THE PROBABILITY OF OCCURRENCE AND THE INTENSITY OF TROPICAL CYCLONES ALONG THE SOUTHERN AFRICAN EAST COAST

by

COBUS ROSSOUW

Thesis prepared as part of the requirements

For the degree

Master in Engineering (Civil)

At the University of Stellenbosch

DR. J ROSSOUW Pr. Ing

Study Leader

STELLENBOSCH

JUNE 1999

Declaration

I the undersigned declare that the work contained in this thesis is my own original work and has not previously in its entirety or in part been submitted at any University for a degree.

Signature: 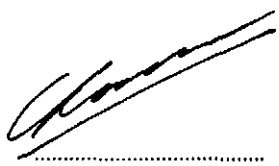 **Date:** 09/11/1999

THE PROBABILITY OF OCCURRENCE AND THE INTENSITY OF TROPICAL CYCLONES ALONG THE SOUTHERN AFRICAN EAST COAST

SYNOPSIS

A tropical cyclone is a non-frontal, synoptic scale, low-pressure system over tropical or sub-tropical waters with organised convection and a definite cyclonic surface wind circulation. The system varies in size between a hundred and a few thousand kilometres in diameter with high winds circulating around a central low pressure. The process of bringing the lower atmospheric layers into thermodynamic equilibrium with the warm tropical waters add the energy to the atmosphere and lower the surface pressure. If favourable climatic conditions exist this leads to the formation of a warm core vortex, which can develop into a tropical cyclone. The occurrence of tropical cyclones follows seasonal variations, the tropical cyclone season for the Southwest Indian Ocean being between November and March. The occurrences peak along the Southern African East Coast between Mid-January and Mid-February.

The data on the location and intensity of tropical cyclones along the Southeast Africa coastline were obtained from the Joint Typhoon Warning Centre and span the period between 1848 and 1999. The available data before 1945 consist of tropical cyclone tracks that influenced populated areas or were encountered by ships. It was assumed that a number of tropical cyclones before 1945 were not recorded and therefore data collected before 1945 were disregarded in the analysis. The development of radar in 1945 significantly improved the detection of tropical cyclones. Some of the tropical cyclone tracks recorded between 1945 and 1956 contain information about the intensity of the tropical cyclone. Since the dawn of the satellite age in the mid 1980's, the detection of tropical cyclones and intensity measurements have improved vastly.

Monte Carlo simulation techniques were used to create long term data series based on the available measured data. Statistical distributions were fitted for each characteristic describing the tropical cyclone at its nearest position to the site under investigation.

Tropical cyclones frequently occur along the Southern African East Coast. The region where more than one tropical cyclone per 100 years can be expected is bordered by latitudes 2.5°S to 32.5°S. The design parameters for structures in these regions should provide for the influence that a tropical cyclone will have on the site. The occurrence rate and expected maximum Intensity of tropical cyclones with a 100-year return period vary with latitude along the Southern African East Coast. The maximum number of tropical cyclones in a 100-year period occurs at latitude 15°S with an expected number of tropical cyclones of 157.2 per 100 years. The

maximum expected tropical cyclone intensity in a 100-year period is 143.5 knots at latitude 17.5°S.

DIE VOORKOMS EN INTENSITEIT VAN TROPIESE SIKLONE LANGS DIE SUIDER-AFRIKAANSE OOSKUS

OPSOMMING

Tropiese Siklone is nie-frontale laagdrukstelsels wat hulle ontstaan het oor tropiese en sub-tropiese oseane. 'n Stelsel bestaan uit 'n sentrale laagdrukstelsel met sirkulerende winde daar om. 'n Sikloon se deursnee kan wissel van 'n honderd tot 'n paar duisend kilometer. 'n Laagdrukstelsel ontstaan as gevolg van 'n termodinamiese wanbalans tussen die atmosfeer en die warm oseaanwater in die trope. Indien die benodigde atmosferiese toestande heers kan die laagdrukstelsel in 'n tropiese sikloon ontwikkel. In die Suidwestelike Indiese Oseaan vorm tropiese siklone tussen November en Maart. Die meeste siklone kom hier voor vanaf middel Januarie tot middel Februarie.

Data is verkry vanaf die "Joint Typhoon Warning Centre" vir die Suidwestelike Indiese Oseaan en strek vanaf 1848 tot 1999. Die data voor 1945 verteenwoordig slegs die tropiese siklone wat bewoonde areas of skeepsvaart beinvloed het. Daar is aangeneem dat 'n betekenisvolle getal van die tropiese siklone voor 1945 nie gedokumenteer is nie en derhalwe is slegs data van sikloon voorkomste na 1945 gebruik in die studie. Vanaf 1945 het die ontwikkeling van radar die opsporing van siklone in onbewoonde areas moontlik gemaak. Die gebruik van weersatelliete vanaf die middel 1980's het die kwaliteit van die data nog verder verbeter.

Monte Carlo simulasie tegnieke is gebruik om langtermyn data vir spesifieke posisies langs die kus te genereer. Statistiese verdelings is gepas op die eienskappe wat die sikloon beskryf wanneer dit die naaste posisie aan die terrein bereik. Die passing van die verdelings is gedoen op die beskikbare historiese data. Die verdelings is dan gebruik om langtermyn data stelle te skep vir die terrein.

Tropiese siklone kom gereeld in die Suidwestelike Indiese Oseaan voor en beïnvloed die Suid-Afrikaanse Ooskus. Meer as een tropiese sikloon kan elke 100 jaar verwag word in kusgebiede tussen breedtegrade 2.5° S en 32.5° S. Die ontwerpe vir strukture in die gebied moet dus voorsiening maak vir die invloed van tropiese siklone. Die voorkoms en intensiteit van tropiese siklone varieër met breedtegraad langs die Suid-Afrikaanse Ooskus. Die meeste siklone word verwag by breedtegraad 15°S met 'n gemiddelde van 157.2 siklone per 100 jaar. Die mees intensiewe siklone kom voor by breedtegraad 17.5°S met 'n verwagte 1:100 jaar intensiteit van 143.5 knope.

Uiteensetting van nagraadse vakkursusse soos deur die kandidaat met sukses afgelê:

Vakkursusse		**Krediete**
DS01	Toegepaste Statistiek	2
DS02	Toegepaste Statistiek	2
IW01	Ingenieurswiskunde	2
TW01	Toegepaste Wiskunde	2
SM03	Vibrasies	4
SM01	Materiale	4
SB02	Struktuurbou – Beton	4
WB01	Waterboukunde	4
WB02	Watergehaltebestuur	4
WB03	Rivierhidroulika	4
WB04	Kusboukunde	4
Totaal		36

THE PROBABILITY OF OCCURRENCE AND THE INTENSITY OF TROPICAL CYCLONES ALONG THE SOUTHERN AFRICAN EAST COAST

TABLE OF CONTENTS

LIST OF FIGURES

LIST OF TABLES

LIST OF SYMBOLS

V_m	-	Maximum average one minute sustained wind speed at 10-m height in knots
λ	-	Recurrence Rate per year
α	-	Tropical Cyclone Track Direction relative to True North
V_f	-	Tropical Cyclone Translational Speed in metres per second
d	-	Closest Distance between Tropical Cyclone Track and the Site in kilometres
θ	-	Angle between the Tropical Cyclone Track (at its Closest Distance) and the Site Relative to True North
Δt	-	time interval
t	-	time
p	-	probability
n	-	Rank of a Data Point
N	-	Total Number of Records in a Data Set
R	-	Radial Distance around a Particular Location (km)
α_I	-	Parameter of the Extreme I Distribution
β_I	-	Parameter of the Extreme I Distribution
α_B	-	Parameter of the Beta Distribution
β_B	-	Parameter of the Beta Distribution
a	-	Lower limit of the Beta Distribution
b	-	Upper limit of the Beta Distribution
X	-	Number of 100-year periods simulated in the Monte Carlo simulation

ACRONYMS

NHC	-	National Hurricane Centre
JTWC	-	Joint Typhoon Warning Centre
ITCZ	-	Inter Tropical Convergence Zone
IR	-	Infrared
VIS	-	Visual

THE PROBABILITY OF OCCURRENCE AND THE INTENSITY OF TROPICAL CYCLONES ALONG THE SOUTHERN AFRICAN EAST COAST

1. INTRODUCTION

Tropical cyclones are intense tropical weather systems that develop in the warm tropical ocean basins. It is known that these systems affect the African South East Coast, but their area of influence has not been studied. Tropical Cyclones are rarely included in establishing the design parameters for locations along the South African East Coast, although extreme winds, waves and rainfall from these systems have been recorded at Richards Bay (Tropical Cyclones Imboa (1984) and Demoina (1987)). Tropical cyclone Imboa caused waves with a significant wave height of 8 m (Figure 1.1 indicates the time series of wave heights measured at Richards Bay (Rossouw (1989)). Before this event, such a wave height was considered an event with a return period exceeding 1:100 years. The extreme wave statistics for this site excluded the effect of tropical cyclones on the site, which led to this under estimation in the prediction of extreme waves.

There has been a steady increase in coastal development in Mozambique since the end of the civil war (1992). The Mozambique coastline is frequently affected by Tropical Cyclones. This created a need to understand the occurrence of tropical cyclones along this coast with a view to establish proper design criteria.

1.1 THE AIM OF THE STUDY

This study will aim to provide the reader with an understanding of the cyclones affecting the East African Coastline.

- The reader will obtain a very brief insight into the internal structure of a cyclone and the climatic conditions required to form cyclones.
- The available data on tropical cyclones are described and the limitations of the data highlighted.
- A detailed method to assess the statistical occurrence rate as well as the maximum expected intensity of a cyclone on a particular site is provided.

This study deals only with the occurrence rate and intensity of cyclones at a particular location and does not include the possible impacts that the cyclone might have on the site. Empirical methods relating the intensity, location and movement of the cyclone to possible wave heights, maximum winds and storm surge levels are briefly discussed in Appendix A.

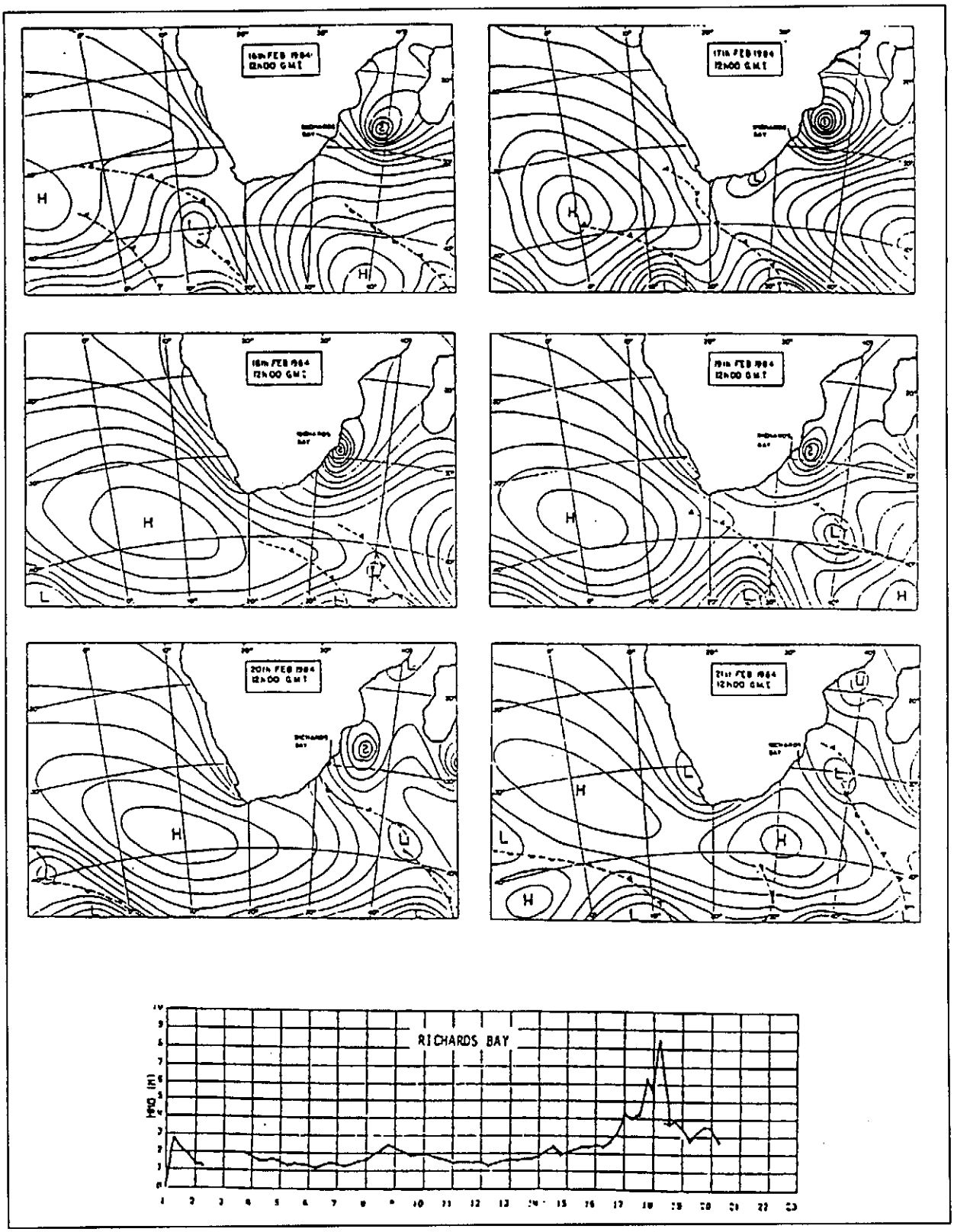

Figure 1.1: Synoptic Chart and Wave Recording Associated with Tropical Cyclone Imboa (Rossouw (1989))

1.2 GLOBAL TROPICAL CYCLONE PATTERNS

Each year 83 tropical cyclones occur throughout the world on average. About two thirds of these cyclones reach severe tropical cyclone status with maximum sustained winds exceeding 33 m/s (McBride (1995)).

1.2.1 Global Tropical Cyclones Occurrences

The location of cyclone formation is presented in Figure 1.2. This map indicates the location of the origin of all cyclones between 1958 and 1977 (20 years). From this map it is clear that the preferred regions of formation are over the tropical oceans. No formations occur within 2.5° latitude of the equator and most formations (87%) occur between 20° N and 20° S. The seasonal formation patterns of tropical cyclones is presented in Figure 1.3. The global distribution of cyclone formation with latitude is indicated in Figure 1.4. About two thirds of all cyclones occur in the Northern Hemisphere, and twice as may cyclones occur in the Eastern as in the Western Hemisphere. These differences are due to the absence of cyclones in the South Atlantic and the Eastern South Pacific Oceans.

The actual number and percentage of the total number of cyclones in this period that originated in a specific area is presented in Figure 1.5. Globally the regions of origin of cyclones are divided into 7 sub areas viz.: Western Atlantic, East Pacific, South Pacific, Western North Pacific, Australian, North Indian and South Indian regions. The statistics for each basin are presented in Table 1.1.

Table 1.1: Statistics on Occurrence of Tropical Cyclones based on data from 1968-1989 (Landsea (1998))

	TROPICAL STORM OR STRONGER (SUSTAINED WINDS > 17 m/s)			SEVERE TROPICAL CYCLONES (SUSTAINED WINDS > 33 m/s)		
BASIN	MOST	LEAST	AVERAGE	MOST	LEAST	AVERAGE
Atlantic	18	4	9.7	12	2	5.4
NE Pacific	23	8	16.5	14	4	8.9
NW Pacific	35	19	25.7	24	11	16.0
N Indian	10	1	5.4	6	0	2.5
SW Indian	15	6	10.4	10	0	4.4
Aus SE Indian	11	1	6.9	7	0	3.4
Aus SW Pacific	16	2	9.0	11	2	4.3
Globally	103	75	83.7	65	34	44.9

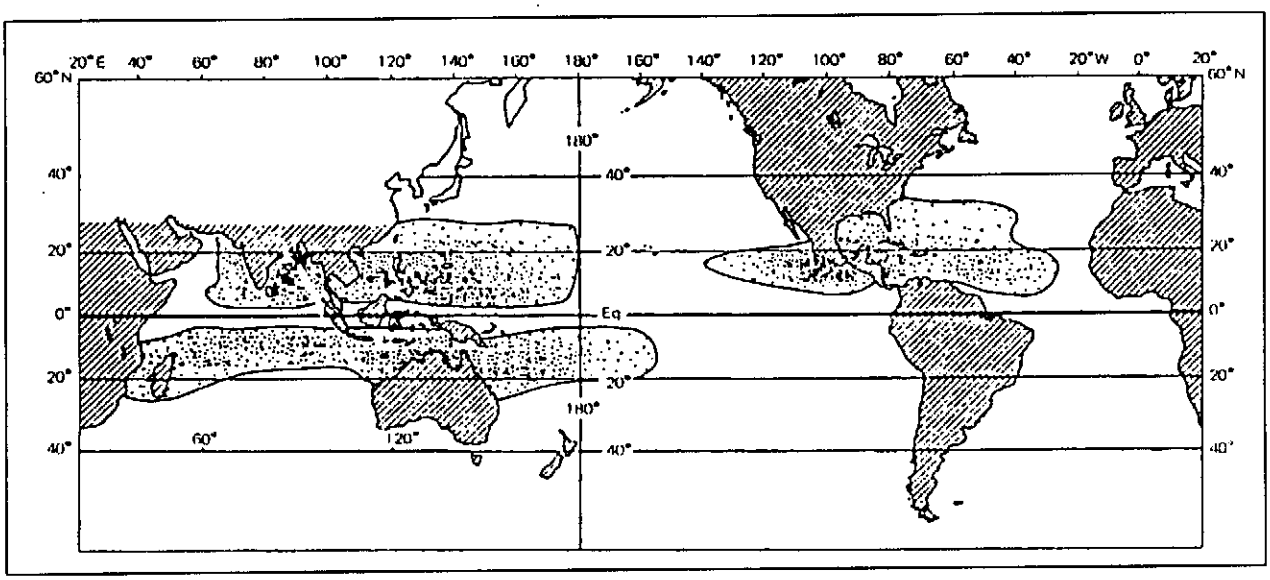

Figure 1.2:

Tropical Cyclone Origin Locations for all Tropical Cyclones between 1958 and 1977

(International Atomic Energy Agency (1984))

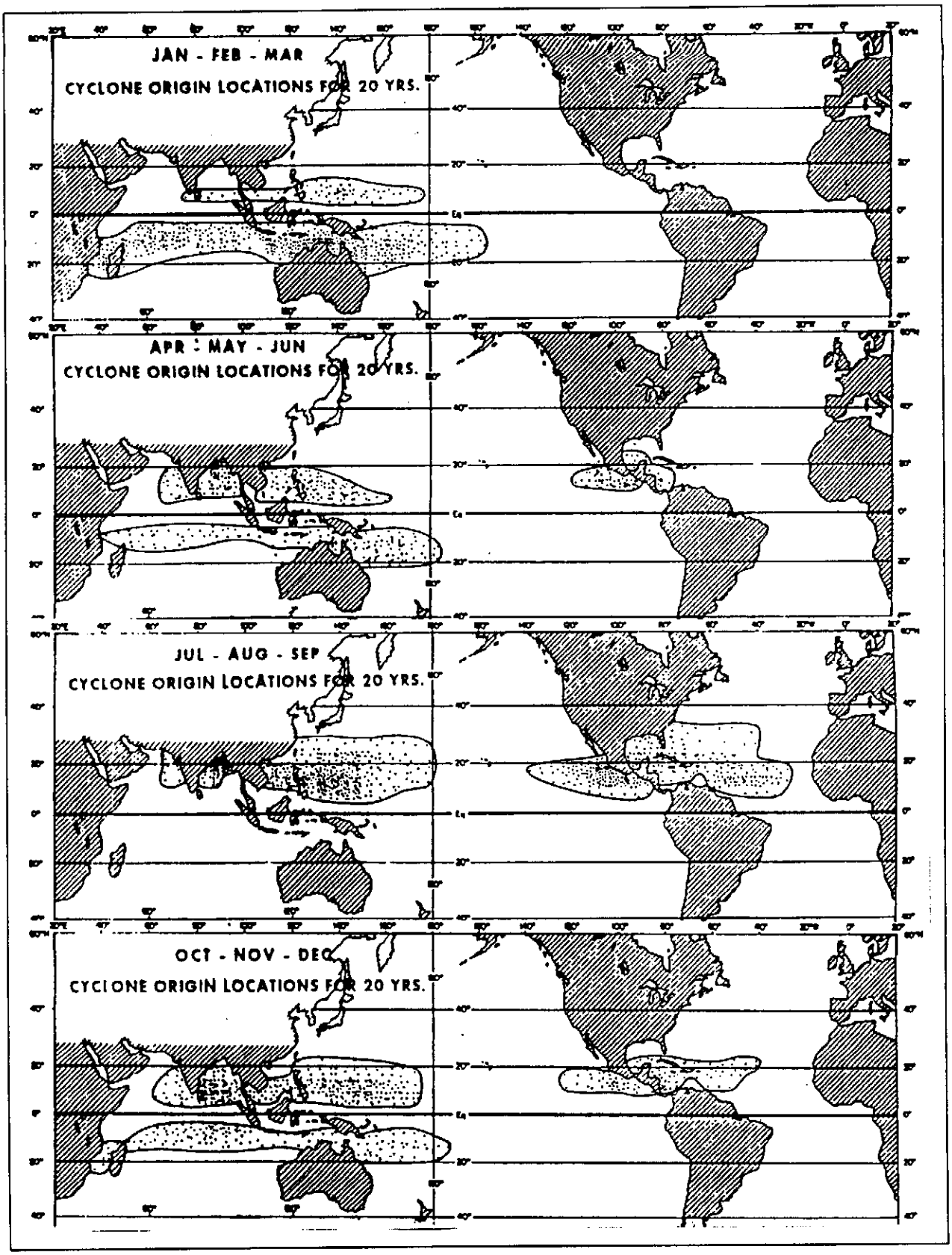

Figure 1.3: Seasonal Tropical Cyclone Formation Patterns (Grey (1975))

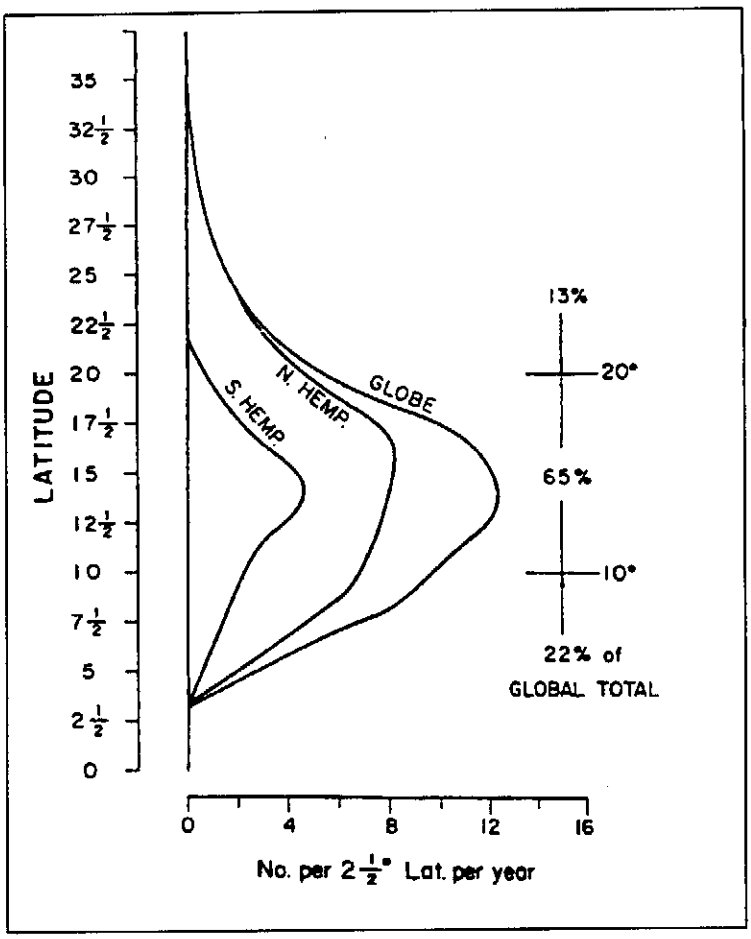

Figure 1.4: Distribution of Tropical Cyclone Origin with Latitude (Grey (1975))

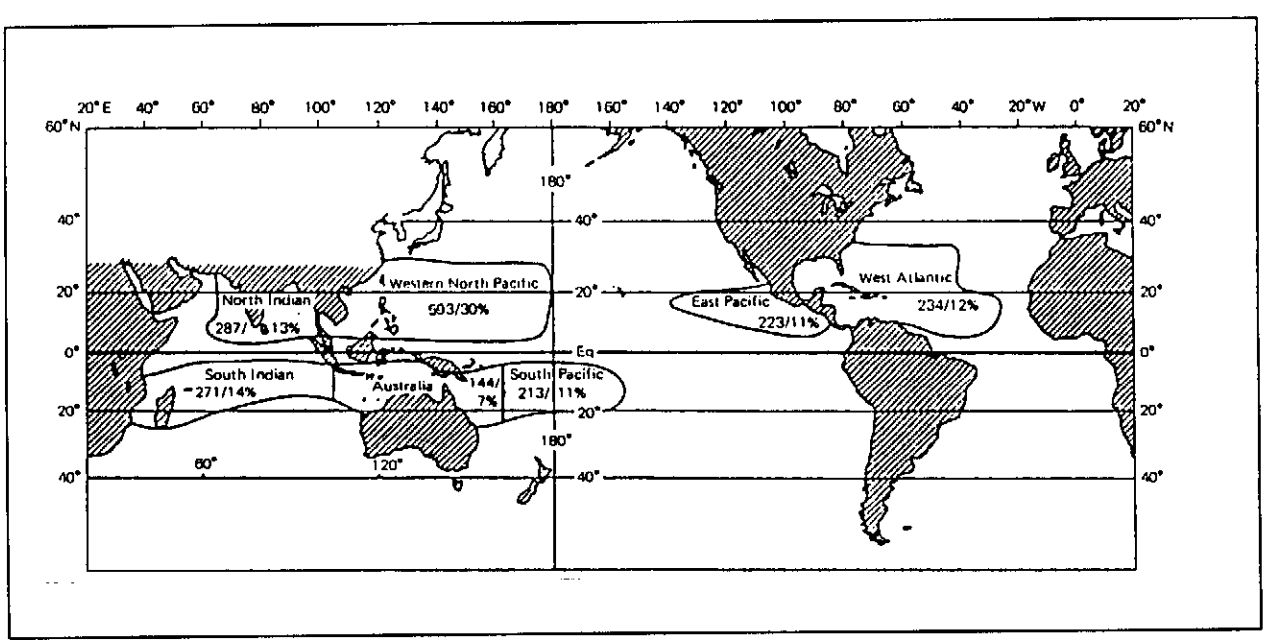

Figure 1.5: Number and Percentage of Global Number of Tropical Cyclone Origins between 1958 and 1977 (International Atomic Energy Agency (1984)

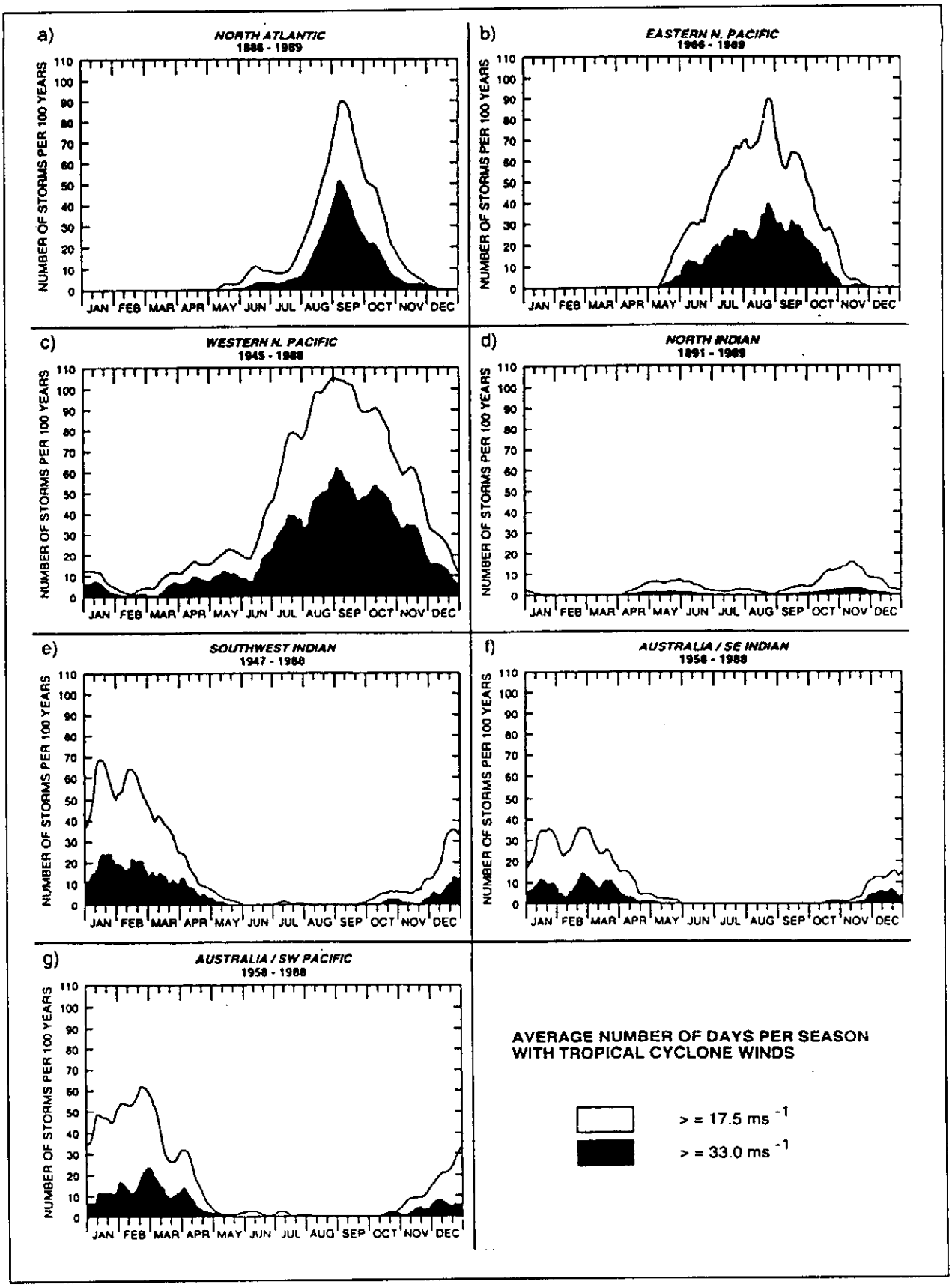

Figure 1.6: Seasonal Distribution of Tropical Cyclone Origins for the Seven Tropical Cyclone Basins (Neumann (1993))

Tropical Cyclones are seasonal phenomena, and most basins have a maximum frequency of formation during the late summer to early autumn period. The Southern Hemisphere peak occurs from January to March and the Northern Hemisphere peak is from July to September. The seasonal distribution of formation locations is governed by two major factors. The first is the warmer sea surface temperatures during late summer. The second is seasonal variations in the location of the monsoon trough. These effects on tropical cyclone formation will be discussed in detail in Chapter 2. The annual seasonal distribution of tropical cyclones is indicated in Figure 1.6 for the seven tropical cyclone basins.

1.2.2 Statistics on the Effect of Severe Tropical Cyclones World Wide

Globally tropical cyclones cause large-scale disasters especially severe tropical cyclones crossing coastal zones in populated areas. The most extreme cases (Landsea (1998)) are mentioned below.

The most intensive tropical cyclone measured to date was Typhoon Nancy in the Northwest Pacific on 12 September 1961. This tropical cyclone had a minimum central pressure of 888 mb with maximum sustained winds of 185 knots. The cyclone that intensified the fastest was Typhoon Forrest. This cyclone formed in the Northwest Pacific in September 1983. The central pressure of the cyclone dropped by 100 mb from 976 to 876 mb in just under 24 hours. This drop in central pressure caused the sustained surface winds to increase by 85 knots in 24 hours from 65 to 150 knots.

The highest recorded storm surge resulting from tropical cyclone activity was 13 m at Bathurst Bay, Australia. This was as a result of the Bathurst Bay Hurricane in 1899. Tropical cyclones also cause excessive rainfall. The highest recorded rainfall associated with tropical cyclones was recorded on Reunion Island. Tropical Cyclone Denise caused 1144mm rainfall in 12 hrs with a total of 1825mm during a 24-hour period. Tropical cyclones vary vastly in size. The largest recorded cyclone to date was Typhoon Tip in the Northwest Pacific. This cyclone had gale force winds (wind speeds greater than 30 kt) which extended over an 1100 km radius. The smallest recorded cyclone to date is Cyclone Tracy near Darwin, Australia. This cyclone only had a 50-km radius of gale force winds.

The intensity of severe tropical cyclones has caused disasters around the world. The most deaths resulting from a single tropical cyclone are estimated at 300 000 people in Bangladesh. This was as a result of the Bangladesh cyclone in 1970. Most of the deaths were related to storm surge set up, resulting from the cyclone, flooding the populated low lying deltas of the area. The largest damage caused by a cyclone is estimated at $77.5 Billion (Inflated to 1997 values) caused by the Great Miami Hurricane in 1926 with Hurricane Andrew (1992) causing the second most damage ($35.5 Billion). Both tropical cyclones affected Florida and Louisiana in the United States of America.

The above statistics emphasise the importance of taking the effect of cyclones into account in establishing the design parameters for the cyclone-affected areas.

1.3 DESCRIPTION OF THE STRUCTURE OF THE THESIS

The thesis is divided into seven sections. Chapter 2 is included to introduce the concept of tropical cyclones. It describes the classification system used for cyclones around the world. A simplified description of the structure of a cyclone is presented and climatic conditions required to form a cyclone are explained. A brief discussion on the formation of tropical cyclones in the Southwest Indian Ocean concludes this chapter. The aim of this chapter is to provide insight into the driving mechanisms of cyclones and to introduce the basic terminology used for describing cyclones. A basic knowledge of the structure and formation of tropical cyclones will also assist in understanding the cyclone motions and data needed to make cyclone predictions.

Chapter 3 provides details with regard to the data presently available on cyclones in the South Western Indian Ocean. The data is briefly discussed and shortfalls in the data set are highlighted. An overview with regard to the behaviour of cyclones affecting the Southern African East Coast is also included in this chapter.

In Chapter 4 a statistical procedure to evaluate the occurrence rate and intensity of cyclones at a particular location is discussed. This model aims to give a statistical base for establishing the appropriate "design cyclone" for a specific location. It provides a combined statistical model of cyclone location, intensity and track direction with regard to a specific location. In Chapter 5 the models described in the previous chapter are applied using data from Chapter 3. Richards Bay is used as an example to clarify the use of the models described in Chapter 4. Chapter 6 provides a summary of the occurrence rate and intensity of tropical cyclones along the Southern African East Coast. The methods described in Chapter 4 are applied at 2.5 degrees latitude intervals from latitude 2.5°S to 32.5°S to produce a tropical cyclone risk map. This map can be

UNIVERSITEITSBIBLIOTEEK U.S.

used to assess the probability and intensity of tropical cyclones along the Southern African East Coast. Only the occurrence rate and intensity are addressed in this thesis. Methods of calculating the possible wave climate, wind speeds and storm surge from a tropical cyclone at a know location, intensity and approach angle are presented in Appendix A of the thesis.

2. TROPICAL CYCLONE CLASSIFICATION, STRUCTURE AND FORMATION

This chapter provides a brief understanding of what a tropical cyclone is. The various different classification systems shall be explained to provide an understanding of the terminology used in publications from different sources. A simplified description of the cyclone structure is also presented. The structure will be explained with a view to understand the occurrence of cyclones along the African Southeast Coast. Details with regard to the thermodynamics and physics of the system and their interaction with global atmospheric conditions are not presented, but references are given. This chapter also discusses the climatic conditions required to form tropical cyclones. A brief discussion on the formation of tropical cyclones in the Southwest Indian Ocean concludes this chapter. This will help to understand the distribution of cyclone patterns across the globe.

2.1 CLASSIFICATION OF TROPICAL CYCLONES

A tropical cyclone is a generic term for a non-frontal synoptic scale low-pressure system over tropical or sub-tropical waters with organised convection and a definite cyclonic surface wind circulation (Holland (1993)). This definition does not contain any reference to maximum winds or minimum pressures, but only describes the structure of the system.

The classification of tropical cyclones globally relates to the maximum sustained surface wind of the system. The maximum sustained wind is defined as the maximum average 10-minute wind speed at 10 m elevation according to the World Meteorological Organisation. Most countries have adopted this definition. However the National Hurricane Centre (NHC) and Joint Typhoon Warning Centre (JTWC) uses the maximum sustained surface wind as the maximum average 1-minute wind speed at 10 m.

This difference in averaging period may provide complications in comparing statistics from one basin to another as the shorter averaging period may slightly raise the maximum sustained surface winds and thus the number of occurrences of storms. The area of responsibility of the NHC is the North Atlantic and Eastern North Pacific Oceans while the JTWC covers the Western North Pacific Ocean.

The classification system according to maximum sustained wind speeds also differs for the various regions. Globally tropical cyclones with maximum sustained surface winds of less than 17 m/s (33 kt) are called tropical depressions. Once the tropical cyclone reaches winds of at least 17 m/s they are typically called a "tropical storm" and assigned a name. If winds reach 33 m/s (65 kt), then they are called: a "hurricane" (the North

Atlantic ocean, the Northeast Pacific Ocean East of the dateline, or the South Pacific Ocean East of 160E); a "typhoon" (the Northwest Pacific Ocean West of the dateline); a "severe tropical cyclone" (the Southwest Pacific Ocean West of 160E or Southeast Indian Ocean East of 90E); a "severe cyclonic storm" (the North Indian Ocean); and a "tropical cyclone" (the Southwest Indian Ocean) (Neumann 1993). This classification system is summarised in Table 2.1. The JTWC has introduced another classification term for the Northwest Pacific Ocean. They call all tropical cyclones with maximum sustained winds exceeding 130 kt, "super typhoons".

Table 2.1: Global Classification System of Tropical Cyclones

Region	Maximum Sustained Surface Wind Speed		
	V < 34 kt	34 kt < V < 64 kt	V > 64 kt
North Atlantic Ocean	Tropical Depression	Tropical Storm	Hurricane
Northeast Pacific Ocean East of the dateline	Tropical Depression	Tropical Storm	Hurricane
South Pacific Ocean East of 160E	Tropical Depression	Tropical Storm	Hurricane
Northwest Pacific Ocean West of the dateline	Tropical Depression	Tropical Storm	Typhoon
Southwest Pacific Ocean West of 160E	Tropical Depression	Tropical Depression	Severe Tropical Cyclone
Southeast Indian Ocean East of 90E	Tropical Depression	Tropical Depression	Severe Tropical Cyclone
North Indian Ocean	Tropical Depression	Cyclone	Severe Cyclonic Storm
Southwest Indian Ocean	Tropical Depression	Tropical Depression	Tropical Cyclone

The above table should aid in understanding the type and severity of the storms mentioned in other publications when they are only referred to under their generic names. This publication only uses the term tropical cyclone and does not distinguish between tropical depressions and tropical cyclones as is customary in the Southwest Indian Ocean.

2.2 THE STRUCTURE OF A MATURE TROPICAL CYCLONE

This section will provide a brief technical discussion on the structure of a mature cyclone. The first part gives a brief description of the cyclone structure as provided in "Design Basis Tropical Cyclone for Nuclear Power Plants, International Atomic Energy

Agency (1984)". This is a very brief description of the overall mechanics of a cyclone without any significant detail about the physics or structure thereof. This section serves as an introduction for the next section where more detail with regard to the physical and atmospheric processes is given.

2.2.1 General Description of a Tropical Cyclone

A tropical cyclone consists of a rotating mass of warm humid air. This rotating mass varies in size from 100 km to several hundreds of kilometres. The atmospheric pressure in the centre is the lowest and was measured as low as 888 mb (Typhoon Nancy (1961)). The central pressure of a cyclone provides an indication of the intensity of the cyclone. The lower the central pressure of a cyclone the higher the maximum sustained surface winds. Atkinson and Holiday (1977) have investigated the relationship between central pressure and intensity for the Northwest Pacific and found good relationships. This relationship is included in Appendix A of the report.

In the Northern Hemisphere the winds of a cyclone spiral inwards towards the centre in an anticlockwise direction, whereas in the Southern Hemisphere the rotation is clockwise. The rotation direction is the result of Coriolis forces, which drives the spiral vortex. This also explains the difference in rotation between the Southern and Northern Hemisphere cyclones. The typical pattern of the wind field of a tropical cyclone in the Northern Hemisphere is presented in Figure 2.1.

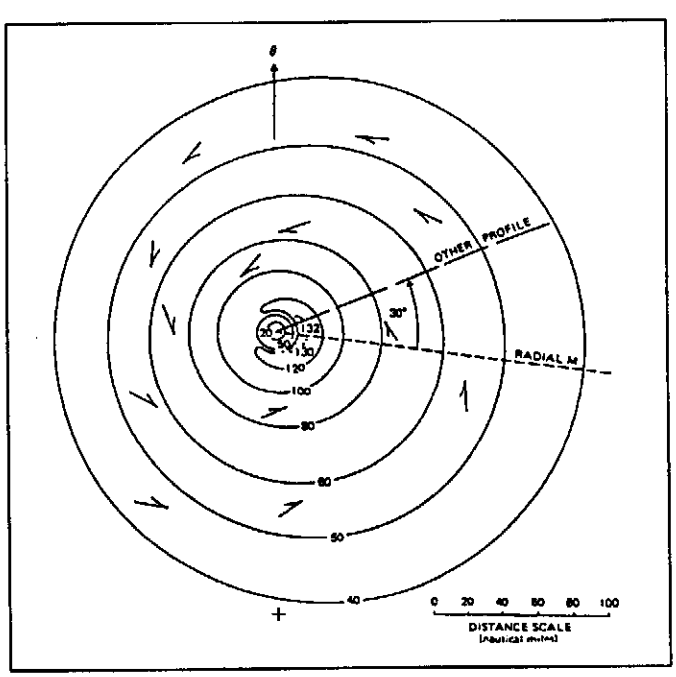

Figure 2.1: Typical Pattern of Tropical Cyclone Wind Fields in the Northern Hemisphere (International Atomic Energy Agency (1984))

Well-developed cyclones have widespread areas of thick cloud cover, extending to great heights, together with bands of torrential rains and violent winds. The strongest winds blow in a tight band around the eye of a tropical cyclone. The eye is a region of light winds and lightly clouded sky, usually circular or elliptical in shape and ranging from a few kilometres to over 150 km in dimension. The winds increase near the outer edges of the eye, called the eye wall, and then diminish gradually with distance from the wall. Figure 2.2 shows a satellite image of Super Typhoon Winnie that occurred in the Northwest Pacific in August 1997. The features of a tropical cyclone are indicated on this figure.

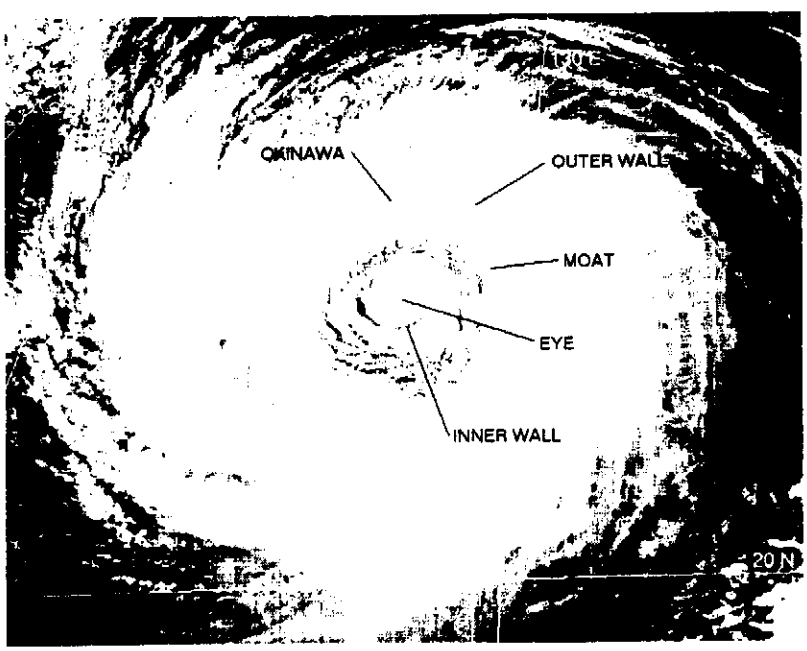

Figure 2.2 Satellite Image of Super Typhoon Winnie (Dillon et. Al. (1998))

Although the winds of tropical cyclones frequently exceed 50 m/s, a cyclone's translational movement is much slower. For example, in the Northwest Pacific, the movement would typically be towards the West or West-Northwest at about 4-5 m/s, although other directions and translational speeds of up to 15 m/s are not uncommon.

The physical process and energy transformations occurring in tropical cyclones are extremely complex. Essentially a tropical cyclone is a vast heat engine where the source of energy is the warm sea providing water vapour which releases latent heat when it condenses and forms rain. Tropical cyclones are warm core storms. Since the warm air of the core is lighter than its surroundings, the surface pressure there is lower and such differences in the surface pressure produce the familiar pattern of circular

isobars. Air starting to move towards the low-pressure centre is deflected because of the rotation of the earth and spiral inwards. A much more detailed description of these processes is presented in Section 2.2.2.

2.2.2 Internal Structure of a Mature Tropical Cyclone

This section provides more detail with regards to the internal circulation processes inside a tropical cyclone. The processes are described qualitatively and no details with regard to the thermodynamic, momentum and energy transfers within the system are presented. Willoughby (1995) provides more detail and mathematical models describing the internal dynamics of the system.

Over much of the tropical oceans in summer, the process of bringing the tropospheric column (lower atmospheric layer up to 15 km from the earth surface) in thermodynamic equilibrium with the sea would add enough energy to lower the surface pressure by 5-10%. The atmosphere's adjustment of the balance wind and mass on a rotating Earth towards the low pressure (attainable at thermodynamic equilibrium) is the primary reason for the formation of tropical cyclones.

The tropical cyclone is thus a warm-core vortex. Winds that rotate around the centre decrease with height, but typically fill the whole troposphere (the lower atmospheric layer up to 15 km from the surface of the earth). The inner region (cyclonic core) contains spiral bands of precipitation, the eyewall and the eye. Figure 2.2 indicates these features as observed in a satellite image. The inner region winds can become intense and may reach speeds of up to 90 m/s just outside the eye.

As the cyclone matures, the spiralling winds rotating around the eye become increasingly axisymetric. The spiralling winds thus rotate in a circular pattern around the eye in a mature cyclone. These winds are referred to as the primary circulation of the cyclone. In addition to the primary circulation, secondary circulation develops in response to surface friction and condensational heating. The secondary circulation has radial inflow near the surface towards the eye, saturated ascent around the eye, forced descent inside the eye and outflow near the tropopause level (upper levels of the troposphere) outside the eye. An idealised profile of the secondary flow of a tropical cyclone is shown in Figure 2.3. As the air of the secondary circulation moves towards the cyclone centre, it loses angular momentum. As the circulation reach the tropopause level and turns outward, all the angular momentum is lost. The air from the secondary circulation starts to turn anticyclonicly about the eye beyond the 100-200 km radius. This secondary circulation supplies additional angular momentum and thermal energy and intensifies the primary circulation. This inflow of energy maintains the primary

circulation against friction and radiative cooling. The primary circulation is much stronger than the secondary circulation, especially in the core of a tropical cyclone.

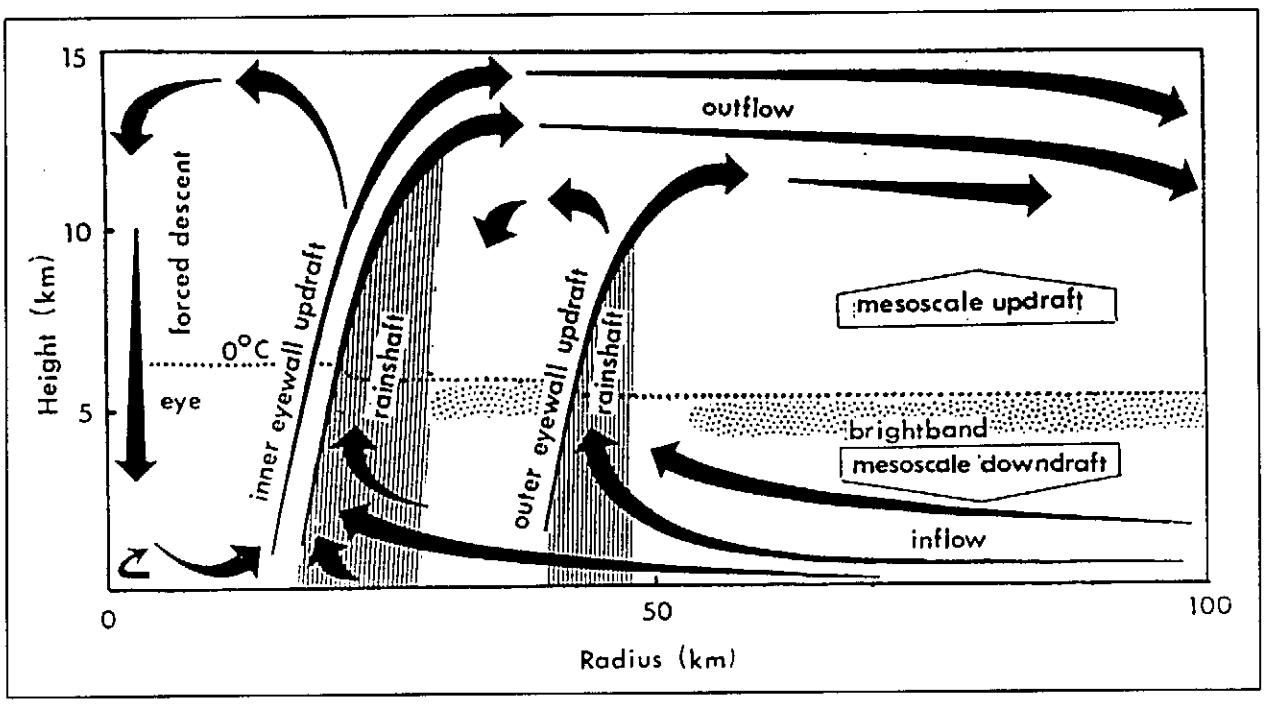

Figure 2.3: Idealised Profile for the Secondary Circulation within a Tropical Cyclone (Willoughby (1988))

Figure 2.4 shows the typical flow patterns for a Southern Hemisphere tropical cyclone. The flow patterns at different levels are shown with the pressures indicated giving an indication of elevation of the flow pattern (The higher the pressure, the closer to the earth surface the flow). It is clear that close to the surface (850-mb) the primary circulation dominates. The airflow is elliptical around the eye of the tropical cyclone angling inward towards the eye. The circulation pattern of the surrounding area follows the motion of the cyclone. In the mid tropopause level (500 mb) the primary circulation is still dominant, but the global airflow from east to west is not changed except in the area close to the eye. The condensed streamlines to the Northwest and the separation of streamlines to the Southeast cause a bigger pressure deficit, forcing the overall translational movement of the cyclone in a Southeasterly direction. In the upper tropopause level (250 mb) the anticyclonic motion of the secondary circulation is visible close to the centre of the tropical cyclone. The separation of the streamlines to the West of the tropical cyclone causes a low-pressure gradient across the cyclone, which also aids the translational movement of the tropical cyclone.

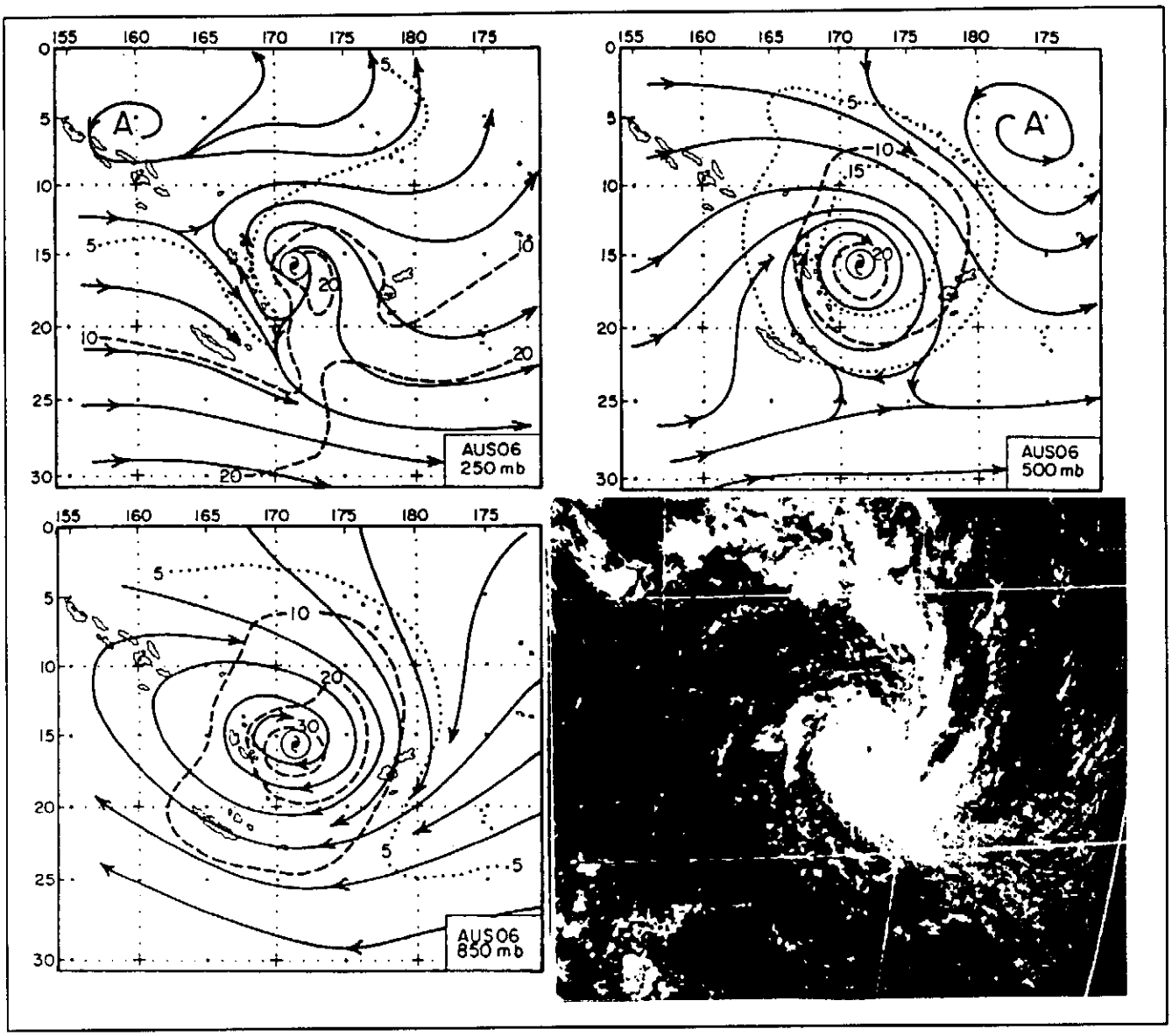

Figure 2.4: Typical Flow Patterns for a Southern Hemisphere Tropical Cyclone (Holland (1984))

From this figure it is clear that the secondary circulation and interaction with the global East West movement of air are responsible for the translational movement of tropical cyclones and the tendency of tropical cyclones to move towards the poles at recurvature. If this environmental forcing is strong enough, the tropical cyclone moves to higher latitudes into cooler water and stronger West East airflow streams. The loss of the fuel (warm sea temperature) and the stronger airflow counter the tropical cyclone primary vortex generally results in a reduction in intensity.

With the information provided on the structure of a tropical cyclone, the systems governing the primary vortex as well as the mechanism forcing translational movements of tropical cyclones we can explore what environmental conditions are needed to form these systems.

2.3 FAVOURABLE ENVIRONMENTAL CONDITIONS FOR THE FORMATION OF TROPICAL CYCLONES

The explanation of the structure of cyclones in Section 2.2 of this study will provide a better insight into the environmental factors required to form tropical cyclones. The aim of this section is to provide an understanding into the mechanism leading to the formation of cyclones. This will also give insight into the reasons for cyclone formation along the African Southeast Coast.

The following environmental conditions must be in place for a tropical cyclone to form (Landsea(1998)):

- Warm ocean waters (at least 26.5° C) throughout sufficient depth. It is unknown exactly what depth of warm water is required, but generally it is accepted that the water must have this minimum temperature to a depth of at least 50 m. If only the surface water is sufficiently warm, surface mixing by wind removes the heat before a significant tropical cyclone can form. As explained in Section 2.2, the primary forming mechanism of tropical cyclones is the low pressure that develops as a result of warm water heating the surface air.

- An atmosphere that cools fast enough with height such that it is potentially unstable to moist convection. It is the thunderstorm activity, which allows the heat stored in the ocean waters to be liberated for the tropical cyclone development.

- Relatively moist layers near the mid-troposphere (5 km above the surface of the earth). Dry mid levels are not conducive for allowing continuing development of widespread thunderstorm activity.

- A minimum distance of at least 500 km from the equator. For tropical cyclone formation to occur there is a requirement of minimum values of the Coriolis force to provide for the near gradient wind balance to occur. Without the Coriolis force, the low pressure of the disturbance cannot be maintained. (This is why no cyclone formations are noted within 2.5° Latitude of the equator as mentioned in Section 1.2.1)

- A pre-existing near surface disturbance with sufficient vorticity and convergence. Tropical cyclones cannot be generated spontaneously. To develop they require a weakly organised system with sizeable spin and low level inflow.

- Low values (less than about 10 m/s difference in wind speeds between the surface layers and the upper troposheric layers) of vertical wind shear between the surface and the upper troposphere. Vertical wind shear is the magnitude of wind change with height. Large values of vertical wind shear disrupt the incipient tropical cyclone and can prevent the formation, or if the tropical cyclone has already formed, weaken or destroy the tropical cyclone by interfering with the organisation of deep convection (secondary circulation) around the eye.

The above conditions are necessary for the formation of cyclones, but tropical cyclones do not always develop even if all the above are in place.

2.4 TROPICAL FLOW PATTERNS ASSOCIATED WITH THE FORMATION OF TROPICAL CYCLONES

Warm sea surface temperatures required to form tropical cyclones extend across the globe in the tropical oceans during the late summer. Tropical cyclone formation however does not occur in all the tropical oceans, but only in the locations indicated in Figure 1.2. McBride (1995) attributes this to the formation of Inter-Tropical Convergence Zones (ITCZ) in certain basins around the globe. The formation and location of these zones set up conditions of low vertical shear winds, which are prerequisites for the formation of tropical cyclones. The mechanism and interaction causing zones of low vertical shear winds are explained below.

The ITCZ extend semi-continuously around the globe. They may occur as a convergence zone between the trade Easterlies from the Northern and Southern Hemispheres, or as a convergence zone in Westerly monsoon flow. In this latter configuration, the monsoon Westerlies usually have trade Easterlies on their poleward side. The shearline between the monsoon Westerlies and the trade Easterlies is known as the monsoon trough and is a climatologically preferred region of tropical cyclone formation. The upper- and lower-level flow patterns for the two modes are illustrated schematically in Figure 2.5. The trade convergence line of the ITCZ typically is associated with strong vertical shear winds, a condition which is not conducive to tropical cyclone formation. When monsoon Westerlies are present, the upper level subtropical ridge overlies the low-level monsoon shearline. This configuration of trade Easterlies overlain with Westerlies and monsoon Westerlies overlain with Easterlies leads to a vertical wind shear of close to zero, with Westerly shear on the poleward side

and easterly shear on the equatorward side. This configuration leeds to both low vertical shear wind as well as a mechanism to develop a weakly organised system with sizeable spin and low level inflow.

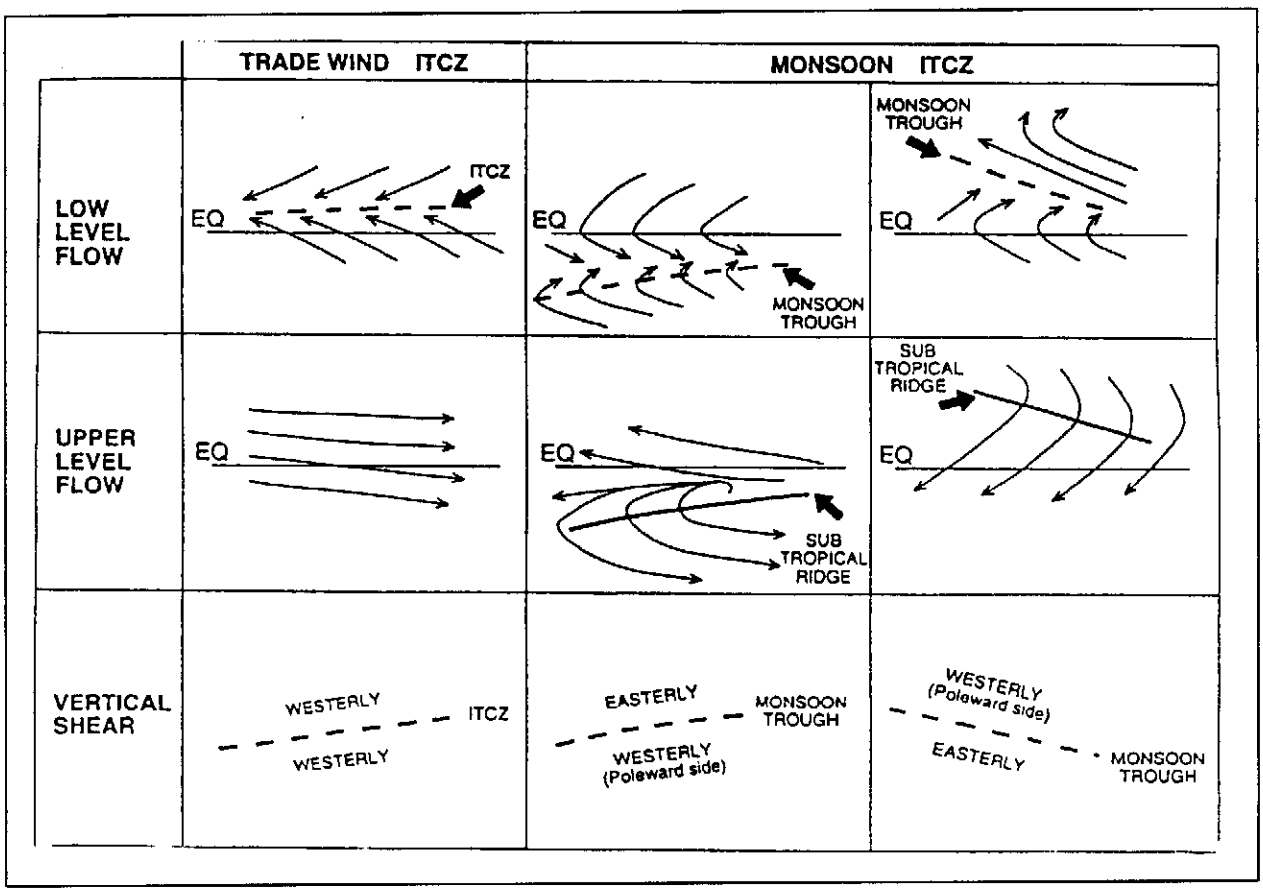

Figure 2.5: Flow Patterns Associated with the Inter Tropical Convergence Zone (McBride (1995))

The seasonal distribution of the mean location of the monsoon-type ITCZs occurring over the oceans is plotted in Figure 2.6. The association between the monsoon trough and occurrences of tropical cyclones in Figure 1.3 is quite marked.

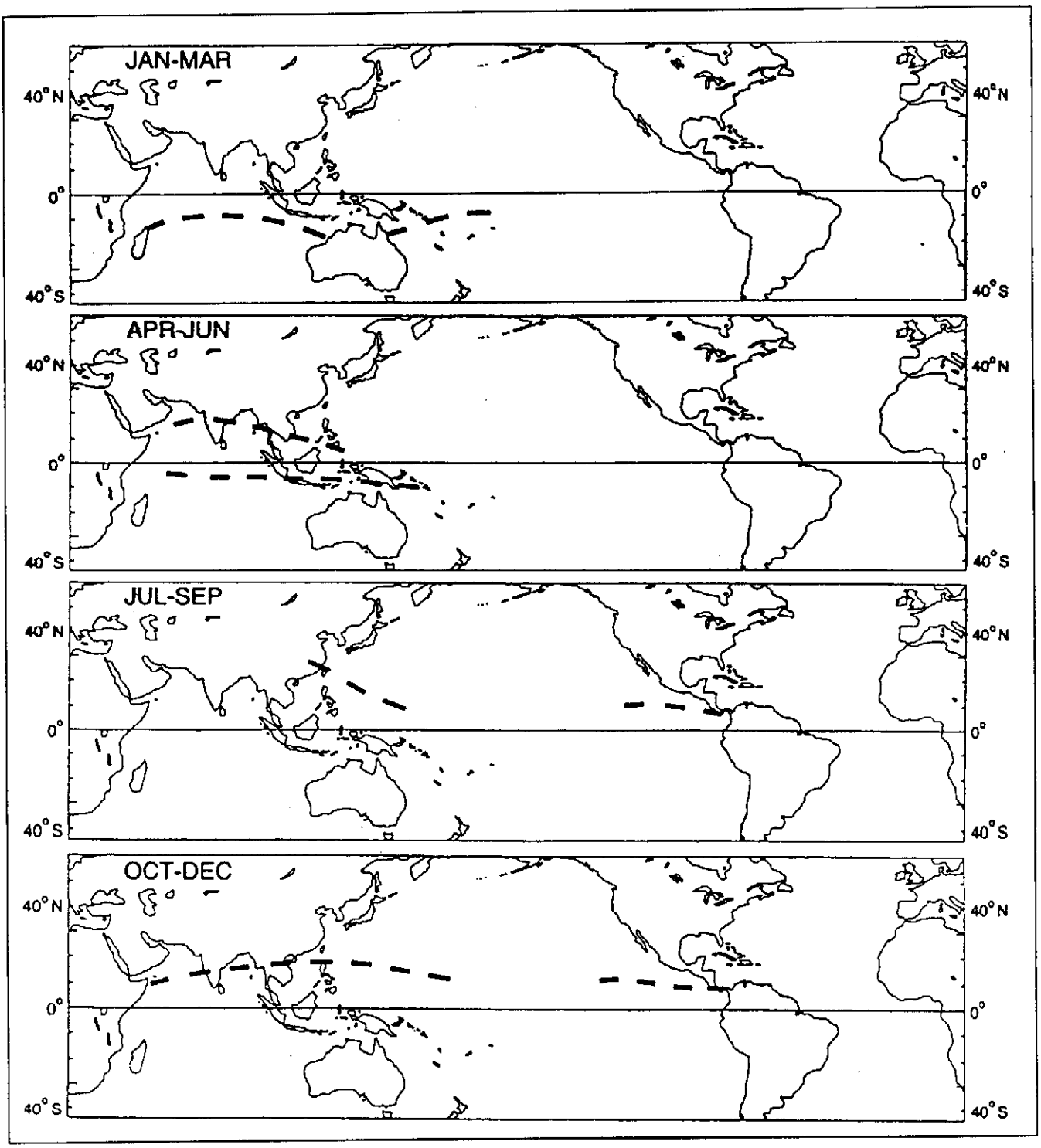

Figure 2.6: Seasonal Distribution of the Location of the Monsoon Type Inter Tropical Convergence Zone (McBride (1995))

2.5 TROPICAL CYCLONE FORMATION IN THE SOUTHWEST INDIAN OCEAN

Figure 1.6 (e) reflects the annual distribution of tropical cyclone formation for the Southwest Indian Ocean. The major part of the cyclone season extends from November though March, with a double peak mid-season maximum in mid-January as well as mid-February. The morphology of formation is poorly documented in this basin due to the sparsity of synoptic and upper-air data. The mean position of the 26°C sea surface temperature isotherm is generally south of 20°S during the peak season, and retreats equatorward to about 10°S during the winter.

The seasonal establishment and retreat of the Southern Hemisphere monsoon shearline are consistent with the seasonal variations of tropical cyclone formation. In particular, the shearline is at its furthest excursion from the equator during January and February and the formation locations follow a similar trend. This can be seen from Figure 2.7, which indicates the mean monthly latitudes of tropical cyclone formation of tropical cyclones with winds of at least 34 knots. From this figure it is clear that the far Western portion of this basin (between Africa and 50°E) displays different behaviour. No formations occur in this region until November. Most of the formation events that do take place in this area are confined to the Mozambique Channel, which leads to a poleward displacement of these initial positions relative to the positions of formation East of 50°E. A distinct transition in the surface wind flow through the Mozambique Channel occurs between November and December with a change in the dominant South-Easterly trade regime in November to a cross-hemispheric Northerly flow in December. This Northerly component remains a prominent feature of the general circulation through February, but the flow retreats equatorward during March. By April, the general flow reverses as South-Easterly trade winds become dominant and tropical cyclone activity cease in the area.

The African Southeast coast is affected by cyclones forming in the Mozambique Channel as well as in the Indian Ocean east of Madagascar. The tropical cyclones forming east of Madagascar generally track west over Madagascar. They lose intensity as they cross the landmass, but can re-intensify in the Mozambique Channel if they pass over sufficiently warm water. Tropical cyclones affecting the African Southeast coast do occur from October to April, with a marked increase in occurrence from December through to March.

The above should give an understanding of the nature of tropical cyclones, the reason for their existence and the mechanisms involved in their structure. This knowledge should aid in understanding the data presented in the following chapter.

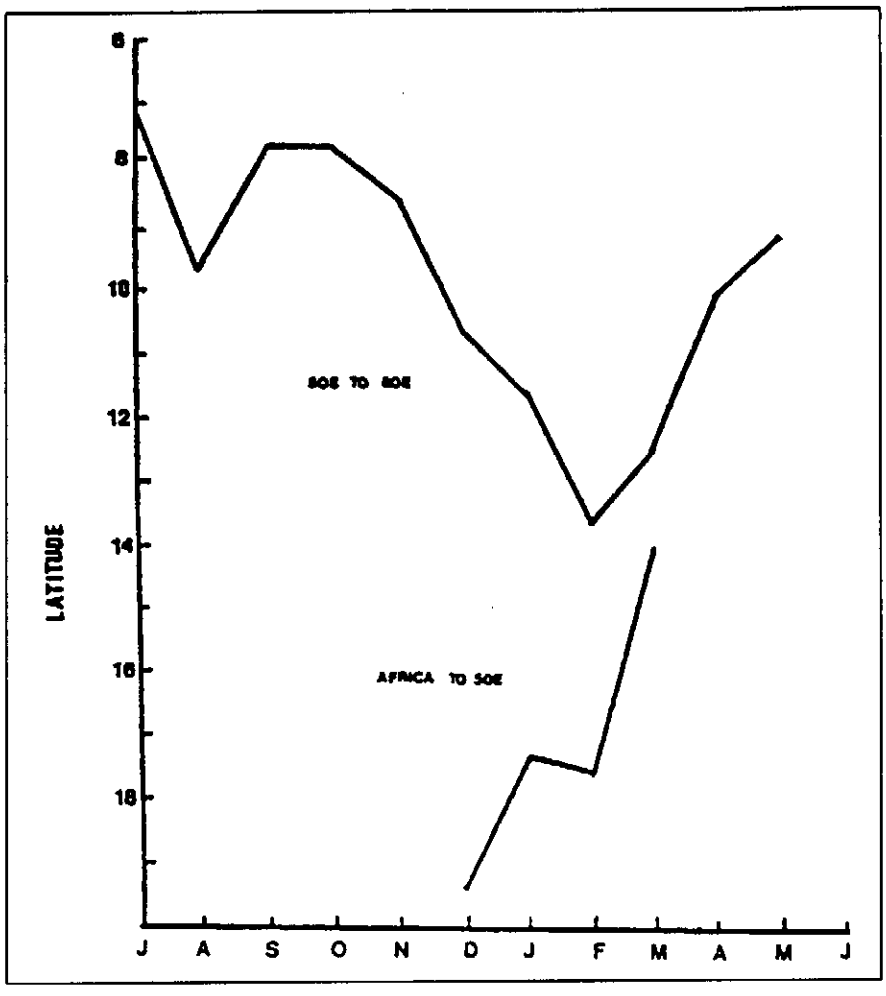

Figure 2.7: Mean Monthly Latitudes of Tropical Cyclone Formation in the Southwest Indian Ocean of Tropical Cyclones with Winds Exceeding 34 knots. (McBride (1995))

3. DESCRIPTION OF THE AVAILABLE DATA ON TROPICAL CYCLONES ALONG THE SOUTHERN AFRICAN EAST COAST

This chapter describes the available data on tropical cyclones and in particular the data for tropical cyclones affecting the Southern African East Coast. A brief description of the methods of data collection globally is provided. This will help to understand the accuracy and limitations of the data sets, especially data collected before satellite measurements were available. The various institutions possessing data on tropical cyclones are also described. The type and format of the data is briefly described. The section concludes by choosing a preferred data set and a description of the tropical cyclones affecting the Southern African East Coast.

3.1 THE HISTORY OF DATA COLLECTION AND POSITION FIXING FOR TROPICAL CYCLONES

Tropical cyclone data for the Southwest Indian Ocean has been collected and stored since 1848. The earlier cyclones were identified by ships that encountered these storms as well as from land stations where a tropical cyclone passed sufficiently close (usually within 200 km from the coast) to a populated landmass to be noticed. This was the only method of collecting data in the Southwest Indian Ocean and continued up to 1962. This data consists of estimated tropical cyclone positions at 6 hourly intervals with no indication of the intensity. The location of the centre of the cyclone was estimated and large errors in the positions can be assumed.

An increase in shipping and commercial airline traffic improved the data from 1945. Data recorded on aircraft and ships are frequently used to fix the position of cyclones. During this period several meteorological stations were brought into operation which also helped with the improvement of the data. The development of radar improved the detection of tropical cyclones since the mid 1940's. Radar had the capability to detect the dense rainstorms around the eye of the cyclone up to 400 km from the tropical cyclone. Since then the accuracy of locations significantly improved. The development of Doppler radar provided scientists with the first method of estimating the intensity of a tropical cyclone remotely. The understanding of the cyclone structure and core also increased significantly, since Doppler radar provides information on the circulation patterns of the rainbands close to the core.

The collection of data with remote sensing improved greatly with the introduction of satellites in the 1980's. Visual images from satellites could easily identify the location of tropical cyclones, while tracking of the cloud movement around the eye gave an indication of the intensity of the tropical cyclone. Today there are two types of satellites

being used to track and collect data from tropical cyclones. Geostationary satellites (GMS, GOES, METEOSAT and INSAT) are located above fixed locations around the equator. These satellites continually monitor the tropics providing infrared (IR) and visible (VIS) data at hourly intervals. The second type of satellites used are the polar orbiting satellites (TIROS, METEOR and DMSP). They orbit the earth in fixed patterns in a North-South orbit crossing the poles. The data from polar orbiting satellites are available twice a day for a particular location. The data also consist of IR and VIS imagery. METEOSAT5 and METEOSAT7 covers Southern Africa including both the Atlantic and Indian Oceans. Figure 3.1 and Figure 3.2 illustrate the VIS images as recorded by these satellites.

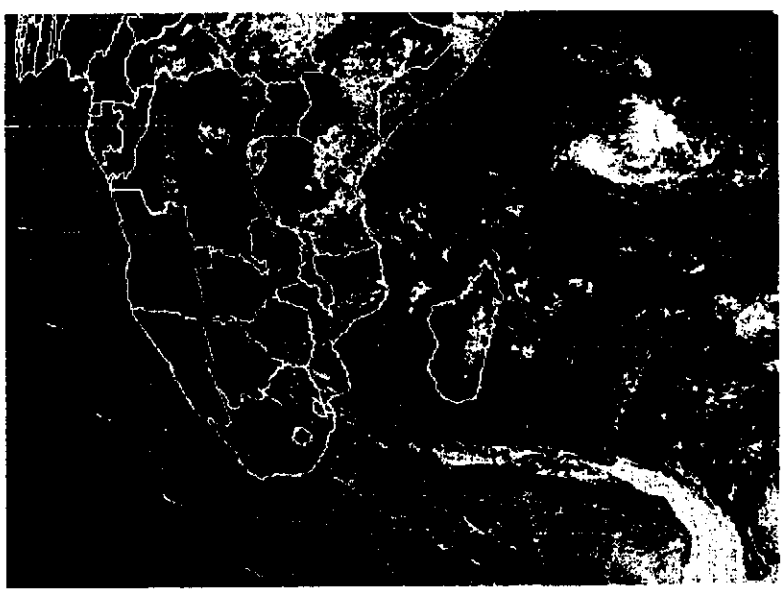

Figure 3.1: Visual Satellite Image of Southern Africa as Observed by METEOSAT5

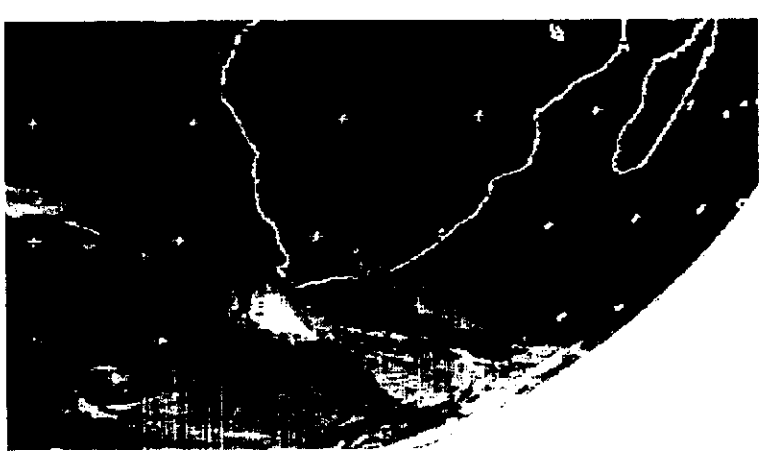

Figure 3.2: Visual Satellite Image of Southern Africa as Observed by METEOSAT7

Over the horizon radar is currently in its final development stage. This type of radar will be able to collect data on tropical cyclones thousands of kilometres away.

Figure 3.3 provides an indication of the available data sources and coverage on a global scale.

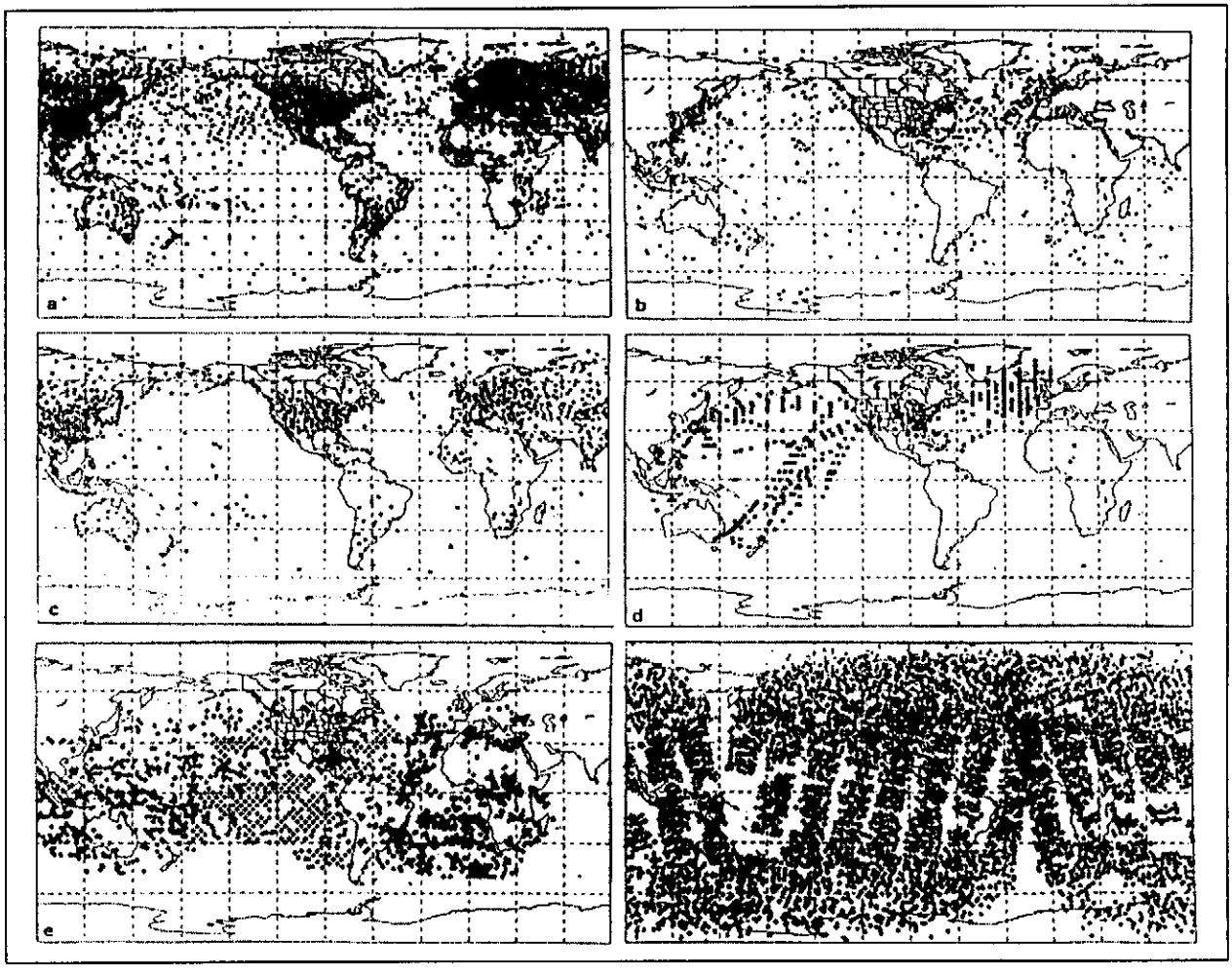

Figure 3.3: Source Data Distribution Globally, (a) Surface Observations; (b) Surface Marine Observations; (c) Upper-Air Soundings; (d) Aircraft Reports; (e) Satellite Cloud-Track Wind Observations; (f) Satellite Temperature Profile Observations (Dey (1989))

3.2 DESCRIPTION OF THE AVAILABLE DATA FOR THE SOUTHWEST INDIAN OCEAN

This section includes a brief review of the methods of data collection for the Southwest Indian Ocean. The sources of data are briefly described and the format of the data from various sources is presented.

Figure 3.3 indicates the data from various sources around the world. From this figure it is noted that the main types of data for this basin are surface observations, surface marine observations, satellite cloud-track wind observations from geostationary satellites and satellite temperature profile observations from polar orbiting satellites. The data collected before the satellite era was very sparse for this basin and therefore the earlier data may contain significant errors in the location of tropical cyclones.

Cyclone data for the period from 1848 to 1996 are available from Meteo France in Reunion. The data for the period between 1848 and 1947 contain only the dates on which cyclones were observed within 200 km of the coastline. 36 cyclones were observed during this period. For the period between 1947 and 1962 the data contain the tracks of cyclones observed within 200 km of the coast. During this period the data contain tracks of 28 cyclones. The data from 1962 to 1996 contain the tracks of 57 cyclones observed within the Mozambique Channel. Maximum 15-minute average wind speed and central pressure data are available for some of these cyclones.

The Joint Typhoon Warning Centre (JTWC) in Guam is a combined Air force and Navy organisation of the USA. Their principal function is to predict areas of tropical cyclone activity globally and issue warnings with regard to the occurrence of tropical cyclones. They have developed prediction models for the various tropical cyclone basins and these models are implemented to produce tropical cyclone track and intensity forecasting. The JTWC has a database containing historical records of the "Tropical Cyclone Best Track Data" for all cyclones. This data set is considered to be the best available for the Western Indian Ocean. It contains data for all cyclones in the Southern Hemisphere between 1945 and 1997 providing the date and position of the cyclones at 6 hourly intervals. Data relating to the estimated maximum sustained one-minute wind speed at 10 m are available from 1956 onwards.

The JTWC data covers a shorter period than the Meteo France data. All the tracks from the Meteo France data are included in the JTWC data. A number of tracks which are included in the JTWC are not included in the Meteo France data, therefore the JTWC data set was used for the analysis of the occurrence rate of tropical cyclones. The Meteo France data was used in Appendix A to establish a relationship between

maximum wind speed and central pressure. The list of all the tropical cyclones that entered the study region between 1945 and 1997 is presented in Appendix C.

There are other institutions that also possess data on tropical cyclones. Most of the data from these sources originate from the data of the JTWC.

3.3 DESCRIPTION OF THE JOINT TYPHOON WARNING CENTRE DATA SET

The JTWC data contain 216 tropical cyclones tracks for the period 1945 to 1997 in the region bordered by Latitude 4.2° S to 42.9° S and Longitude 17.7° E to 50° E. Fifty five of the 216 tracks for this region include maximum wind speed data. Maximum wind velocities up to 130 knots are present in the data.

The data are available in ASCII format. The filename indicates the tropical basin, cyclone number and year of the data. An example is BSH0145, which contains the first (BSH**01**45) cyclone track for the Southern Hemisphere (**BSH**0145) during 1945 (BSH01**45**). Each file consists of six hourly locations and maximum sustained one minute wind velocities at 10 m for that particular cyclone. For every six hourly reading there is a 22 character long entry. The first 10 digits reflect the cyclone number, year, month, day and hour, each 2 characters in length. The following three characters give the latitude of the storm multiplied by 10 followed by an S or an N indicating Southern or Northern Hemisphere. The following four numbers give the Longitude of the storm multiplied by 10 followed by an E or W indicating Eastern or Western Hemisphere. The last three digits indicate the average one-minute mean wind speed at 10-m height in knots. If no intensity information is available, the last digits –999 are used. An example of such a data file is presented in Appendix B.

The following chapter deals with the use of the data to predict the occurrence rate as well as the expected intensity of tropical cyclones at a particular location.

4. A STATISTICAL MODEL TO PREDICT THE PROBABILITY OF OCCURRENCE AND INTENSITY OF TROPICAL CYCLONES AT A PARTICULAR SITE

Tropical cyclones display fairly random behaviour. There are only 53 years of reasonably accurate data available. This data show a great variation in the track, direction, intensity and forward motion from one cyclone to the next. This variation makes the prediction of tropical cyclone occurrence very difficult. This randomness of tropical cyclone behaviour is experienced around the world and various techniques have been developed to try and assess the risk associated with the occurrence of tropical cyclones at a particular location. The climatic influences driving the intensity and movement of the tropical cyclone are also not fully understood. The data needed to predict tropical cyclone occurrences and characteristics in terms of the physical and thermodynamic processes inside the tropical cyclone are also not available for most of the tropical cyclone basins around the world. The lack of understanding of the physical processes and data, forces the use of empirical statistical models to predict the occurrence of tropical cyclones at a location.

The general trend in dealing with the occurrence rate and intensity of tropical cyclones is to construct statistical models from the known data and generate long term data sets using Monte Carlo simulation techniques. These methods have become increasingly popular since the increase of the power of desktop computers made such simulations less time consuming. With the use of a modern PC, data sets of several thousand years can be simulated in a matter of a few minutes. Chouinard et .al.(1997) used this method to evaluate the severity and recurrence rate of tropical cyclones for the Gulf of Mexico. Scheffner et. al. (1996) used a similar technique coupled with a storm surge model to evaluate the storm surge levels associated with tropical cyclone activity along the Coast of Delaware. Hatada et. al. (1996) used this method to estimate storm surge levels and wave heights for selected locations on the Pacific Coast of Japan. Cheng et. al. (1990) applied similar Monte Carlo simulation techniques to evaluate tropical cyclone occurrence rates for Shanghai, China. Vickery et al. (1995) completed a recent review of the predicted hurricane wind speeds along the East Coast of the United States of America using the techniques explained in the following sections of this chapter.

This chapter provides a method of constructing a statistical model for tropical cyclone predictions. Guidelines with regard to the distributions fitted to the various parameters required to describe tropical cyclone behaviour and the possible impacts of tropical cyclones on a site are provided.

4.1 METHODOLOGY

Rare and extreme natural phenomena (floods, earthquakes, etc.) are often modelled as Poisson processes in space and time. The assumptions associated with the Poisson process are that events are completely random and independent of each other in space and time. The process is characterised through a parameter λ, which is the recurrence rate in space and time of the events. If this parameter (λ) remains constant in space and time, the process is said to be a homogeneous Poisson process. If this parameter is found to vary in either space or time, the process is an inhomogeneous Poisson process. In this model, the tropical cyclone is modelled as a homogeneous Poisson process in time and an inhomogeneous Poisson process in space.

The available data contain information about the location, direction of movement, speed of the forward movement and in some instances the intensity of a particular tropical cyclone. This model optimises the use of the data by simulating the characteristics of the tropical cyclone at the closest distance to a particular location as a vector indicating the position, intensity (V_m), track direction (α) and forward speed (V_f). The position of the tropical cyclone is presented using a polar co-ordinate system with the closest distance (d) and angle with regard to the site (θ) as parameters. The parameters are defined in Figure 4.1. In this thesis the sites are located on the coastline at 2.5° latitude intervals.

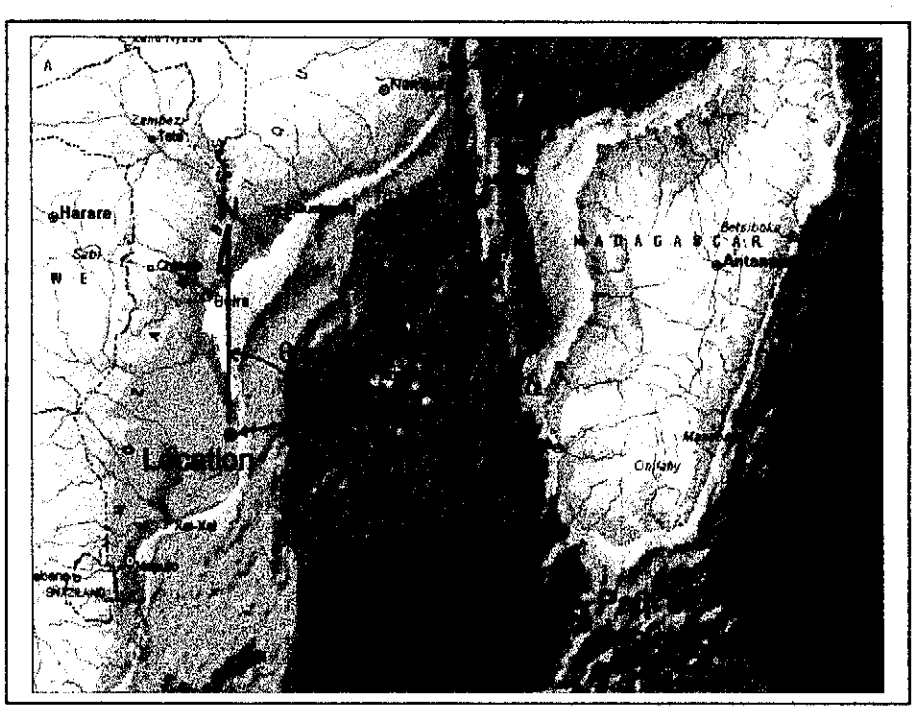

Figure 4.1 Definition of the Parameters Describing the Tropical Cyclone Characteristics

On the basis of these assumptions, the number of occurrences of an event in t is given by the Poisson distribution; that is, if X_t is the number of occurrences in time interval t, then:

$$P(X_t = x) = \frac{(\lambda \cdot t)^x}{x!} e^{-\lambda \cdot t}$$

for x=0,1,2,.....

where λ is the mean occurrence rate; that is the average number of occurrences of the event per unit time interval.

In the 53 years of available data, 216 tropical cyclones occurred in the region, thus the mean occurrence rate is 216/53 = 4.075 tropical cyclones per year.

Ang et al (1975) continues by stating that the inter-arrival time of a Poisson process is exponentially distributed. The probability mass function of the exponential distribution is given by:

$$F(T_1 \leq t) = 1 - e^{-\lambda \cdot t}$$
$$F((T_1 > t) = e^{-\lambda \cdot t}$$

The above distribution is used in the Monte Carlo simulation to simulate the annual number of cyclones occurring per year as follows:

The probability mass function is used to establish the times of arrivals between events. A random number (p) between 0 and 1 is generated and the associated inter-arrival time (t) between two events calculated for that probability:

$$t_i = -\frac{1}{\lambda} \times \ln(p)$$

This procedure is repeated i times until:

$$t_1 + t_2 + ... + t_i \leq 1 year < t_1 + t_2 + ... + t_{i+1}$$

The amount of cyclones occurring in that particular year is therefor i.

The occurrence rate of 4.075 cyclones per year is expressed as 4.075/12 = 0.340 cyclones per month for simulation purposes. The amount of cyclones is counted until:

This statistical model is based on the data of all cyclone tracks that entered the region bordered by Latitude 4.2° S to 42.9° S and Longitude 17.7° E to 50° E between 1945 and 1997. During this period 216 tropical cyclones entered this region and 55 of these tropical cyclone tracks contain information with regard to maximum wind velocity. The closest distance between each tropical cyclone track and a particular site is identified. The distance (d), angle toward the site relative to true North (θ), forward speed of the tropical cyclone (V_f), the direction of movement relative to true North (α) as well as the intensity (V_m) (where available) are extracted. These data are then used to fit statistical distributions to the various parameters. These distributions are then used in a Monte Carlo simulation to generate further data to predict the expected occurrence rate and intensity of tropical cyclones at a specific location.

The following section will provide details with regard to the distribution fitting to the data. The chosen distribution for each parameter is presented in sections 4.2.1 to 4.2.6. Details with regards to other distributions that were tested for each parameter are presented in Appendix D.

4.2 DISTRIBUTIONS FITTED TO THE EXISTING DATA

4.2.1 Occurrence Rate of Tropical Cyclones along the East African Coastline

L.E. Chouniard et al (1997) suggests that the occurrence rate of tropical cyclones be modelled as a homogeneous Poisson process in time. This assumption is supported by various other studies for example Batts et al. (1980) and Vickery et al. (1995). Ang et al. (1975) gives the following conditions that must be satisfied for a process to be Poisson distributed:

- An event can occur at random and at any time or any point in space.
- The occurrence(s) of an event in a given time (or space) interval is independent of that in any other non-overlapping intervals.
- The probability of occurrence of an event in a small interval (Δt) is proportional to Δt, and can be given by $\lambda\Delta t$, where λ is the mean occurrence rate of the occurrence of the event (assumed to be constant for a homogeneous Poisson process); and the probability of two or more occurrences in Δt is negligible.

$\sum_{1}^{i+1} t_{i+1} > 12 months$

Section 2.5 highlights the seasonal variation in tropical cyclone occurrence in the Southwest Indian Ocean with occurrences generally between November and April of the following year. This seasonal variability is not taken into account since the occurrence rates as presented in this study cover periods of more than one year.

4.2.2 Distribution of the closest distance of tropical cyclones to a site

The distribution of closest distance (d) between a tropical cyclone track and the particular site is fitted using the location of the site as the origin of the distribution (d=0). This assumption is valid only if the position of the tropical cyclone is not correlated to the closest distance to the site. A correlation analysis was done for latitude 20° S where approximately the same number of tropical cyclones pass to the north and the south of the site. The correlation coefficient between the closest distance and the angle with regard to the site yields a correlation coefficient of –0.259, which is considered insignificant. The closest distance (d) between a particular site and the 216 tropical cyclone tracks during the period 1945 to 1997 were extracted for each track. These distances were ranked in increasing order and plotted using the following plotting position:

$$p = \frac{n}{N+1}$$

where: p is the plotting position
n is the rank of the particular distance
N is the total number of available cyclone track (216)

A further test was performed at the location at 20°S to validate that the distribution of closest distance for tropical cyclones passing to the north and the south of the site is part of the same distribution. This was done to ensure that there is no discontinuity in the distribution fitted to the closest distance values. The distribution of closest distance (d) for tropical cyclones passing to the north and the south of the site is similar and is indicated in Figure 4.2. Therefore the choice of the site as origin for the distribution of closest distance is justified.

The Extreme I, Lognormal, Normal and Uniform distributions were fitted to all the data. None of these distributions fitted all the data.

Vickery et al. (1995) studied the occurrence rate of hurricanes along the Gulf of Mexico and the United States East Coast using Monte Carlo simulation techniques. He found that the distribution of closest distance followed a Uniform distribution. He fitted the data only to cyclones that came within a predetermined radius (R) from the site. The International Atomic Energy Agency (1984) suggests that all tropical cyclones within a radius of 300-400 km from a site should be included in the tropical cyclone risk analysis. For this study a radius of influence, R, of 400 km was used.

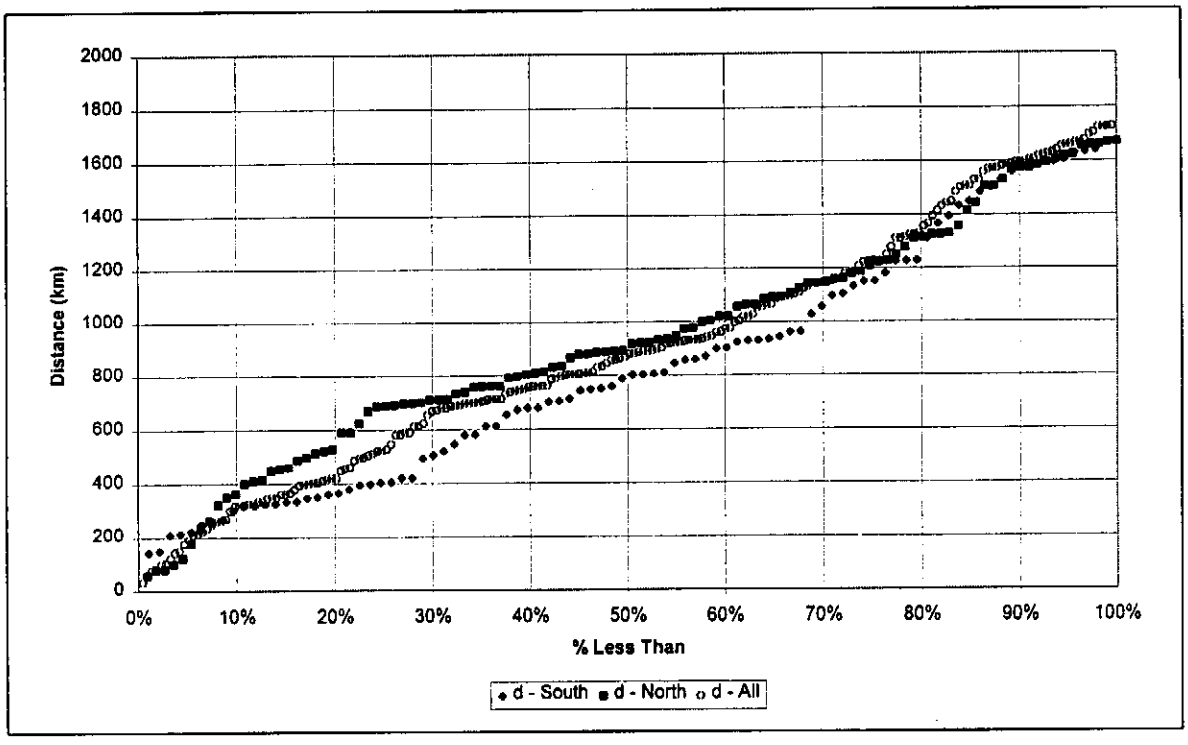

Figure 4.2: Distribution of Closest Distance to the Site at Latitude 20°S.

It was decided not to fit distributions to all the data, but limit the data to the closest 10% of the cyclones or all cyclones closer than 400 km from the site, which ever was greater. The plotting position was still kept in terms of all the data (216).

The Extreme I distribution provided the best fit for the reduced data set. The relationship between probability of non-exceedance (p) and closest distance (d) is given by:

$$d = \alpha_I + \beta_I \cdot \ln(-\ln(p))$$

where: d - Closest distance to the site in kilometres

α_l - Constant

β_l - Constant

p - The probability of non-exceedance

The constants α_l and β_l were obtained by linear regression between d and ln(-ln(p)).

4.2.3 Distribution of the angle between the tropical cyclone at the closest location to the site relative to true North

The angle (θ) between the tropical cyclone at its closest distance and the site measured clockwise from true N, is calculated for each tropical cyclone track in the data set. The definition of this angle is indicated in Figure 4.1.

The same ranking method and plotting position as described in Section 4.2.2 is used for the distribution of θ. Distribution fitting is done to all the data and not just the section of the closest cyclones as used for the distribution of the closest distance.

Vickery (1995) found that the Bi-Normal distribution fitted the data for the Miami region. The data for the East African Coastline seem to follow the Normal distribution.

4.2.4 Distribution of the translational speed of the tropical cyclone

The translational speed of the tropical cyclone (V_f) when at its closest to a particular location, is derived from the difference in position of the tropical cyclone the six hours preceding the nearest location and the position at the nearest location to the site. This parameter is affected by the accuracy of the recorded position of the tropical cyclone at six hourly intervals.

The translational velocity for each tropical cyclone track is calculated from the tropical cyclone track data. The ranking and plotting position methods described in Section 4.2.2 are followed and distributions fitted to the data. It was found that in the data of tropical cyclone tracks affecting the Southern African East Coast there are some excessive translational speeds of up to 70 m/s. It is very uncommon for tropical cyclones to move at such high translational speeds. Speeds of up to 20 m/s have been noted, but this maximum speed has an extremely low occurrence rate. During the analysis it was found that one or two of the data points exceed 20 m/s. These values are possibly due to errors in the position fixing of the cyclones and are discarded from the data set.

Various data distributions have been fitted to the data. Vickery (1995) found that the Lognormal distribution fitted the tropical cyclones in the Miami region. The best fit for the Southwest Indian Ocean data seems to be the Extreme I distribution. Linear regression between ln(-ln(p)) and V_f fits the data extremely well especially if abnormally high speeds are discarded from the data set.

4.2.5 Distribution of the direction of travel of the tropical cyclone at its closest position to the site.

The direction of travel of the tropical cyclone at its closest location to the site is defined as the angle measured clockwise from true N from the position six hours preceding the closest position to the closest position of the track to the site. Figure 4.1 contains a graphical presentation of this definition.

This angle has been obtained for each of the 216 tracks in the data set. They are ranked and assigned a plotting position in accordance with the method described in Section 4.2.2. Normal, Lognormal and Extreme I distributions were fitted to the data without any reasonable fit being obtained. The aforementioned distributions did not fit the angles between North-Northwest and North-Northeast well. The upper and lower values generally fell outside of the 0 to 360 degree angle range. The Beta distribution was fitted with reasonable results. This distribution has the advantage that upper and lower bound values for the distribution can be specified. It was therefore used as the preferred distribution of the track direction.

4.2.6 Distribution of the intensity of tropical cyclones

The intensity of a tropical cyclone is given as the average one minute mean wind speed (in knots) at 10-m height in the data set. Only 55 of the 216 tracks for tropical cyclones contain information on their intensities. It was therefore decided to use a different approach to estimate the intensity from the approach followed in Sections 4.2.2 to 4.2.5. This approach aims to maximise the use of the available intensity data through using all the intensity measurements in the study region and not just that for each tropical cyclone at the point where it is nearest to the site.

All the intensity measurements were binned per 2.5 degree latitude in 5 knot speed bins. The percentage exceedance of intensity table is presented in Table 4.1.

The intensity for the latitudes which enclose most of the data (15°S to 20°S) is distributed Lognormally. It was assumed that this distribution fits the intensity of all the latitude bins, but the lack of data at this stage prevents conclusive evidence thereof. The Lognormal fit to the data per 2.5° Latitude bin is shown in Figure 4.2 for latitudes 15°S to 20°S.

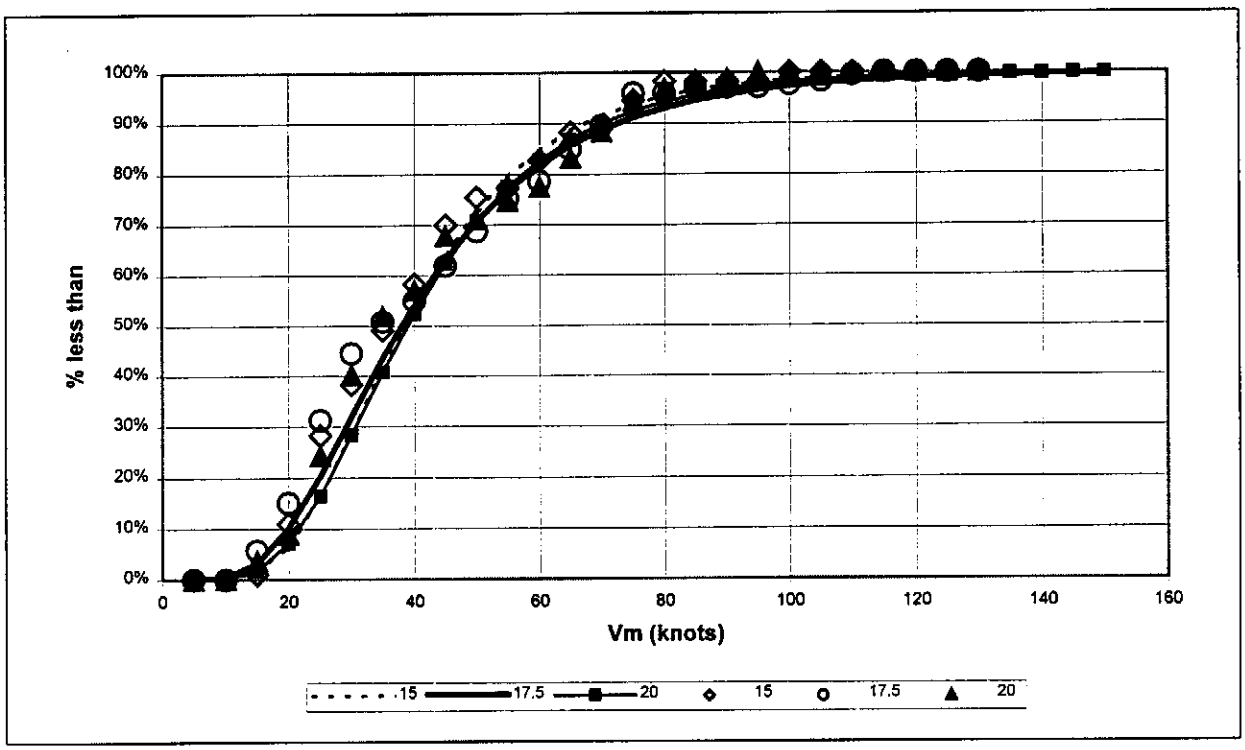

Figure 4.3: Lognormal Fit of the Distribution of Intensity of Tropical Cyclones Between Latitudes 15°S and 20°S Along the Southern African East Coast

Table 4.1 Percentage exceedance of Intensity per 2,5 ° Latitude

Intensity	Latitude												
V_m (Knots)	2.5	5	7.5	10	12.5	15	17.5	20	22.5	25	27.5	30	32.5
5	100%	100%	100%	100%	100%	100%	100%	100%	100%	100%	100%	100%	100%
10	100%	100%	100%	100%	100%	100%	100%	100%	99%	100%	100%	100%	100%
15	86%	96%	95%	97%	98%	99%	94%	96%	94%	100%	100%	100%	100%
20	71%	94%	86%	92%	92%	89%	85%	91%	83%	94%	100%	100%	100%
25		70%	66%	75%	86%	72%	69%	76%	69%	88%	99%	100%	81%
30		46%	55%	59%	76%	62%	55%	60%	59%	79%	93%	93%	44%
35		29%	45%	47%	61%	51%	49%	48%	47%	63%	81%	74%	38%
40		20%	39%	41%	56%	42%	45%	43%	41%	54%	74%	63%	38%
45		14%	29%	30%	36%	30%	38%	32%	24%	27%	57%	59%	38%
50		12%	24%	26%	32%	25%	31%	29%	21%	24%	46%	52%	31%
55		11%	21%	23%	27%	23%	25%	25%	17%	21%	33%	52%	25%
60		11%	18%	21%	25%	17%	21%	22%	17%	18%	15%	41%	19%
65		10%	12%	16%	23%	12%	15%	17%	16%	15%	11%	26%	13%
70		8%	10%	14%	22%	11%	10%	12%	14%	14%	8%	19%	13%
75		4%	6%	7%	19%	5%	4%	6%	13%	12%	7%	11%	13%
80		4%	4%	5%	16%	2%	4%	3%	12%	9%	6%	11%	13%
85		4%	3%	4%	13%	2%	3%	2%	10%	8%	4%	7%	
90		4%	2%	3%	7%	2%	3%	1%	6%	2%	3%	7%	
95		2%	2%	2%	6%	2%	3%		6%	2%	3%	7%	
100		2%	1%	2%	6%		2%		4%	2%	3%	4%	
105		2%		1%	5%		2%		3%	2%	3%		
110		2%		1%	4%		1%		2%	2%	1%		
115													
120													
125													
130													

These distributions were used in the Monte Carlo simulation to predict the intensity of the tropical cyclone. The distribution fit corresponding to the closest latitude bin to the site is used in the simulation.

4.3 DESCRIPTION OF THE MONTE CARLO SIMULATION

The Monte Carlo simulation technique is a numerical simulation technique that uses the statistical distributions fitted to measured data to simulate or extend existing data realistically. This method entails the generation of random numbers between 0 and 1. These numbers represent the probability of exceedance of a statistical distribution reflecting the measured data. From the statistical distribution the actual value of the simulated parameter is calculated from the probability mass function fitting the data. The use of Monte Carlo simulation techniques provides a statistical method to extend existing data sets, providing that the distribution of the existing data is known. The distributions fitted to the data and used in the Monte Carlo simulation are mentioned in Section 4.2. These distributions are used to simulate the closest tropical cyclone vectors to a site for a number of 100-year periods.

The simulation is repeated X times with a 100-year period simulated each time. Every year in the 100 years is simulated separately. Firstly the number of tropical cyclones in the year is generated using the method described in Section 4.2.1. For each of these cyclones a random number is generated and the distribution of closest distance (Section 4.2.2) is used to calculate the distance of that particular tropical cyclone to the site. If this distance is closer than 400 km from the site, the other parameters (θ, V_f, V_m and α) are generated using separate random numbers for each parameter and it's appropriate statistical distribution. The data are then written to a file for further statistical analysis. After the completion of the X simulations of 100-year periods all the parameters of tropical cyclones, which came within 400 km of the site, are analysed. The average number of tropical cyclones in 100 years, the average maximum intensity in 100 years as well as the absolute maximum intensity of any tropical cyclone in the simulation period are calculated. The flow chart of the Visual Basic code combined with Microsoft Excel spreadsheet is presented in Figure 4.4. The number of simulations (X) needs to be increased until the results in terms of the average number of tropical cyclones in a 100 year period and the average maximum intensity of the tropical cyclones, having an influence on the site, stabilise. The Monte Carlo simulation was repeated for 100 to 500 runs in steps of 100 and from 1000 to 10 000 runs in steps of 1000 to assess the number of runs needed to produce stable results. This analysis indicated that 1000 runs produce results that are within 1% of the 10 000 run average. Therefore 1000 runs (100 000 years of data) seems an adequate number of 100 year simulations.

The above chapter describes a method to analyse and predict the occurrence rate, intensity and other characteristics of tropical cyclones having an influence on the

Southern African East Coast. The use of the above methods will be further explained with an example given in the following chapter.

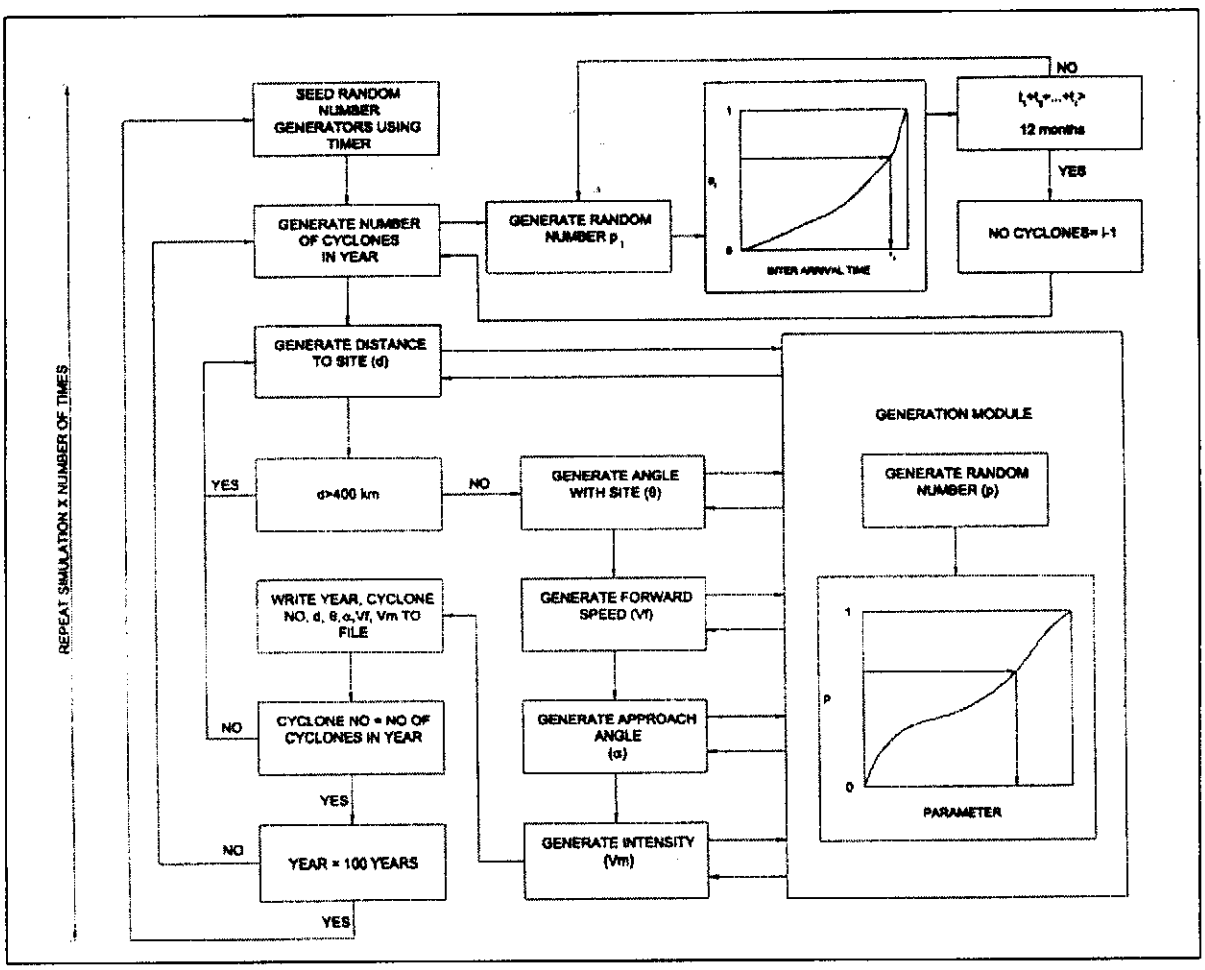

Figure4.4: Flow Chart for the Monte Carlo Simulation

4.4 VALIDATION OF THE MONTE CARLO SIMULATION TECHNIQUE USING RESULTS OF A PREVIOUS STUDY ON BEIRA, MOZAMBIQUE

Rossouw (1998) has investigated the occurrence rate and intensity of tropical cyclones influencing Beira, Mozambique. Beira is located at latitude 19° 51'S on the Mozambique Coast. He found that 31 came within 400 km of the site during the period 1945 to 1996. Wind data is available for 9 of the 31 cyclones and V_m ranges between 15 and 65 knots. This means that the expected number of tropical cyclones in a 100-year period based on the data is 60.7. The Monte Carlo simulation gives the average number of tropical cyclones in a thousand, 100-year simulation as 66.8. This agrees well with the prediction using the limited data set. An exponential distribution was fitted through the 9 measured intensities that were available for the Beira location. This distribution leads to a 1:100 year tropical cyclone intensity of 76 knots based on the available measured data. The Monte Carlo gives the 1:100 year intensity for tropical cyclones as 117 knots. This is significantly higher than the prediction using the measured data. The predicted intensity using the measured data is based on only 9 measurements, therefore the confidence in terms of the distribution used to extrapolate these measurement to a 1:100 year intensity is low. The distribution used in the Monte Carlo simulation is based on 55 tropical cyclone tracks with 214 data points in the 20°S latitude bin. The confidence in the results of the Monte Carlo Simulation is therefore higher.

The Monte Carlo simulation technique is therefore accepted as a valid method for the prediction of the occurrence rate as well as the intensity of tropical cyclones along the Southern African East Coast.

5. EXAMPLE OF THE USE OF MONTE CARLO SIMULATION TECHNIQUES TO PREDICT THE OCCURRENCE RATE AND INTENSITY OF TROPICAL CYCLONES INFLUENCING RICHARDS BAY, SOUTH AFRICA

The following example is an application of the use of the data described in Chapter 3 with the methods given in Chapter 4 to assess the tropical cyclone risk at Richards Bay, South Africa.

Richards Bay is located at approximately 28.8°S Latitude; 32.1°E Longitude. Since the construction of the port at Richards Bay two cyclones, Demoina and Imboa, have passed close to the port and caused severe waves, winds and rainfall. The impact of tropical cyclones was not taken into account in establishing the design parameters of this port. This port is of mayor economical importance to South Africa since the bulk of the coal exported from South Africa is exported from it.

5.1 EXTRACTION OF THE TROPICAL CYCLONE CHARACTERISTICS AT THE CLOSEST DISTANCE TO RICHARDS BAY

The 216 tropical cyclones that entered the study area were analysed and their characteristics at the closest distance to Richards Bay were extracted. The characteristics of the 10% of the tropical cyclones which came closest to Richards Bay are listed in Table 5.1. The full data set of all the tropical cyclones that entered the study area is given in Appendix C.

From Table 5.1, 3 tropical cyclones entered within a 400 km radius of the site between 1945 and 1997. The tropical cyclone that came closest to the site occurred in 1968. This tropical cyclone came within 268 km from Richards Bay. Unfortunately no intensity measurements are available for this cyclone (V_m=-999 knots). The tropical cyclone that came closest to Richards Bay for which intensity measurements are available was tropical cyclone Imboa that occurred in 1984 and had an intensity of 30 knots at its closest position.

Table 5.1: Characteristics of the 10% Closest Tropical Cyclones to Richards Bay

Cyclone No	Day	Month	Year	Hour	Lat. °S	Long °E	Distance km	V_m Knots	θ °	V_f m/s	α °N
105	12	1	68	0600	27.1	33.8	268	-999	45.0	6.7	212.5
97	6	1	66	1800	27.8	34.6	300	-999	68.2	7.9	168.7
175	29	1	84	1200	25.3	32.3	390	30	3.3	4.2	240.3
40	31	1	56	0600	29.7	36.1	456	-999	102.7	6.2	228.4
121	14	2	72	0600	25.3	35.2	520	-999	41.5	4.4	290.6
214	28	1	97	1200	26.3	36.1	525	50	58.0	1.2	243.4
199	25	2	91	0000	25.5	35.6	535	60	46.7	1.2	153.4
141	26	2	75	0600	29.2	37.0	547	-999	94.7	4.6	180.0
83	18	12	64	1800	25.7	36.0	555	-999	51.5	69.0	263.6
76	14	2	62	0600	23.9	34.0	585	-999	21.2	6.2	128.4
37	20	1	53	1200	28.4	37.8	636	-999	86.0	6.8	188.7
184	20	3	86	0000	27.7	38.0	668	25	79.4	2.8	201.8
122	21	2	72	1800	24.1	36.0	680	-999	39.7	1.6	198.4
120	20	3	71	0600	25.1	37.1	692	-999	53.5	1.9	146.3
177	15	2	84	0600	26.4	38.0	709	35	67.9	2.1	256.0
189	31	1	88	0600	27.5	38.4	716	110	78.3	6.3	170.5
57	17	1	57	0600	26.7	38.2	718	-999	71.0	4.2	172.9
145	27	1	76	1800	22.8	35.0	742	-999	25.8	6.3	235.0
106	23	1	68	0000	23.4	36.1	748	-999	36.5	2.8	291.8
178	15	2	84	0000	26.3	38.4	754	40	68.4	2.3	243.4
152	23	12	78	0600	22.9	35.4	758	-999	30.0	4.2	209.7

5.2 DISTRIBUTION OF THE OCCURRENCE RATE OF TROPICAL CYCLONES IN THE STUDY AREA

During the study period 216 tropical cyclones occurred in 53 years, thus the mean occurrence rate is 4.075 tropical cyclones per year. This is converted to the mean monthly occurrence rate of 4.075/12 =0.340 tropical cyclones per month, ignoring the seasonal distribution of the occurrences.

It is assumed that these occurrences follow a Poisson distribution which is applied to simulate the annual number of occurrences per year.

5.3 DISTRIBUTION OF THE CLOSEST DISTANCE OF ALL TROPICAL CYCLONES TO RICHARDS BAY

The closest distance (d) for each of the tropical cyclones is ranked in ascending order and a plotting position is assigned according to their rank. This plotting position is given by:

$$p = \frac{n}{(N+1)} = \frac{n}{217}$$

where: n = the rank of the distance
N = the total number of tropical cyclones in the data set (216)

A linear regression analysis is performed between ln(-ln(p)) and the lowest 10% of d values to obtain the distribution of the closest distance of tropical cyclones to the site. This distribution has a probability mass function:

$$d = \alpha_I + \beta_I \cdot \ln(-\ln(p))$$

where: d - Closest distance to the site in kilometres
α_I - Constant
β_I - Constant
p - The probability of non-exceedance

The fit of the closest distance is presented in Figure 5.1. The coefficients α_I and β_I are 1310.8 and –626.7 respectively. The data fitted the distribution with a correlation coefficient of 99.1%.

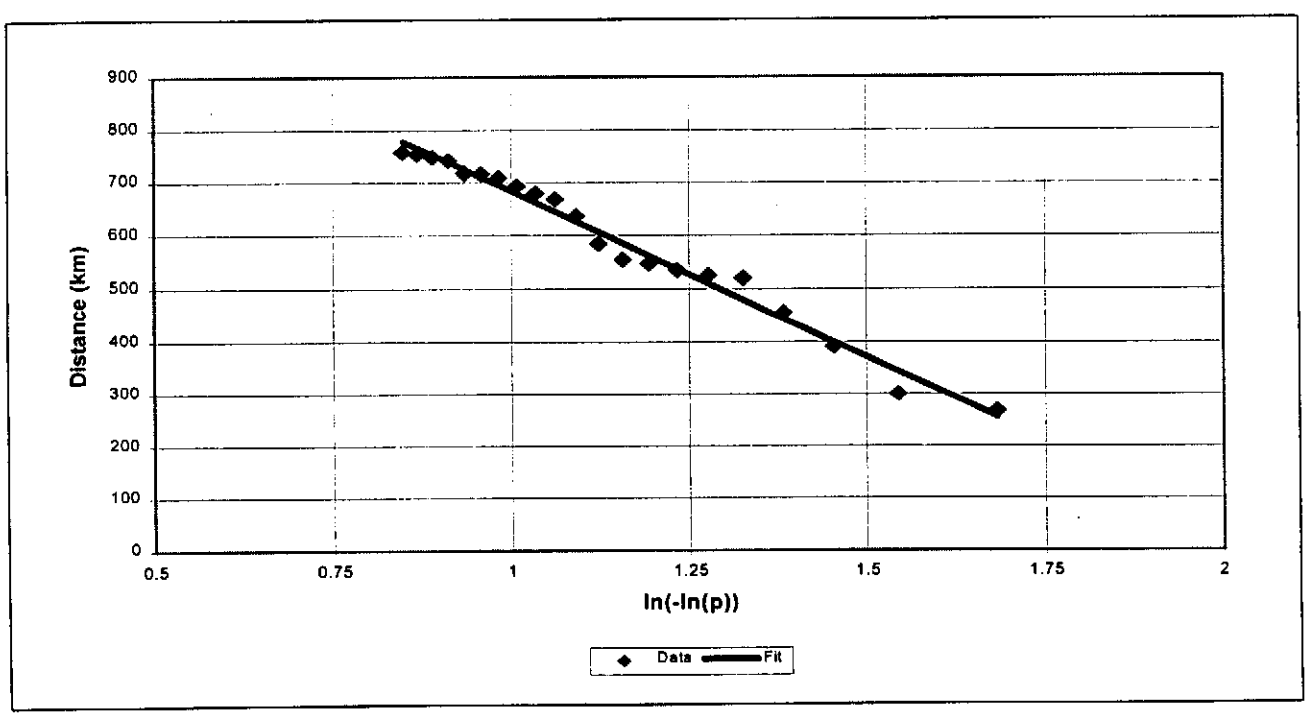

Figure 5.1: Fit of the Closest Distance of Tropical Cyclones to Richards Bay

5.4 DISTRIBUTION OF THE ANGLE BETWEEN THE TROPICAL CYCLONE AT ITS CLOSEST DISTANCE TO THE SITE RELATIVE TO TRUE NORTH

The angles that all the tropical cyclones have at their closest distance to the site are presented in Table 5.1. It is assumed that these angles are Normal distributed with an average of 51.5° and a standard deviation of 19.1°. This means that the tropical cyclones influencing Richards Bay occur on average to the Northeast of the site. The fit of the normal distribution to the data is presented in Figure 5.2.

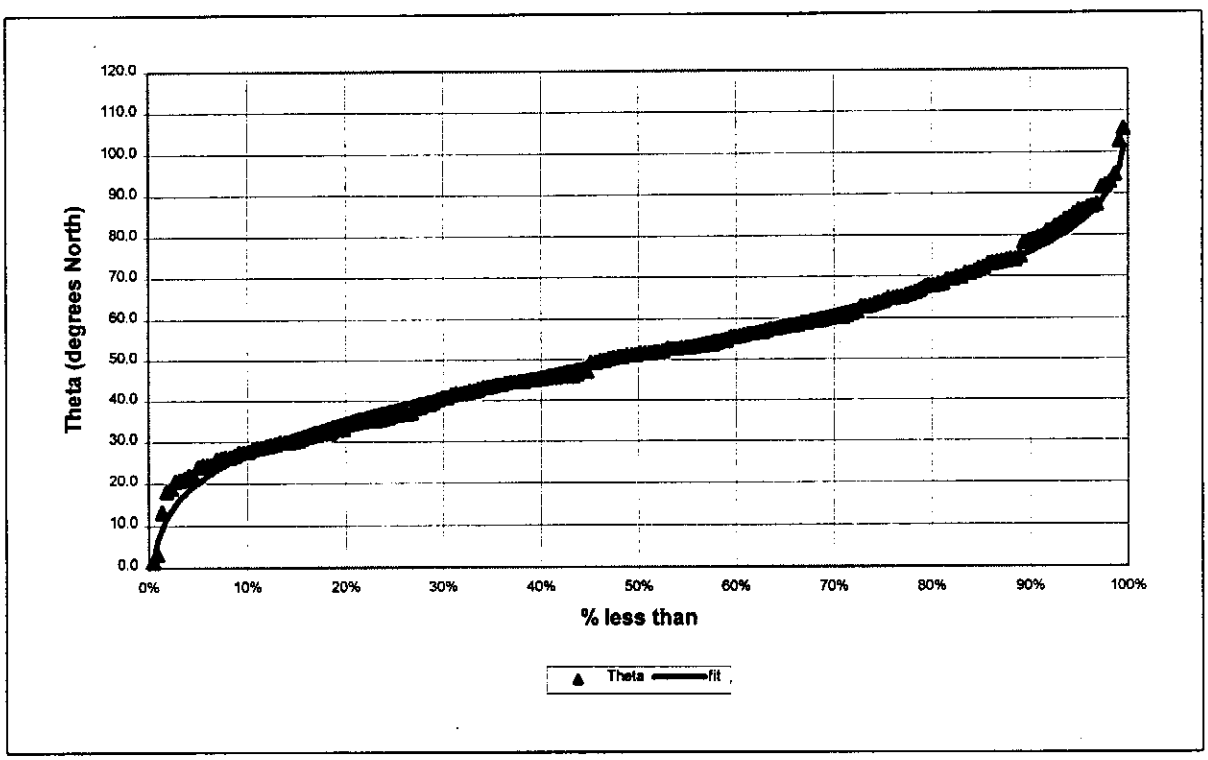

Figure 5.2: Fit of the Angle of the Tropical Cyclone at its Closest Distance with the Site Relative to True North

5.5 DISTRIBUTION OF THE TRANSLATIONAL SPEED OF THE TROPICAL CYCLONE AT ITS CLOSEST DISTANCE TO THE SITE

208 of the 216 tropical cyclones entering the study area remained in the area for six hours or more. The translational speeds (V_t) of these 208 tropical cyclones are ranked and a plotting position assigned according to:

$$p = \frac{n}{(N+1)} = \frac{n}{209}$$

where: n = the rank of the translational velocity
N = the total number of tropical cyclones in the data set (208)

Three of the translational speeds exceeded 20 m/s. These excessively high translational speeds are considered unrealistic and are discarded from the data. Therefore a linear regression analysis was performed between ln(-ln(p) and V_f for all the data where V_f<20 m/s. The probability mass function of the fitted distribution is:

$$V_f = \alpha_l + \beta_l \cdot \ln(-\ln(p))$$

where: V_f - Translational speed of the tropical cyclone in m/s
α_l - Constant
β_l - Constant
p - The probability of non-exceedance

The linear regression yields α_l and β_l as 3.322and –1.929 respectively. The data fit this distribution with a correlation coefficient of 99.2%. The distribution and fit to the data is presented in Figure 5.3.

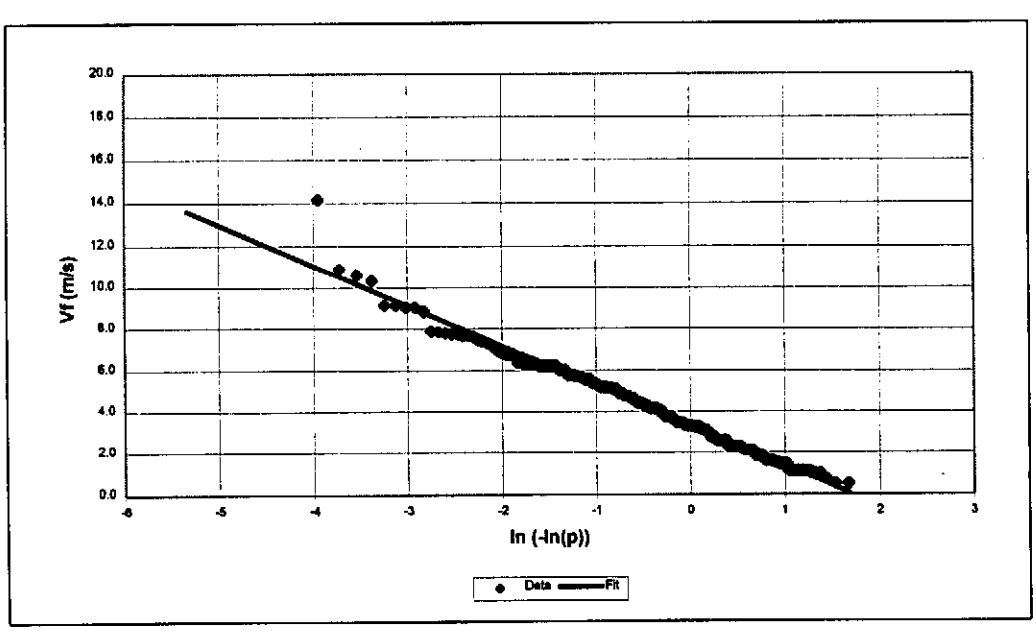

Figure 5.3: Distribution of the Translational Velocities of Tropical Cyclones at its Closest Distance to Richards Bay

5.6 DISTRIBUTION OF THE DIRECTIONS OF TRAVEL OF TROPICAL CYCLONES AT THEIR CLOSEST DISTANCES TO RICHARDS BAY

The directions of travel (α) for all 216 tropical cyclones are calculated at their closest distances to Richards Bay. 208 of the 216 tropical cyclones remained in the study area for more than 6 hours. The average direction of travel for the six hours preceding the closest distance of the tropical cyclone to Richards Bay are extracted, sorted in ascending order and ranked. The plotting position for each angle is presented by:

$$p = \frac{n}{(N+1)} = \frac{n}{209}$$

where: n = the rank of the direction of travel
N = the total number of tropical cyclones in the data set (208)

The data is fitted according to the Beta distribution with limiting values of 0 and 360 degrees. The fit of the data to the Beta distribution yields α_B and β_B parameters of 5.009 and 4.040 respectively. The fit of the data to the distribution is indicated in Figure 5.4.

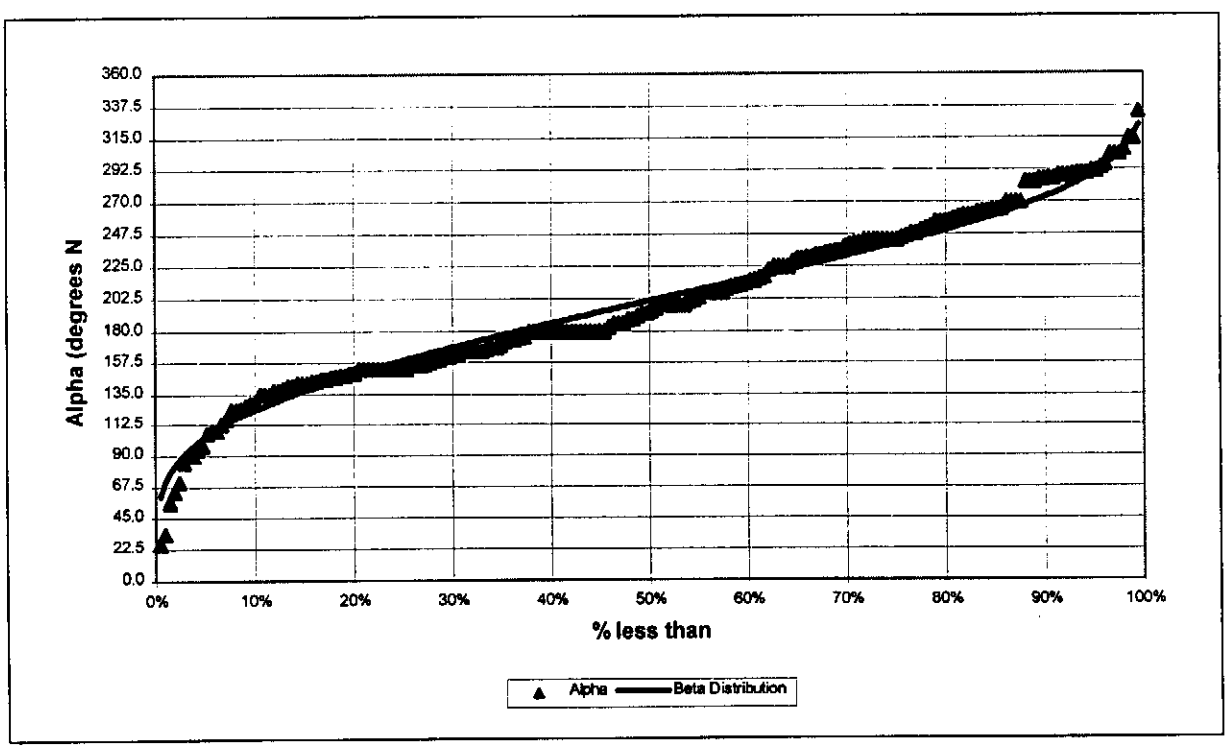

Figure 5.4: Distribution of the Direction of Travel of Tropical Cyclones at its Closest Distance to Richards Bay

5.7 DISTRIBUTION OF INTENSITY OF TROPICAL CYCLONES AFFECTING RICHARDS BAY

All the available intensity measurements (V_m) of the tropical cyclones entering the study area are used to establish the distribution of intensity of tropical cyclones. These intensities are binned in 2.5° Latitude bins and a Lognormal fit is applied to the data. The nearest 2.5° Latitude bin to Richards Bay is 30° S. In this latitude bin, 27 intensity records are available. The maximum intensity included is 105 knots with an average of 56.3 knots and standard deviation of 20.7 knots. The average of ln (V_m) and the standard deviation of ln (V_m) is calculated and used as the parameters of the Lognormal distribution. For the 30°S latitude the average of ln(V_m) is 3.97 with a standard deviation of 0.37. The fit of the available data is shown in Figure 5.5.

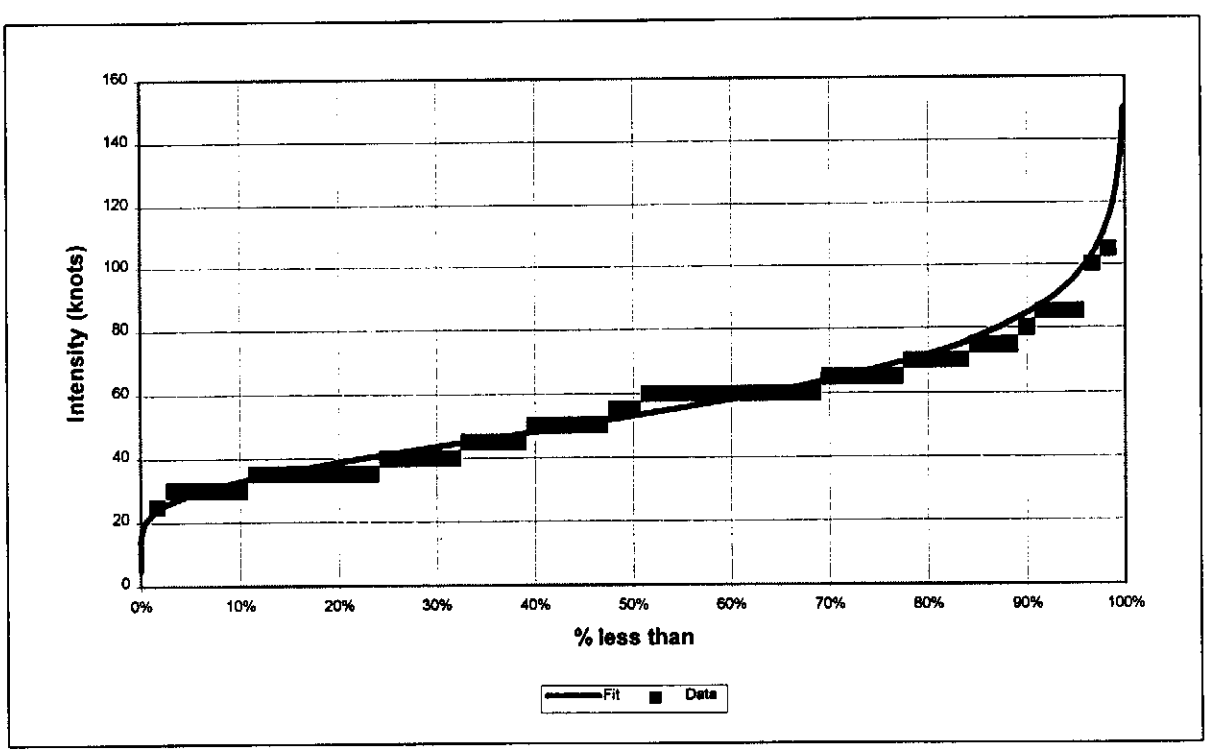

Figure 5.5: Distribution of Tropical Cyclone Intensity at 30°S Applied to Tropical Cyclones Influencing Richards Bay

Table 5.2: Distributions fitted to Tropical Cyclone Characteristics for Richards Bay

Parameter	Distribution	Statistical Parameters	
Occurrence Rate	Poisson	λ Inter Arrival Time	4.075 per Year 0.340 months
Closest Distance	Extreme I	α_I β_I	1310.837 -626.687
Angle at Closest Distance (θ)	Normal	Average Standard Deviation	51.452 19.112
Forward Velocity (V_f)	Extreme I	α_I β_I	3.322 -1.929
Approach Angle (α)	Beta	α_B β_B a b	5.009 4.040 0 360
Intensity (V_m)	Log Normal	Average Ln(V_m) Standard Deviation Ln (V_m)	3.966 0.366

5.8 RESULTS OF THE MONTE CARLO SIMULATION

The Monte Carlo simulation described in Section 4.3 was run to simulate 1000 x 100 years of data. The distributions fitted in Sections 5.1 to 5.7 and summarised in Table 5.2 were used to simulate the various parameters. The results of the simulation are indicated in Table 5.3.

Table 5.3: Results of the Monte Carlo Simulation for Richards Bay

Average Number of Tropical Cyclones in 100 Years	5.6
Maximum Number of Tropical Cyclones in 1000x 100 year simulations	14
Average Intensity of Tropical Cyclones for 1000x 100 year simulations	56.12 knots
Average Maximum Intensity in 100 Years	82.9 knots
Absolute Maximum Intensity in 1000x 100 Year Simulations	174 knots

The method described in Chapter 4 and illustrated by the example given in this Chapter is applied to the Southern African East Coast. The input parameters and results are presented in the following Chapter.

6. TROPICAL CYCLONE DISTRIBUTION MAP FOR THE SOUTHERN AFRICAN EAST COAST

The assessment of the probability of occurrence and intensity of tropical cyclones is done for 2.5° latitude intervals from 2.5° S to 32.5° S for all locations along the coast. The methods outlined in Chapter 4 and explained with the example in Chapter 5, were applied to all coastal locations. This chapter provides information on the statistical distribution parameters that fitted the existing data at 2.5° latitude intervals. It also provides the results for the simulations of these locations. These results are summarised in a tropical cyclone occurrence and intensity chart. The chapter concludes with a brief description of the tropical cyclone occurrence and intensity patterns based on the results of the analysis.

6.1 PARAMETERS OF THE STATISTICAL DISTRIBUTIONS FITTED TO SITES AT 2.5° LATITUDE INTERVALS BETWEEN 2.5°S AND 32.5°S.

The location of the East African coastline was determined at 2.5° latitude intervals. The closest distance to the particular location that each of the 216 tropical cyclones that entered the study area between 1945 and 1997, was calculated and the tropical cyclone parameters extracted. The distributions associated with each parameter as presented in Chapter 4 were fitted to this data. Table 6.1 contains the parameters describing the statistical distributions for each of the locations. The variation of the parameters with latitude is shown in Figures 6.1 to 6.5.

Table 6.1: Statistical Distributions fitted to locations at 2.5° Latitude Intervals

Parameter	Distribution		Latitude (°S)												
			2.5	5	7.5	10	12.5	15	17.5	20	22.5	25	27.5	30	32.5
Distance d (km)	Extreme I	α_I	1790.40	1519.80	1210.81	819.35	574.98	387.60	462.28	607.31	584.18	891.20	1179.08	1493.50	1840.19
		β_I	-843.47	-753.15	-638.58	-427.92	-320.22	-254.21	-295.65	-372.06	-381.31	-541.86	-614.28	-635.66	-633.77
Translational Speed V_t (m/s)	Extreme I	α_I	3.22	3.19	3.12	3.17	3.12	3.15	3.08	3.00	3.02	3.16	3.27	3.35	3.40
		β_I	-1.93	-1.95	-1.95	-1.92	-1.91	-1.80	-2.16	-1.79	-1.90	-1.87	-1.95	-1.94	-1.97
Angle with Site θ (deg)	Normal	Avg	162.24	155.96	151.56	145.71	141.58	132.56	109.94	87.36	71.90	61.25	56.12	50.90	49.93
		Std	14.83	17.77	23.42	29.69	42.83	57.21	49.42	38.18	39.17	26.56	28.99	17.07	14.40
Direction of Travel α (deg)	Beta	α_B	3.39	3.52	3.47	3.45	3.57	3.47	3.64	3.86	3.62	4.08	4.59	4.39	4.35
		β_B	2.26	2.36	2.34	2.40	2.53	2.58	2.75	2.88	2.81	3.22	3.66	3.56	3.55
Intensity V_m (knots)	Log Normal	Avg	3.11	3.53	3.60	3.66	3.80	3.65	3.64	3.66	3.62	3.76	3.91	3.97	3.67
		Std	0.20	0.40	0.47	0.46	0.48	0.44	0.50	0.46	0.53	0.41	0.30	0.37	0.44

These statistical distributions were used in the Monte Carlo simulation to simulate 1000 x 100-year periods for each site.

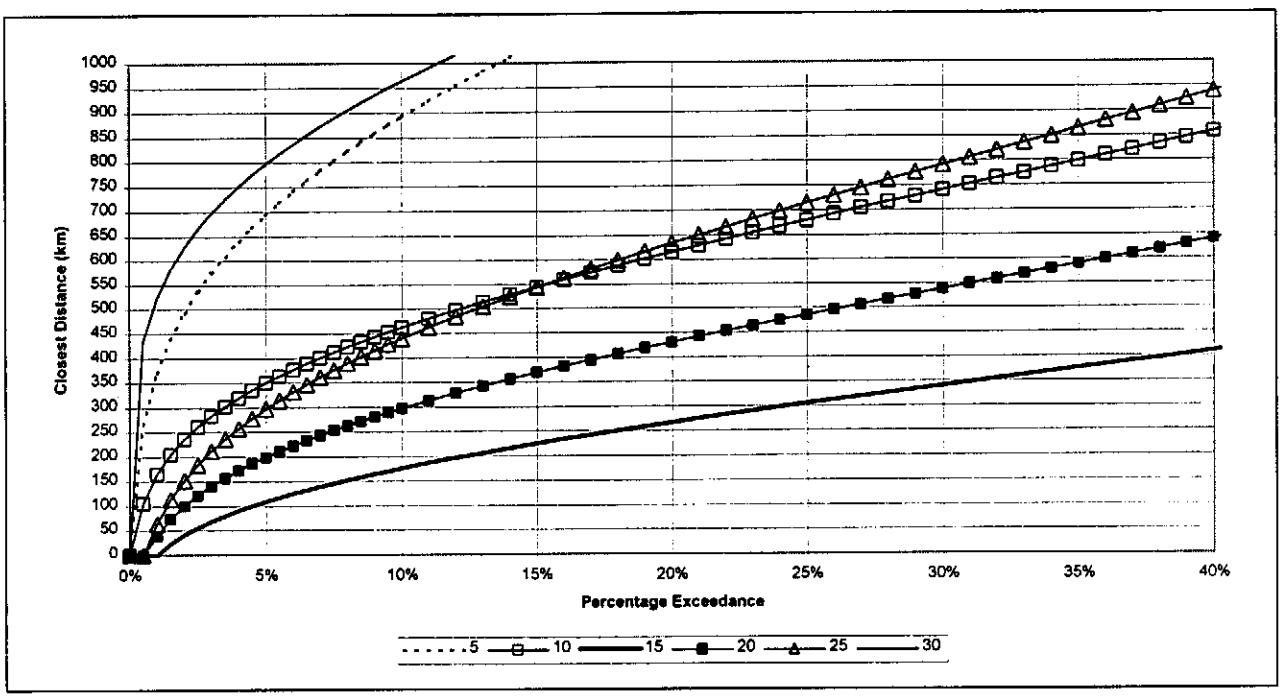

Figure 6.1: Variation of Closest Distance with Latitude (d)

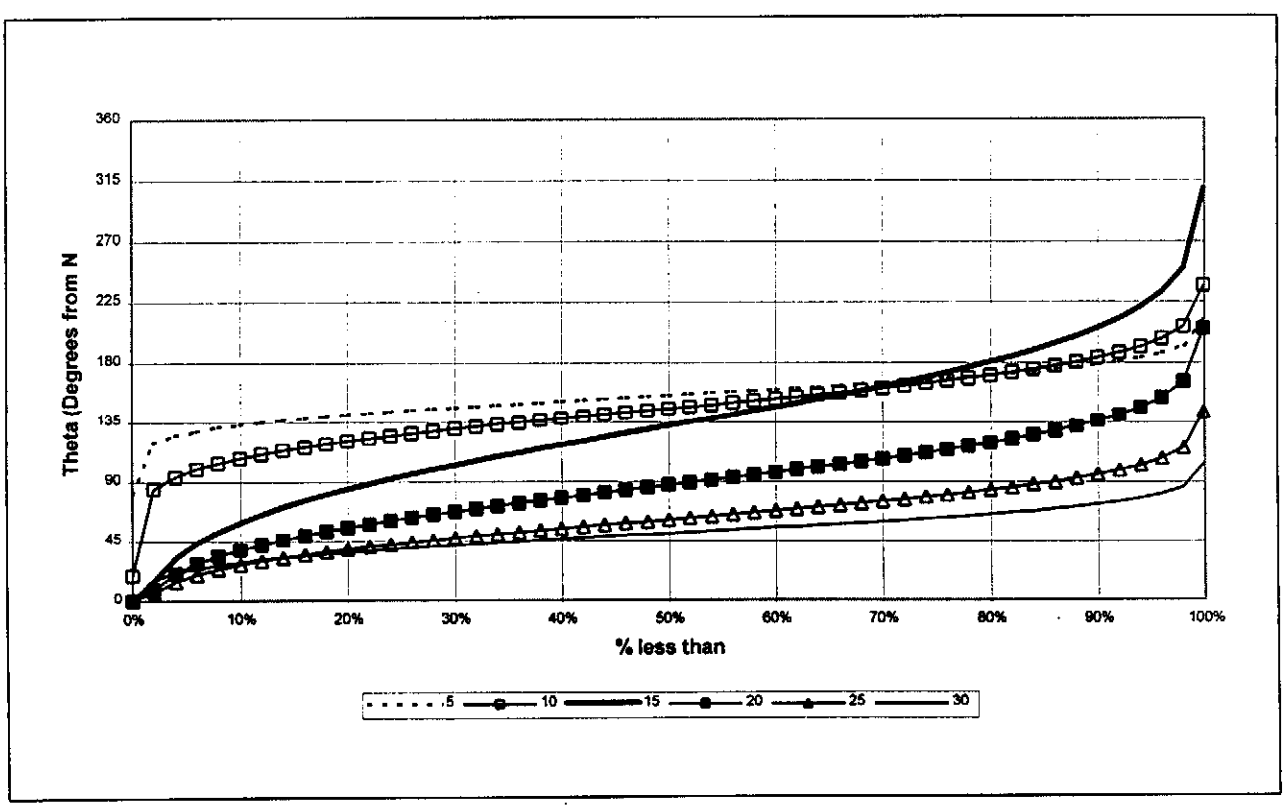

Figure 6.2: Variation of Angle with Site with Latitude (θ)

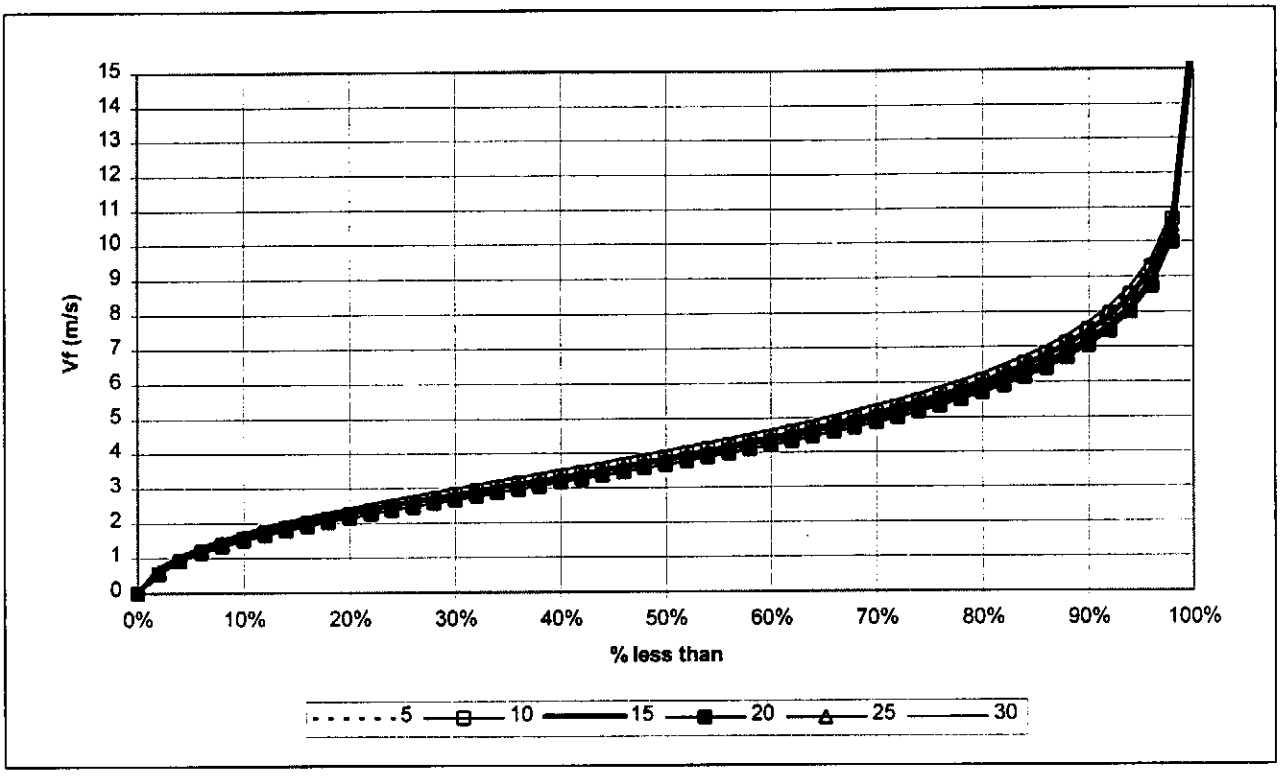

Figure 6.3: Variation of Tropical Cyclone Translational Speed with Latitude (V_f)

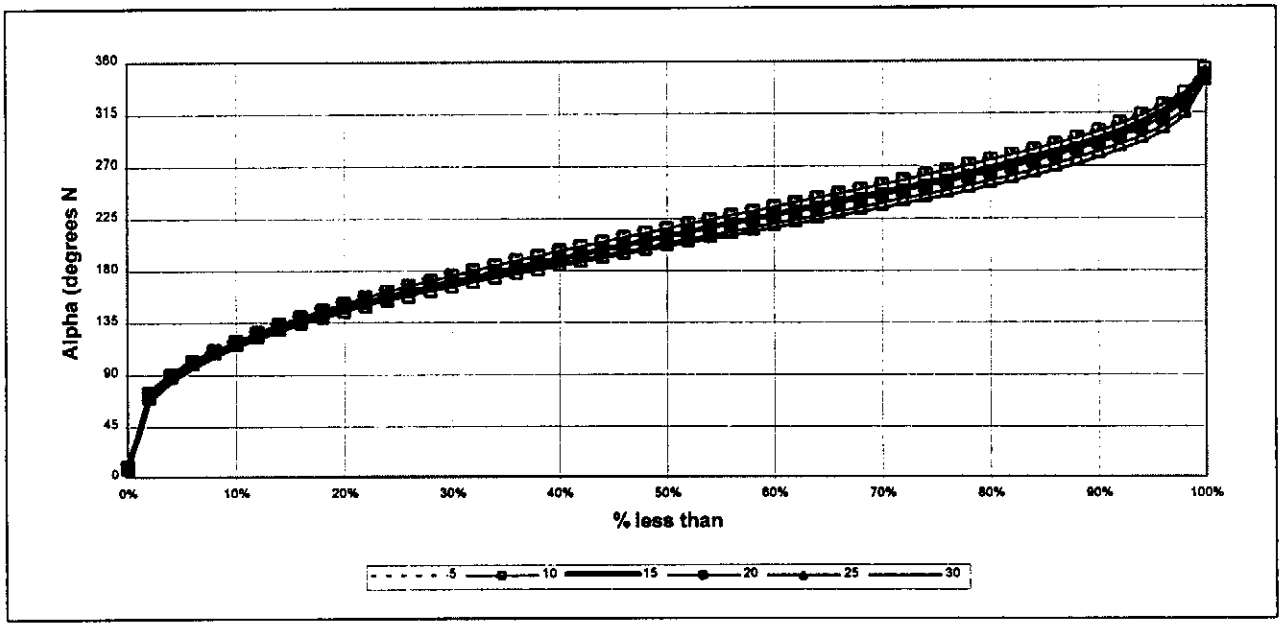

Figure 6.4: Variation of Approach Angle with Latitude (α)

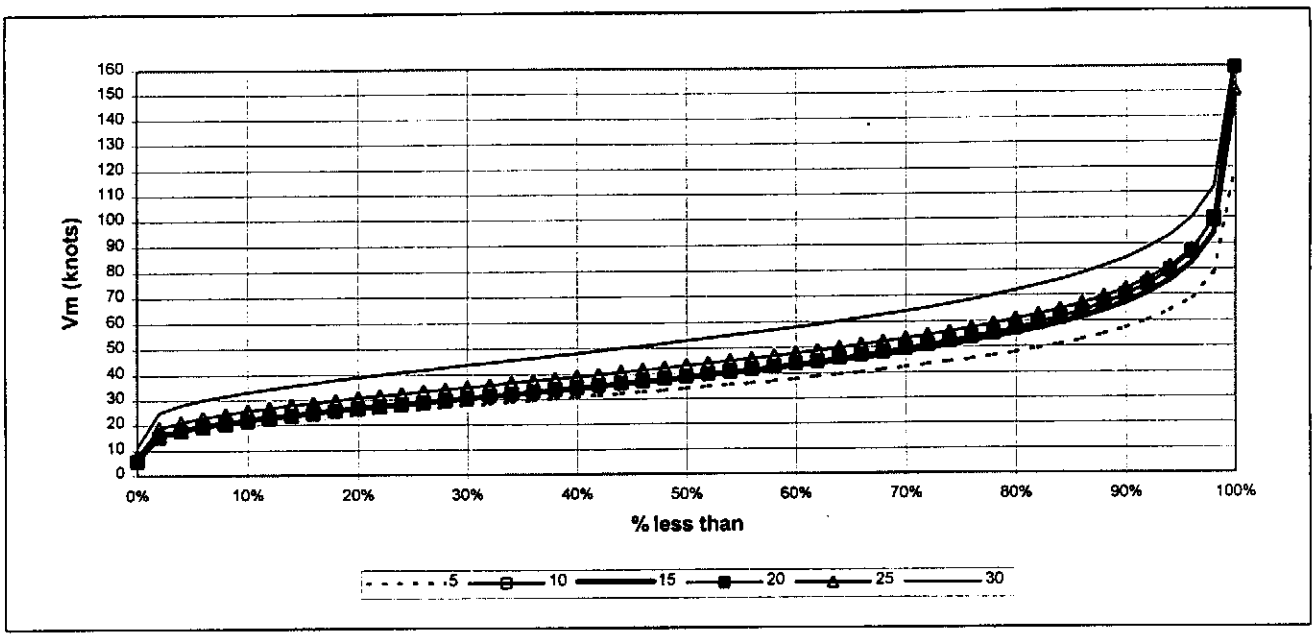

Figure 6.5: Variation of Intensity with Latitude (V_m)

6.2 DISCUSSION ON THE VARIATION OF THE STATISTICAL PARAMETERS WITH LATITUDE ON THE SOUTHERN AFRICAN EAST COAST

Table 6.1 and Figure 6.1 indicate that the risk of a tropical cyclone path intersecting the site is the highest at 15° S. There is a 38% probability that a tropical cyclone that enters the study region will pass within 400 km from the site. The risk of a tropical cyclone passing within 400 km of the site rapidly reduces to the North and the South of Latitude 15°S. The risk of a tropical cyclone passing within 400 km of the site reduces to 17.5% and 2.4% for latitudes 20°S and 10°S respectively.

The angle between the tropical cyclone and the site (α) varies with latitude. This is clearly illustrated in Figure 6.2. Angles of less than 90° indicate that the tropical cyclone is passing to the North of the site from the East. Angles between 90° and 180° indicates that the tropical cyclone is passing South of the site from the East while angles greater than 180° represent the tropical cyclones that approach the site from the African Continent. For latitudes North of 10°S more than 97% percent of the tropical cyclones pass to the South of the location. For latitude 15°S, 20% of the tropical cyclones pass to the North while 60% pass to the South. At latitude 20°S half of the tropical cyclones are located to the South and the other half located to the North of the site. As you move further Southward toward latitude 30°S, the percentage of tropical cyclones passing to the North of the site increases until almost all (98% at 30°S) of the tropical cyclones occur to the North of the site.

The forward velocity of tropical cyclones does not vary significantly with latitude as indicated on Figure 6.3. Figure 6.4 indicates that the translational angle of tropical cyclones does not vary significantly with latitude on the Southeast African Coastline.

Figure 6.5 indicates a slight variation in the intensity of tropical cyclones with latitude. The lowest intensities are noted for latitude 2.5°S. The breakdown of the Coriolis force near the equator provides a possible explanation for this reduction in intensity. The intensities of tropical cyclones between latitudes 10°S and 25°S seem fairly constant, while there is a sharp increase in intensity from latitude 25°S to 30°S. Madagascar protects the Southern African East Coast against tropical cyclones between latitudes 10°S and 25°S. Tropical cyclones reduce in intensity when passing over land because the heat source, warm tropical waters, is isolated from the system.

6.3 RESULTS OF THE ANALYSIS

The results of the Monte Carlo Simulation are summarised in Table 6.2. This table provides the average number of tropical cyclones expected during a 100 year period and the average maximum intensity that occurs within a 100 year period, averaged for the 1000 simulations. This information was used to construct the tropical cyclone occurrence and intensity map given in Figure 6.6.

Table 6.2: Results of the Monte Carlo Simulations done at 2.5° Latitude Intervals for the Southern African East Coast.

Latitude	Average No of Tropical Cyclones in 100 Years	Average Maximum Intensity in 100 years (knots)
2.5	2.2	25.4
5	4.9	54.4
7.5	11.4	80.7
10	28.4	99.6
12.5	72.5	146.2
15	157.2	124.4
17.5	118.5	143.5
20	70.9	117.8
22.5	80.2	136.3
25	34.3	102.6
27.5	11.5	80.6
30	1.5	65.4
32.5	0.0	-

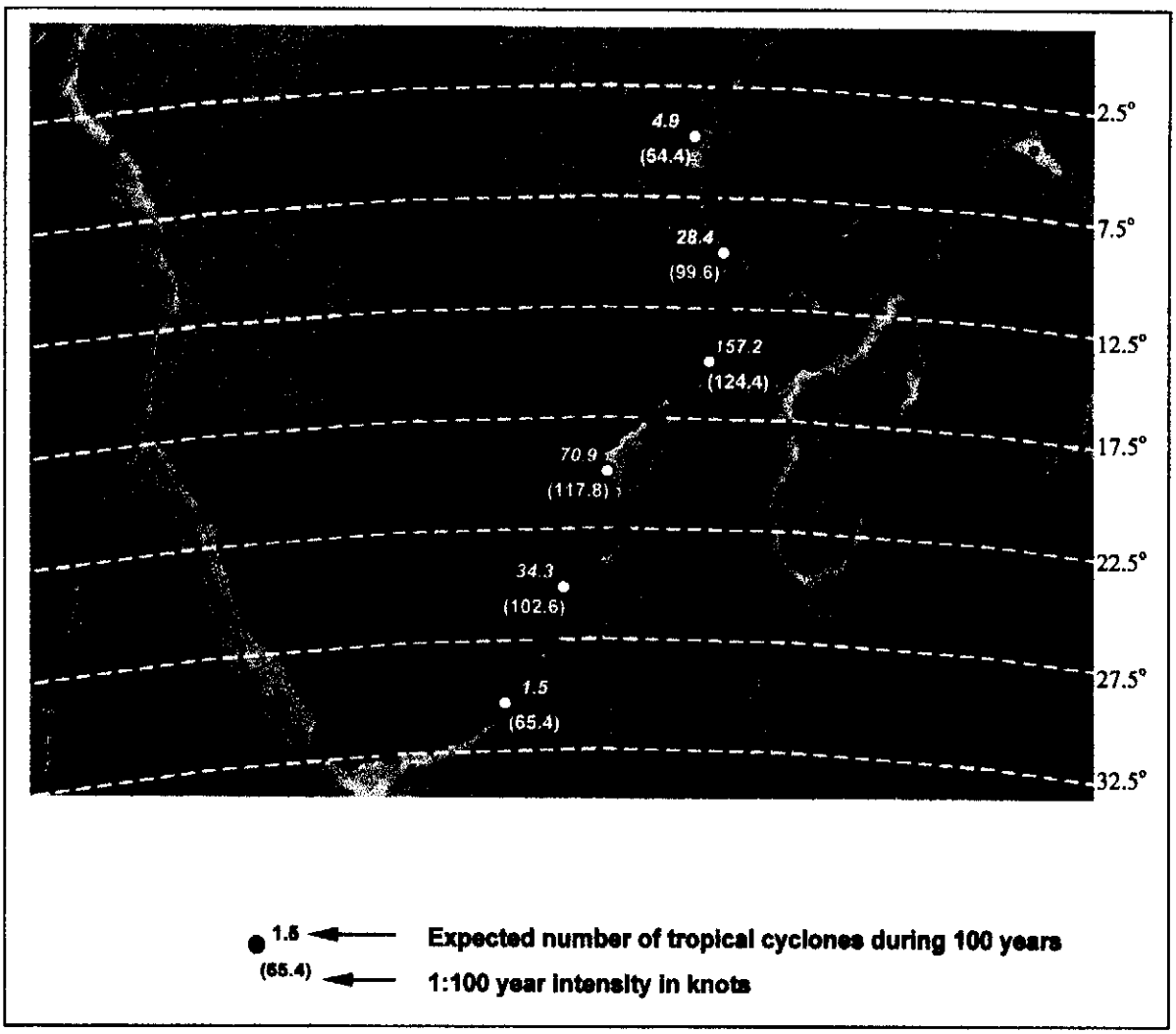

Figure 6.6: Tropical Cyclone Occurrence and Intensity Map for the Southern African East Coast

6.4 DISCUSSION OF THE RESULTS OF THE MONTE CARLO SIMULATION

Tropical Cyclones occur most frequently at 15°S Latitude with an average expected number of tropical cyclones in a 100-year period of 157.2. The expected average maximum intensity at this latitude is 124 knots. Tropical cyclones affect only regions North of 32.5°S with less than 1 tropical cyclone expected per 100 years for latitudes South of 30° S. If a structure is designed for a return period of 1:100 years, it is suggested that the design should include tropical cyclone effects for latitudes up to 32.5°S.

The maximum expected intensity of tropical cyclones in a 100-year period show a variation with latitude. The region within Latitudes 12.5°S to 25°S can expect a tropical cyclone with an intensity of at least 100 knots in a 100-year period. The maximum expected intensity of tropical cyclones in a 100-year period occurs at latitude 17.5°S with an intensity of 144 knots.

7. CONCLUSIONS

A tropical cyclone is a large low-pressure system that forms over tropical and sub-tropical oceans. The process of bringing the lower atmospheric layers into thermodynamic equilibrium with the warm tropical waters adds energy to the atmosphere and lowers the pressure. Organised convection patterns and cyclonic wind circulation around the low pressure develops and forms the tropical cyclone. The following climatic conditions are necessary before a tropical cyclone can develop:

- Warm ocean waters (at least 26.5°C) to a depth of at least 50 m.
- An atmosphere that cools rapidly with height and is potentially unstable to moist convection.
- Relatively moist layers near the troposphere to allow continuing development of thunderstorm activity.
- Minimum values of Coriolis force to maintain the low-pressure disturbance.
- A pre-existing surface disturbance with sufficient vorticity and convection.
- Low values of vertical wind shear between the surface and the upper troposphere.

Data on tropical cyclones are available from various sources. The data obtained from the Joint Typhoon Warning Centre have been used in the analysis. This data set contains information on the position and intensity of tropical cyclone tracks at six hourly intervals and spans a period between 1848 and 1999. The data recorded before 1945 only contain information on tropical cyclone tracks that influenced populated areas or ships. It was assumed that a number of tropical cyclones before 1945 were not recorded and therefore only data recorded after 1945 were used in the analysis. Intensity measurements are available for some tropical cyclone tracks from 1945. The detection of tropical cyclones and intensity measurements have vastly improved since the dawn of the satellite age in the mid 1980's.

Tropical cyclones occur frequently along the Southern African East Coast. The average number of tropical cyclone occurrences per year is 4.1 in a region bordered by Latitudes 4.2°S and 42.9°S and Longitude 17.7°E to 49°E. The maximum measured intensity is 130 knots for the period 1956 to 1997.

Monte Carlo simulation techniques can be used to extend the existing data set. A thousand repeat simulations of 100 year periods seem to lead to stable answers with respect to the number and average maximum intensity of tropical cyclones expected in a 100 years.

The simulations were done at 2.5° latitude intervals along the Southern African East Coast. The results indicate that tropical cyclones should occur at least once every hundred years at coastal locations with latitudes between 2.5°S and 32.5°S and should therefore be accounted for in the design conditions in these locations. The maximum occurrence rate is at 15°S with an expected number of tropical cyclones of 157.2 in a 100-year period. Tropical cyclones with intensities exceeding 100 knots can be expected between latitudes 12.5°S and 25°S at least once every 100 years.

8. FURTHER RESEARCH REQUIRED ON TROPICAL CYCLONES ALONG THE SOUTHERN AFRICAN EAST COAST

In this study the occurrence rate and expected intensity of tropical cyclones along the Southern African East Coast only, were studied. Appendix A provides empirical methods on using the results of the study to establish first order estimates of design waves, winds and water levels based on empirical relationships developed in other areas of the world. Little is known about the actual wind profiles for Southwest Indian tropical cyclones. Further data collection is required to establish the wind profiles for Southwest Indian Ocean tropical cyclones.

The data generated through the Monte Carlo simulation technique can be coupled with more sophisticated wind wave generation and storm surge models to establish proper design criteria for the Southern African East Coast. Little is known about the rainfall intensity resulting from tropical cyclones along the Southern African East Coast. The rainfall associated with tropical cyclones can lead to severe flooding (as was the case in South Africa with tropical cyclones Demoina and Imboa). Further investigations into the rainfall intensity patterns resulting from tropical cyclone activity will provide vital inputs in designing flood control structures in the areas affected by tropical cyclones.

The statistical distributions that were used to represent the measured data should be re-evaluated from time to time as more reliable data on tropical cyclones becomes available.

The collection of wave data in tropical cyclone affected areas is advised. Wave recordings that include waves generated by tropical cyclones are needed to fully understand the wave climate of the Southern African East Coast. This will lead to the establishment of design wave height curves that includes both waves generated by frontal systems passing the Southern tip of Africa as well as the wave generated by tropical cyclones.

9. ACKNOWLEDGEMENTS

During this study I received help from various people and institutions. I would in particular like to thank the following:

i) Professor A. Rooseboom for his valuable input into the definition of the scope of this thesis.

ii) Dr J. Rossouw for his aid as supervisor of the thesis as well as his assistance in obtaining data on tropical cyclones from Meteo France.

iii) Dr A.R. Wijnberg on his valuable comments on the structure and contents of the thesis.

iv) Ms A. Banchieri from the World Meteorological Organisation for the valuable publications provided.

v) Mr Frank Wells of the Joint Typhoon Warning Centre in providing technical input in terms of the quality and limitations of the JTWC data set.

vi) Ms H. Arendse for assisting in the final preparation of this document.

REFERENCES

Ang A.H.S et al (1975)	Probability Concepts in Engineering Planning and Design, Volume 1, New York, John Wiley & Sons, pp. 114-116, pp.120 – 121.
Ang A.H.S. et al (1975)	Probability Concepts in Engineering Planning and Design, Volume 2, New York, John Wiley & Sons, pp. 288.
Atkinson G.D. and Holiday C.R. (1977)	Tropical Cyclone Minimum Sea Level Pressure – Maximum Sustained Wind Relationship for the Western North Pacific, Monthly Weather Review 105, pp 421-427.
Batts M.E. et al (1980)	Hurricane Windspeeds in the United States, National Bureau of Standards Report No. BSS-124, U.S. Department of Commerce, Washington DC.
Cheng E.D.H. et al (1990)	Simulation Technique For Tropical Cyclone Occurrences, Journal of Wind Engineering and Industrial Aerodynamics, 1990 , Volume 36, pp. 393 – 401.
Chouniard L.E. et al (1997)	Model for Recurrence Rate in Gulf of Mexico, Journal of Waterway, Port, Coastal and Ocean Engineering, May/June 1997, pp. 113 - 119
Chouniard L.E. et al (1997)	Model for the Severity of Hurricanes in Gulf of Mexico, Journal of Waterway, Port, Coastal and Ocean Engineering, May/June 1997, pp. 120 – 129
Dey C.H. (1989)	The evolution of objective analysis methodology at the National Meteorological Centre, Weather and Forecasting, Volume 4, pp. 297-312.
Dillon C.P. et al (1998)	1997 Annual Tropical Cyclone Report, U.S. Naval Pacific Meteorology and Oceanography Centre West/ Joint Typhoon Warning Centre, pp. 70.
Grey W.M. (1975)	Tropical Cyclone Genesis, Department of Atmospheric Sciences, Paper No. 323, Colorado State University, pp. 121.
Hatada Y. et al (1996)	A Stochastic Typhoon Model and its Application to the Estimation of Extremes of Storm Surge and Wave Heights, Proceedings, Coastal Engineering 1996, pp. 1389 - 1401

Holland G.J. (1984)	On the climatology and structure of tropical cyclones in the Australian Southwest Pacific. Region II. Hurricanes, Australian Meteorology Magazine, Volume 32, pp. 17-31.
Holland G. J.(1993)	"Ready Reckoner" - Chapter 9, Global Guide to Tropical Cyclone Forecasting, WMO/TC-No. 560, Report No. TCP-31, World Meteorological Organization, Geneva.
International Atomic Energy Agency (1984)	Design Basis Tropical Cyclone for Nuclear Power Plants, Safety Series No. 50-SG-S11B, Vienna.
Landsea C. W. (1998)	Hurricanes, Typhoons and Tropical Cyclones, Frequently Asked Questions, Internet Web site, http://www.aoml.noaa.gov/hrd/tcfaq
McBride J. L. (1995)	Tropical Cyclone Formation, Global Perspectives on Tropical Cyclones, R.L. Elsberry (ed.). World Meteorological Organization, Report No. TCP-38, Geneva, 63 pp.
Neumann C. J. (1993)	"Global Overview" - Chapter 1, Global Guide to Tropical Cyclone Forecasting, WMO/TC-No. 560, Report No. TCP-31, World Meteorological Organization, Geneva, pp. 63 – 105.
Rossouw C. (1998)	Design Conditions Associated with the Occurrence of Tropical Cyclones, Watermeyer Prestedge Retief, (Unpublished).
Rossouw J. (1989)	Design Waves for the South African Coastline, PhD Thesis, University of Stellenbosch, pp 37.
Scheffner N. W. et al (1996)	Empirical Simulation Technique Based Storm Surge Frequency Analysis, Journal of Waterway, Port, Coastal and Ocean Engineering, March/April 1996, pp. 93 – 101.
Vickery P. J. et al (1995)	Prediction of Hurricane Wind Speeds in the United States, Journal of Structural Engineering, November 1995, pp. 1691 – 1699.
Willoughby H. E. (1988)	The dynamics of the tropical cyclone core, Australian Meteorological Magazine, Volume 36, pp. 183-199.
Willoughby H. E. (1995)	Mature structure and evolution. Global Perspectives on Tropical Cyclones, R.L. Elsberry (ed.). World Meteorological Organization, Report No. TCP-38, Geneva, pp. 21 – 62.

APPENDIX A

EMPIRICAL METHODS TO CALCULATE THE DESIGN WAVE HEIGHT, PERIOD AND WATER LEVEL ASSOCIATED WITH TROPICAL CYCLONES

TABLE OF CONTENTS

LIST OF FIGURES

1. INTRODUCTION

This Appendix contains a method for using the intensity values, that are obtained according to methods given in Chapter 4 of the thesis, and convert these answers to design wave height, period and water level for a site. It must be noted that these methods were developed for other tropical cyclone affected regions and should only be used as a first approximation. An in depth study into the assumed relationships needs to be carried out before using these methods for design. Very little is known about the wind profiles for Southwest Indian Ocean tropical cyclones. The wind speed profile is vital in calculating the wave height, wave period and storm surge level.

Section 2 provides a brief outline of the methodology used in obtaining the design cyclone. Section 3 gives an outline of the assumptions used to estimate the various parameters needed to establish the design parameters. Richards Bay is used as an example in Section 4 to further explain the methods presented in Section 3. Conclusions and recommendations are made in Section 5.

2. METHODOLOGY USED FOR OBTAINING DESIGN PARAMETERS

The methods outlined in Chapter 4 of the thesis are used to obtain the expected maximum intensity of tropical cyclones affecting the site in a 100 year period. This value is then used to calculate the other parameters needed to obtain the design wave height, wave period and storm surge.

The other parameters needed to establish the significant wave height (H_s) and period (T_p) are calculated using empirical relationships. These parameters are:

- Radius to maximum winds - R
- Central pressure - P_c
- Central pressure deficit - Δp
- Coriolis parameter - f

All the above parameters are related to the intensity of the tropical cyclone (V_m) and latitude.

The 1:100 year V_m with the latitude of the site is used to establish the 1:100 wave height and period. The wave height and period are calculated using the procedure described in the SHORE PROTECTION MANUAL (1984). The maximum H_s and T_p are used with no corrections for position, distance or angle of the cyclone at its nearest point to the site.

A first estimate of storm surge is obtained from Conner et al. (1957). They plotted observed storm surge level as a function of central pressure of the cyclone for the Gulf of Mexico. Various site-specific characteristics determine the storm surge level, therefore this only serves as a guideline. A more detailed study will be required to obtain an accurate estimate of the maximum storm surge.

3. ASSUMPTIONS

The predictions were based on the following general assumptions:

- All cyclones within a 400 km radius of the site will influence the site
- The site will experience the maximum winds generated by cyclones within a 400 km distance from the site
- The storm path of the cyclone with the 1:100 year maximum wind will correspond to the path resulting in the maximum wave height and storm surge level for the site.

3.1 CENTRAL PRESSURE - P_C

It is assumed that the relationship between P_c and V_m is given by the relationship presented by Atkinson and Holiday (1977):

$$V_m = a(\Delta p)^b$$

where:

$$\Delta p = (P_a - P_c)$$

P_a - Ambient far field atmospheric pressure (Taken as 1013 mb (Constant))

P_c - Central Pressure of the Tropical Cyclone (at sea level)

The data from Meteo France containing both V_m and P_c were used to establish the a and b constants, while P_a (Ambient far field atmospheric pressure) was taken as a constant 1013 mbar.

The constants were established by using linear regression between ln (V_m) and ln (Δp). The constants a and b were found to be 4.4548 and 0.6797 respectively with a correlation coefficient of 99.5%. A graph indicating the fit with the measured data is presented in Figure A1.

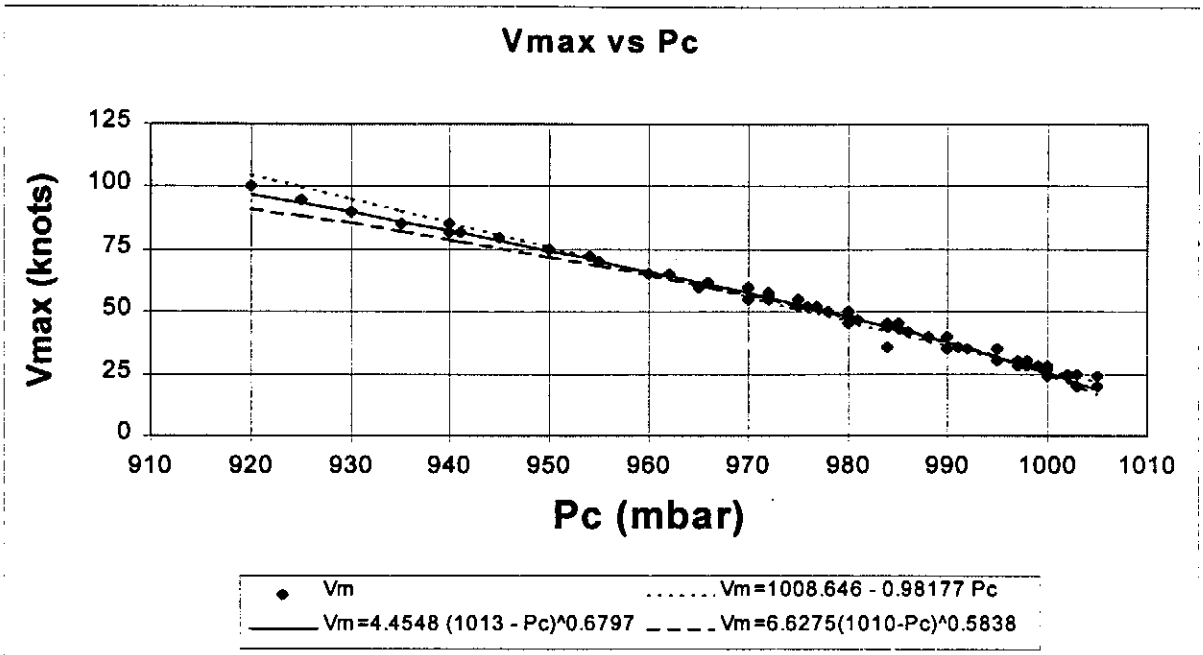

Figure A1

3.2 RADIUS TO MAXIMUM WINDS -R

No data with regards to the radius to maximum wind speed is available for the cyclones in the Southwestern Indian Ocean.

The Joint Typhoon Warning Centre suggested measuring the diameter of the eye of the cyclone from satellite observations to give an indication of the radius to maximum wind. The outer wall of the eye of the cyclone represents the region of maximum winds of the cyclone. The satellite images was not available at the time of this report, thus another approach was followed. This approach can be verified with the satellite images as soon as they become available.

Neumann (1987) used V_m and the latitude of the storm to establish R. He assumed that R has a normal distribution with a mean $\mu(V_m; Lat)$ and standard deviation $\sigma(V_m; Lat)$. Based on the available data for the Gulf of Mexico he found the mean and standard deviation presented by:

$$\mu(V_m; Lat) = 11.671 + 0.014487 \times Lat - 0.1660035(10^{-5})V_m^3$$
$$\sigma(V_m; Lat) = 4.02853 + 0.2822473 \times Lat - 0.03148963 \times V_m$$

These above equations were used to establish R.

3.3 CALCULATION OF H_S AND T_P

The maximum H_s and T_p associated with the tropical cyclone were estimated using the method described in Shore Protection Manual (1984). The significant wave height and period were calculated using the following equations:

$$H_s = 5.03e^{\frac{R\Delta p}{4700}}\left[1+\frac{0.29\alpha V_f}{\sqrt{U_R}}\right]$$

$$T_p = 8.6e^{\frac{R\Delta p}{9400}}\left[1+\frac{0.145\alpha V_f}{\sqrt{U_R}}\right]$$

Where:

$$U_R = 0.865\times V_m + 0.5\times V_f$$

α is a parameter used to correct for the forward motion of the cyclone. Due to a lack of data α is taken as 1.

These equations give an approximation of the maximum wave height and period within the wave field of the cyclone. It was assumed that the cyclone track crosses the site in a way to produce the maximum wave height and period at the site. No reductions in wave height were made from the calculated values.

3.4 STORM SURGE - S_M

The maximum storm surge at the site depends on the wind and wave field over the site as well as the local bathymetry. There are various mathematical models available to calculate the maximum expected storm surge resulting from a cyclone. These methods require accurate wind field data as input. The available knowledge on the wind fields of tropical cyclones in the Southwest Indian Ocean does not include wind speed profiles, therefore the use of more sophisticated models are not justified.

Conner et al (1957) presented a relationship between surge height and central pressure (P_c) for the Gulf of Mexico. This relationship reads:

$$S_{\max} = 0.0433(1023 - P_c)$$

It is assumed that this relationship will give an approximation of the conditions on the Southern African East Coast. The relationship must be validated with a more detailed study before proceeding with a detailed design.

4. RESULTS

4.1 MAXIMUM SUSTAINED 1 MINUTE AVERAGE WIND VELOCITY (V_M)

The simulation of 1000 x 100 year periods for Richards Bay provides an average maximum intensity of tropical cyclones of 82.9 knots (42.6 m/s). Details of this calculation and simulation are presented in Chapter 5 of the thesis.

4.2 PRESSURE ASSOCIATED WITH THE 1:100 YEAR WIND

Based on the relationship proposed by Atkinson and Holiday (1997) and the Meteo France data the relationship between pressure deficit and V_m is given by:

$$V_m = 4.4548(1013 - P_c)^{0.6797}$$

Where V_m is the average 1 minute mean wind speed in knots and P_c in millibars.

Using the above equation for the 1:100 year V_m of 82.9 knots; **P_c is calculated as 939 millibar** and the pressure deficit **(Δp) = 74 millibar**.

4.3 MAXIMUM FORWARD CELERITY OF THE CYCLONE - V_f

The average maximum forward celerity of the tropical cyclones generated in a 100 years is 7 m/s.

4.4 RADIUS TO MAXIMUM WINDS - R

It is assumed that the relationship between latitude and V_m presented by Neumann (1987) is valid. With the 1:100 year V_m and the latitude of 28.8° S the following results were obtained for R:

μ= 12.0 km

σ= 10.8 km

The values of H_s and T_p respond to the exponent of R/4700 and R/9600 respectively. Therefore the accuracy of estimate of R is not considered to be important if the accuracy of the other assumptions is considered. The mean value of R is used for further calculations.

4.5 ESTIMATION OF H_S AND T_P

Using the results presented in Sections 4.1 to 4.5 with the SHORE PROTECTION MANUAL (1984) procedure presented in Section 3.3, the following 1:100 year values for H_s and T_p are obtained:

H_s= 8.0 m
T_p= 11 s

4.6 STORM SURGE

Assuming the relationship between storm surge and central pressure as given by Conner et al. (1957) is valid a maximum 1:100 storm surge height is estimated at **3.63 m**.

This value is based on values fitted for the Gulf of Mexico. The characteristics of the site influence the amount of surge significantly. Therefore this value should be seen as indicative.

5. CONCLUSIONS AND RECOMMENDATIONS

The aim of the Appendix is to provide order of magnitude estimates of the design wave height, wave period and water level. Due to a lack of reliable data, several assumptions were made to establish the design parameters. These assumptions were based on published relationships. The 1:100 year wind velocity, wave height, wave period and water level as calculated for Richards Bay is presented in Table A1.

Table A1

Maximum Sustained 1 minute Average Wind Speed at 10 m. (V_m)	42.6 m/s
Minimum Pressure (P_c)	939 millibar
Significant Wave Height (H_s)	8.0 m
Peak Period (T_p)	11 s
Maximum Surge Height (S_m)	3.63 m

The values of P_c, H_s, T_p and S_m are based on empirical relationships developed for other cyclone areas in the world. These relationships have been transferred to the Western Indian Ocean. Due to the lack of data no attempt was made to validate these relationships for this region. Therefore the confidence in the values reported is fairly low. There are mathematical models available to predict the influence of tropical cyclones on a site based on the physical processes occurring inside the cyclone and therefore are more applicable than the methods used in this report.

The following recommendations are made in order to improve the results for detailed design conditions:

1. Combine these models with the Monte Carlo simulation to evaluate the influence of each generated tropical cyclone separately. The influence of the track direction and distance from the site can be taken into account for each tropical cyclone together with the actual intensity and forward velocity. The above method only uses the average maximum intensity and forward velocity in a 100 year period.
2. Confirm the distribution of radius to maximum winds with satellite images.
3. Base the wind profile and conditions at the site on a large scale mathematical model (CE wind model)
4. Calculate the H_s and T_p at the site using a large scale mathematical model (WAM model)
5. Use the wind and wave models with the local bathymetry of the site as an input to a mathematical surge model (SLUSH) to get accurate predictions of maximum water levels.

6. REFERENCES

Atkinson, G. D. and C. R. Holliday, (1977)	Tropical cyclone minimum sea level pressure – maximum sustained wind relationship for the western North Pacific. Mon. Wea. Rev.,105, 421-427
Neumann, C. J. (1987)	The national hurricane centre risk analysis program (HURISK), NOAA Tech. Memo. NWS NHC 38
Shore Protection Manual (1984)	4th Ed., 2 Vol, U.S. Army Engrs. Wtrwy. Experiment Station, U.S. Government Printing Office, Washington DC.
Conner, W. C. , Kraft, R. H. and Harris, D. L. (1957)	Empirical methods for forecasting the maximum storm tides due to hurricanes and other tropical storms. Monthly Weather Rev. , 85, 113-116

APPENDIX B

EXAMPLE OF A DATA FILE OBTAINED FROM THE JOINT TYPHOON WARNING CENTRE

FILE NAME: **BSH0184**

```
0183071106  48S 887E  25
0183071112  53S 880E  30
0183071118  58S 872E  30
0183071200  63S 865E  30
0183071206  67S 857E  30
0183071212  73S 849E  35
0183071218  78S 842E  35
0183071300  81S 837E  35
0183071306  83S 832E  35
0183071312  85S 827E  35
0183071318  87S 822E  35
0183071400  88S 816E  35
0183071406  90S 809E  30
0183071412  96S 803E  30
0183071418 104S 797E  30
0183071500 112S 800E  30
0183071506 121S 812E  25
```

APPENDIX C

LIST OF ALL THE TROPICAL CYCLONES THAT ENTERED THE STUDY AREA BETWEEN 1945 AND 1997

File Name	Start Date	End Date	Maximum Intensity
BSH0245	15/1/45	18/1/45	-999
BSH0345	12/12/45	15/12/45	-999
BSH0645	02/05/45	02/07/45	-999
BSH0745	14/2/45	18/2/45	-999
BSH0146	29/11/46	30/11/46	-999
BSH0246	12/10/46	12/12/46	-999
BSH0546	28/12/46	30/12/46	-999
BSH1246	02/10/46	16/2/46	-999
BSH1547	02/05/47	02/08/47	-999
BSH1947	03/05/47	03/09/47	-999
BSH0448	22/12/48	26/12/48	-999
BSH1348	02/12/48	14/2/48	-999
BSH1848	16/3/48	19/3/48	-999
BSH0749	01/05/49	01/09/49	-999
BSH1649	19/2/49	28/2/49	-999
BSH1849	03/07/49	03/09/49	-999
BSH2249	31/3/49	04/03/49	-999
BSH2549	06/05/49	06/05/49	-999
BSH0650	21/12/50	25/12/50	-999
BSH0950	30/1/50	31/1/50	-999
BSH1050	02/05/50	02/07/50	-999
BSH1150	13/2/50	15/2/50	-999
BSH0151	25/11/51	30/11/51	-999

BSH0851	28/1/51	02/02/51	-999
BSH1051	13/1/51	27/1/51	-999
BSH1251	31/1/51	02/02/51	-999
BSH2051	20/2/51	03/02/51	-999
BSH0352	20/12/52	21/12/52	-999
BSH0452	01/03/52	01/08/52	-999
BSH0652	01/11/52	22/1/52	-999
BSH1852	03/12/52	24/3/52	-999
BSH2052	18/3/52	20/3/52	-999
BSH2352	14/4/52	16/4/52	-999
BSH2452	24/5/52	28/5/52	-999
BSH0153	30/12/53	31/12/53	-999
BSH0553	01/10/53	16/1/53	-999
BSH0753	14/1/53	21/1/53	-999
BSH1153	02/09/53	02/10/53	-999
BSH1253	18/2/53	22/2/53	-999
BSH0154	01/01/54	01/01/54	-999
BSH0254	20/10/54	20/10/54	-999
BSH0554	17/1/54	23/1/54	-999
BSH0954	03/02/54	03/05/54	-999
BSH1054	27/2/54	03/04/54	-999
BSH1354	30/3/54	31/3/54	-999
BSH2355	24/3/55	28/3/55	-999
BSH0856	01/07/56	01/10/56	-999
BSH1256	26/1/56	31/1/56	-999
BSH1856	02/05/56	02/08/56	-999
BSH2056	02/10/56	13/2/56	-999
BSH2356	26/2/56	28/2/56	-999
BSH2756	21/3/56	23/3/56	-999
BSH2956	04/01/56	04/04/56	-999

BSH3256	04/01/56	04/04/56	-999
BSH0357	13/12/57	16/12/57	-999
BSH0457	26/12/57	31/12/57	-999
BSH1257	13/1/57	17/1/57	-999
BSH1957	02/03/57	02/05/57	-999
BSH2757	13/3/57	14/3/57	-999
BSH0558	18/12/58	21/12/58	-999
BSH1158	23/1/58	29/1/58	-999
BSH1758	23/2/58	28/2/58	-999
BSH1958	03/06/58	03/07/58	-999
BSH0159	11/02/59	11/03/59	-999
BSH0359	12/06/59	12/10/59	-999
BSH1059	01/12/59	15/1/59	-999
BSH1359	24/1/59	26/1/59	-999
BSH2159	14/2/59	15/2/59	-999
BSH2659	18/3/59	24/3/59	-999
BSH2859	26/3/59	29/3/59	-999
BSH1160	28/1/60	31/1/60	-999
BSH2060	21/3/60	23/3/60	-999
BSH0261	19/12/61	24/12/61	-999
BSH1061	01/01/61	01/06/61	-999
BSH0762	18/1/62	23/1/62	-999
BSH1262	02/09/62	16/2/62	-999
BSH2062	22/2/62	22/2/62	-999
BSH2462	03/12/62	15/3/62	-999
BSH1463	17/1/63	17/1/63	15
BSH1563	17/1/63	19/1/63	-999
BSH2963	14/2/63	19/2/63	-999
BSH3463	27/2/63	03/02/63	-999
BSH0864	01/10/64	21/12/64	-999

BSH1264	23/12/64	25/12/64	-999
BSH1464	02/09/64	02/09/64	-999
BSH1764	24/2/64	24/2/64	-999
BSH1864	03/01/64	03/04/64	-999
BSH2264	03/07/64	15/3/64	-999
BSH0665	27/12/65	31/12/65	-999
BSH1565	01/06/65	01/08/65	-999
BSH1865	15/1/65	16/1/65	-999
BSH1965	21/1/65	26/1/65	-999
BSH2265	02/09/65	02/09/65	-999
BSH2865	20/2/65	26/2/65	-999
BSH0166	10/05/66	10/06/66	-999
BSH0566	14/12/66	16/12/66	-999
BSH0666	01/01/66	01/09/66	-999
BSH0866	22/12/66	26/12/66	-999
BSH1066	28/12/66	30/12/66	-999
BSH2466	14/2/66	17/2/66	-999
BSH2566	20/2/66	23/2/66	-999
BSH3666	27/4/66	05/01/66	-999
BSH0967	30/12/67	31/12/67	-999
BSH0968	01/01/68	01/02/68	-999
BSH1068	01/08/68	14/1/68	-999
BSH1168	15/1/68	30/1/68	-999
BSH0269	13/10/69	14/10/69	-999
BSH0469	18/11/69	20/11/69	-999
BSH0869	01/03/69	01/03/69	-999
BSH1769	02/03/69	02/09/69	-999
BSH2269	13/2/69	19/2/69	-999
BSH0170	10/08/70	10/09/70	-999
BSH0870	01/07/70	01/10/70	-999

BSH1170	15/1/70	19/1/70	-999
BSH1470	22/2/70	26/2/70	-999
BSH2470	19/3/70	19/3/70	-999
BSH0771	17/12/71	23/12/71	-999
BSH0971	20/1/71	02/05/71	-999
BSH1971	15/2/71	22/2/71	-999
BSH2571	15/3/71	24/3/71	-999
BSH1472	02/02/72	14/2/72	-999
BSH1772	14/2/72	21/2/72	-999
BSH2372	03/06/72	03/11/72	-999
BSH0373	22/9/73	23/9/73	-999
BSH0473	26/10/73	28/10/73	-999
BSH0873	01/04/73	01/08/73	-999
BSH1073	01/11/73	13/1/73	-999
BSH1373	31/12/73	31/12/73	-999
BSH1473	19/1/73	21/1/73	-999
BSH1673	28/1/73	02/01/73	-999
BSH2173	15/2/73	19/2/73	-999
BSH0874	23/12/74	23/12/74	-999
BSH1374	01/01/74	01/02/74	-999
BSH1874	20/1/74	20/1/74	-999
BSH3374	19/4/74	23/4/74	-999
BSH0675	12/12/75	14/12/75	-999
BSH0975	01/07/75	01/11/75	-999
BSH1075	14/1/75	20/1/75	-999
BSH1475	24/1/75	28/1/75	-999
BSH1975	31/1/75	02/02/75	-999
BSH2275	22/2/75	26/2/75	-999
BSH2475	03/11/75	03/11/75	-999
BSH0176	13/10/76	15/10/76	-999

BSH0876	01/10/76	15/1/76	-999
BSH0976	22/1/76	27/1/76	-999
BSH2176	03/10/76	03/12/76	-999
BSH2276	26/3/76	26/3/76	-999
BSH2376	29/3/76	04/10/76	-999
BSH0977	17/1/77	23/1/77	-999
BSH1077	02/01/77	02/10/77	-999
BSH1777	22/2/77	03/02/77	-999
BSH0278	13/12/78	28/12/78	-999
BSH1578	27/1/78	02/01/78	-999
BSH1878	02/10/78	14/2/78	-999
BSH2478	03/08/78	03/09/78	-999
BSH1279	02/04/79	14/2/79	-999
BSH1479	17/2/79	18/2/79	-999
BSH1579	17/2/79	18/2/79	-999
BSH0280	29/11/80	12/01/80	-999
BSH0380	12/09/80	12/09/80	-999
BSH0780	28/12/80	31/12/80	-999
BSH0880	20/1/80	21/1/80	55
BSH1880	03/08/80	13/3/80	50
BSH0581	19/12/81	24/12/81	-999
BSH1381	02/02/81	02/04/81	35
BSH1781	17/2/81	22/2/81	35
BSH2281	03/01/81	03/03/81	10
BSH2681	04/03/81	04/04/81	35
BSH1682	02/03/82	02/06/82	30
BSH2082	22/2/82	25/2/82	25
BSH2482	18/3/82	25/3/82	60
BSH0783	12/10/83	16/12/83	130
BSH0883	01/10/83	16/1/83	25

BSH0184	16/11/84	17/11/84	25
BSH1484	21/1/84	29/1/84	35
BSH2084	19/2/84	20/2/84	45
BSH2284	02/12/84	15/2/84	30
BSH2384	02/12/84	15/2/84	30
BSH3284	04/09/84	04/12/84	95
BSH1985	02/10/85	02/11/85	40
BSH2385	13/2/85	19/2/85	25
BSH0486	01/06/86	01/10/86	25
BSH2086	18/2/86	25/2/86	25
BSH2686	15/3/86	20/3/86	75
BSH0287	20/11/87	26/11/87	20
BSH2487	22/4/87	25/4/87	35
BSH0588	01/01/88	01/01/88	25
BSH0888	15/1/88	18/1/88	50
BSH0988	26/1/88	02/01/88	35
BSH1488	24/2/88	03/02/88	25
BSH1888	28/3/88	04/01/88	30
BSH0689	01/06/89	15/1/89	25
BSH1889	03/07/89	03/11/89	20
BSH1989	26/3/89	31/3/89	65
BSH0890	01/01/90	01/05/90	75
BSH2790	04/10/90	14/4/90	15
BSH0291	19/10/91	21/10/91	35
BSH1091	16/2/91	18/2/91	25
BSH1291	23/2/91	03/04/91	20
BSH0492	12/07/92	12/11/92	30
BSH1092	01/02/92	01/02/92	30
BSH1193	16/1/93	21/1/93	20
BSH0894	13/1/94	16/1/94	95

BSH1394	02/02/94	02/05/94	105
BSH2094	15/3/94	17/3/94	115
BSH2394	23/3/94	04/02/94	80
BSH0995	19/1/95	27/1/95	15
BSH1695	03/04/95	03/12/95	15
BSH0496	22/10/96	23/10/96	25
BSH0696	01/11/96	15/1/96	110
BSH1496	14/2/96	19/2/96	30
BSH1696	26/2/96	29/2/96	85
BSH1497	01/04/97	01/09/97	50
BSH2097	24/1/97	31/1/97	110
BSH2397	02/09/97	17/2/97	50
BSH3097	25/2/97	03/02/97	20

APPENDIX D:

DISTRIBUTION FITTING TO TROPICAL CYCLONE PARAMETERS

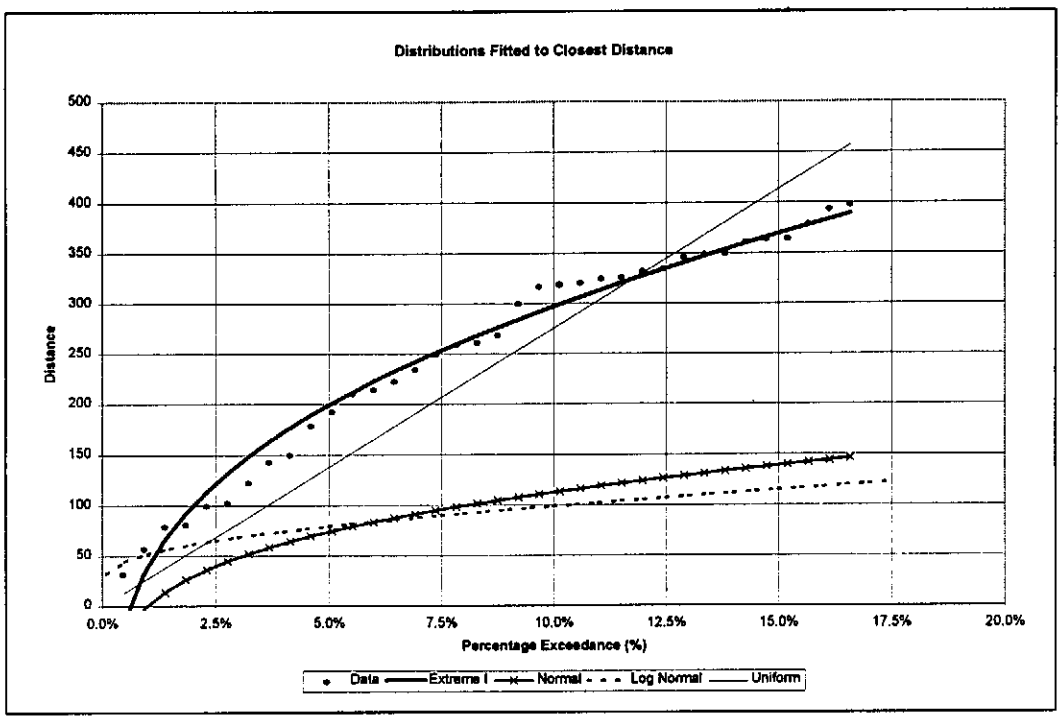

Figure D1: Distributions Fitted to Closest Distance (d)

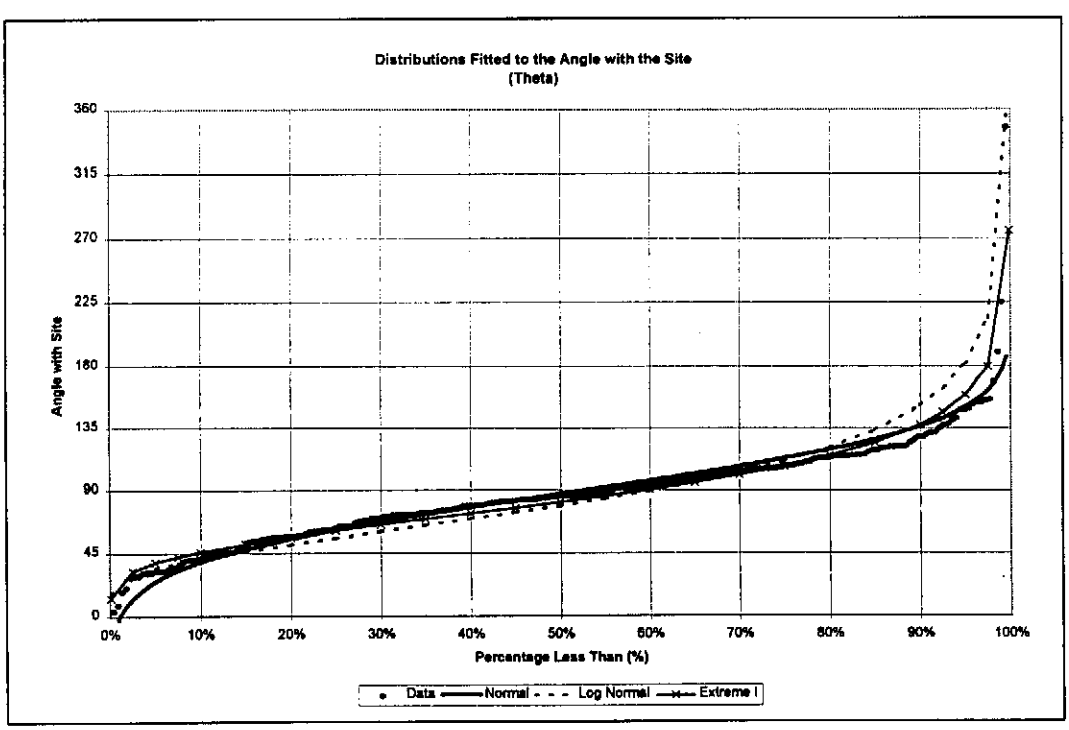

Figure D2: Distributions Fitted to Angle with Site (θ)

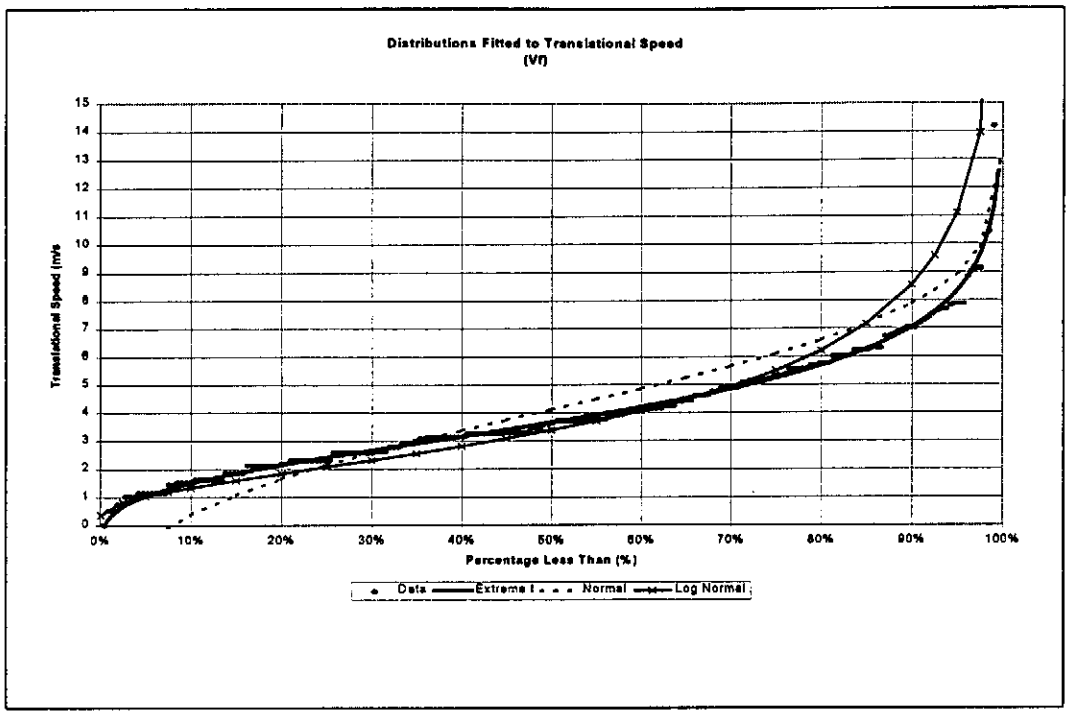

Figure D3: Translational Speed (V_t)

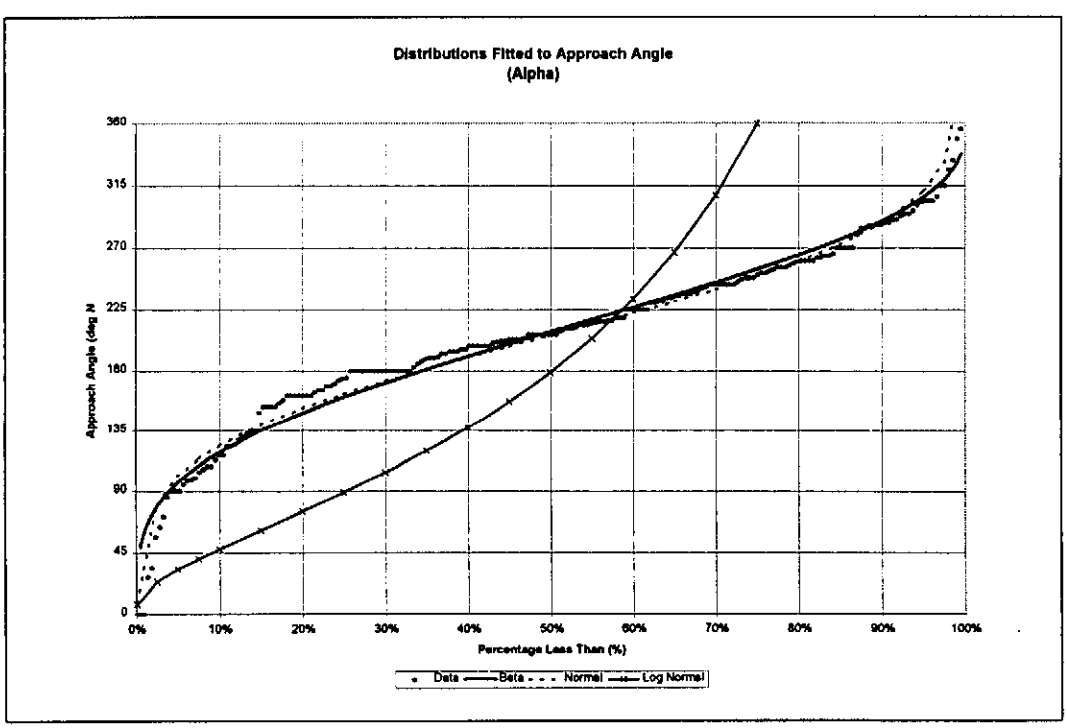

Figure D4: Direction of Travel of the Tropical Cyclone (α)

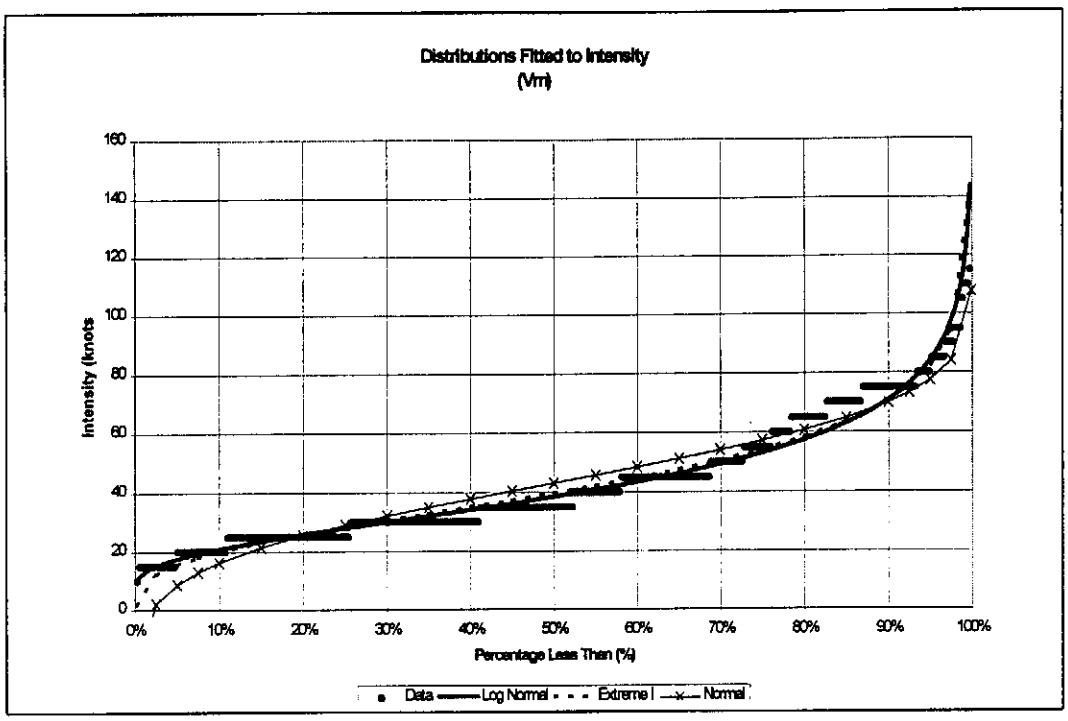

Figure D5: Distributions Fitted to Intensity (V_m)